JAERI 1310

JAERI 1310

Study on the Solid State Chemistry of Ternary Uranium Oxides

March 1988

日 本 原 子 力 研 究 所

Japan Atomic Energy Research Institute

JAERI レポートは，日本原子力研究所が研究成果編集委員会の審査を経て不定期に公刊している研究報告書です。

入手の問合わせは，日本原子力研究所技術情報部情報資料課（〒319-11茨城県那珂郡東海村）あて，お申しこしください。なお，このほかに財団法人原子力弘済会資料センター（〒319-11 茨城県那珂郡東海村日本原子力研究所内）で複写による実費頒布をおこなっております。

JAERI reports are reviewed by the Board of Editors and issued irregularly.

Inquiries about availability of the reports should be addressed to Information Division Department of Technical Information, Japan Atomic Energy Research Institute, Tokai-mura, Naka-gun, Ibaraki-ken 319-11, Japan.

編集兼発行　日本原子力研究所
印　　刷　いばらき印刷㈱

Study on the Solid State Chemistry of Ternary Uranium Oxides

Toshiyuki Yamashita

Department of Chemistry
Tokai Research Establishment
Japan Atomic Energy Research Institute
Tokai-mura, Naka-gun, Ibaraki-ken

Received September 9, 1987

Abstract

With the increase of burnup of uranium oxide fuels, various kinds of fission products are formed, and the oxygen atoms combined with the consumed heavy atoms are freed. The solid state chemical and/or thermodynamic properties of these elements at high temperatures are complex, and have not been well clarified.

In the present report, an approach was taken that the chemical interactions between UO_2 and these fission products can be regarded as causing overlapped effects of composing ternary uranium oxides, and formation reactions and phase behavior were studied for several ternary uranium oxides with typical fission product elements such as alkaline earth metals and rare earth elements. Precise determination methods for the composition of ternary uranium oxides were developed. The estimated accuracies for x and y values in $M_yU_{1-y}O_{2+x}$ were ±0.006 and ±0.004, respectively. The thermodynamic properties and the lattice parameters of the phases in the Ca-U-O and Pr-U-O systems were discussed in relation to the composition determined by the methods. Crystal structure analyses of cadmium monouranates were made with X-ray diffraction method.

Keyword: Ternary Uranium Oxides, Phase Behavior, Crystal Structure Analyses, Ca-U-O system, Pr-U-O system, Cadmium Monouranates, Thermodynamic Properties, Uranium Oxide fuels, Alkaline Earth Metals, Rare Earth Elements.

三元系ウラン酸化物の固体化学的研究

日本原子力研究所東海研究所化学部

山下利之

1987年9月9日受理

要旨

酸化物燃料の照射に伴い，多種類にわたる核分裂生成物が発生すると共に，重元素の消耗により結合酸素が遊離する．高温での，これら元素の固体化学反応および熱力学的挙動は複雑であり，充分解明されていない．

本報告では，UO_2とこれら核分裂生成物との化学的相互作用を三元系酸化物の重畳現象とみなして解明するアプローチをとり，アルカリ土類金属や希土類元素などの代表的な核分裂生成物を含む三元系ウラン酸化物について，生成反応を調べ，相挙動を求めた．本研究においては三元系ウラン酸化物の組成の精密分析が不可欠であることから，少量の試料量（約20 mg）に対して，酸素量および金属比の定量精度が，それぞれ，±0.006と±0.004である組成分析法を開発した．これを用いてカルシウムおよびプラセオジムを含む各三元系ウラン酸化物の熱力学的性質を，組成との関連において議論した．また，これら固溶体の格子定数の組成依存性を定めた．X線回折法により，カドミウム—ウラン酸塩の結晶構造を解析した．

CONTENTS

目　　次

1. Introduction

1.1 Background and objectives of this study

As nuclear fuels, pressed and sintered pellets of uranium dioxide, UO_2, has widely been used in light water reactors such as pressurized and boiling water type reactors. Uranium dioxide crystallizes in cubic fluorite type structure, and it has several advantages when used as nuclear fuels. That is to say, UO_2 has high chemical and thermodynamical stability and shows no phase transformation up to its melting point, and it can retain fission products in its crystal lattice to a large extent.

Recently, the demand to use the nuclear fuels until such higher burnups as 40,000–45,000 MWd/t seems to become rather pressing from economical reason. However, the increase in burnup makes the following chemical phenomena prominent in the UO_2 fuel:

(1) accumulation of solid and/or gaseous fission products,

(2) oxygen nonstoichiometry of the uranium dioxide,

(3) redistribution of fission products and actinides under high thermal gradients.

Fission products react with the fuel matrix UO_2 to form ternary or polynary uranium compounds or separate oxide phases. The chemical compounds formed are greatly dependent on the oxygen potential of the system which gradually increases with the increase of burnup accompanied by augmentation of O/U ratio of the UO_2 fuel due to fission. Besides that, if the fission products are transported to the outer surface of the fuel through the solid and/or gas phase, there is a possibility that they react with the cladding material, which may cause its failure. It has been reported that the oxygen potential also governs the chemical interaction between fission products and the cladding materials [1]. The study of fission products' behavior in relation to the oxygen potential is, therefore, of basic importance for the assessment of the irradiation behavior of nuclear fuels.

There have been considerable amounts of works on the irradiation behavior of fuels which are, for example, reviewed in the references [2-5]. In most of these works, efforts have been exerted for the whole system including the fuel and numerous fission products. The standpoint of the present study is a little different: In the present study, the complicated behavior of the UO_2 fuel is investigated from chemical and thermodynamic point of view. For this purpose, the whole system is to be divided into ternary uranium oxide systems with individual fission product, and the phase relations and thermodynamic properties of each system are studied to elucidate the effects of the added element on the chemical and thermodynamic properties of UO_2 fuels. Then, the results obtained are combined together to clarify the behavior of the regarded oxide fuel. This kind of knowledge on the phase relations and the thermodynamic properties is supposed to contribute in clarifying the chemical form of fission products in nuclear fuels and the change of thermodynamic properties of the fuels with the accumulation of fission products, and in investigating the chemical interaction between the fuel and the cladding. It may be worthwhile to note here that the composition of the specimens used in these studies should be determined with high accuracies because the properties of ternary uranium oxides depend strongly on their compositions.

The main purpose of the present work is to develop useful analytical methods for the determination of the composition of ternary uranium oxides and to have the knowledge on the phase relations of ternary uranium oxide systems by investigating the formation reactions,

the crystal structures and the phase behavior of these systems. Alkaline earth metals and rare earth elements are selected as foreign metals in UO_{2+x} phase since some of them have high fission yields and can react with UO_2 to form ternary solid solutions.

In order to make this point clear, literatures concerning ternary uranium oxides with alkaline earth metals are first reviewed. For ternary uranium oxide compounds with discrete compositions, the basic properties such as preparative conditions, crystal structures, and physicochemical properties are fairly well known. For ternary uranium oxide solid solutions, however, such knowledge is so far poor. Considering that the concentration of fission products is not very high in the present commercial light water reactors (less than one atomic percent for the fission product having the highest fission yield), the fission products are supposed to dissolve in the UO_2 matrix forming solid solution rather than to form the discrete ternary uranium compounds. This is the reason that the crystal chemical properties were studied for the ternary solid solutions in the present work.

Because the oxygen content in the solid solutions varies with the amount of doped metals as well as reaction conditions, it is very important to know the accurate composition of the solid solution for the precise discussion of changes in their physicochemical properties with the composition. Then analytical methods which can be easily applicable to ternary uranium oxides were first developed to determine the compositions with high accuracies.

Alkaline earth monouranates are used as starting materials when the ternary solid solutions are prepared. Then, these materials need to be well-characterized. Next, the formation reactions and thermal stabilities of the alkaline earth monouranates are investigated to establish preparative conditions of these monouranates. In the course of the study, an anomalous change in oxygen nonstoichiometry was found when the phase transformation took place in strontium monouranate from α to β phase. Thermal stability of the compound depends on its crystal structure and is supposed to be attributed to the bond strength and hence to intra-atomic distances between oxygen and metal atoms. This kind of information is obtained by the crystal structure analyses. Because cadmium monouranate which shows a similar anomalous change in oxygen nonstoichiometry to that of strontium monouranate was considered to give good supporting data for this purpose, and therefore its crystal structure was analyzed in detail.

With use of the techniques and the results obtained above, the phase relations of ternary calcium-uranium-oxygen and praseodymium-uranium-oxygen systems were studied to clarify not only the single phase region of the solid solution but the relation of lattice parameter and composition. Another aim is to study the change in thermodynamic properties with oxygen nonstoichiometry. Calcium and praseodymium were chosen considering their crystal radii since the formation of the solid solution would be easier in the case where they have closer crystal radii to that of uranium ion.

Fuel dissolution in nuclear fuel reprocessing is one of big problems to be surmounted for establishing the nuclear fuel cycle. The dissolution problem will, however, be reduced to a large extent if the oxide fuel can be converted into soluble compounds without a significant increase of high level wastes. Alkali and/or alkaline earth metal polyuranates were found to be generally soluble in a diluted acid through the present work: They seem to be a possible candidate of the materials to be converted. Then, the reactivity and reaction conditions between alkali metals and uranium oxides were studied in order to know the minimum amounts of alkali metal salts required to form uranates.

As most of the results obtained in the present study are generally applicable for the investigation of ternary uranium oxide systems, we hope that they provide a basis of the individual data for further important measurements such as the oxygen potentials and trans-

port properties of the oxide solid solutions to establish the irradiation behavior of nuclear fuels.

The outlines of this study are as follows:

In Chapter 1, ternary uranium oxides with alkaline earth metals will be reviewed in regard to their phase relationships, crystal structures and some thermodynamic properties.

In Chapter 2, two analytical method, i.e., a gravimetric method by addition of alkali or alkaline earth metal nitrates and a cerium(IV)-iron(II) back titration method, will be described together with various another methods for determining the composition of ternary uranium oxides. The present methods are devised to give high accuracies for even small amount of sample with easy operations and without expensive equipments.

In Chapter 3, formation of alkaline earth metal monouranates (MUO_4, M = Ca, Sr, Ba) is studied by means of thermogravimetry and X-ray diffractometry. Compositions and phase behavior of these monouranates are discussed in relation to the kind of alkaline earth metals and their crystal structures.

In Chapter 4, the structural parameters of cadmium monouranates, α and β-$CdUO_4$, are determined by X-ray powder diffraction method. The detailed structures of cadmium monouranates are compared with those of strontium monouranates which show similar crystal modifications and phase behavior in the phase transformation from α to β.

In Chapter 5, the phase behavior of $Ca_yU_{1-y}O_{2+x}$ solid solution is studied by means of X-ray diffraction and chemical analysis. The phase relations ($y \leq 0.4$) and the lattice parameter of the solid solution are determined. The oxidation state of uranium is discussed using an ionic model. The partial molar enthalpy of oxygen is also estimated.

In Chapter 6, the phase relations for praseodymium-uranium-oxygen ternary system are investigated by means of X-ray diffraction and chemical analysis. Region of existing phases in this system and the lattice parameter of a fluorite solid solution are determined. Discussion is made on the phase regions of this system in term of the oxidation state of uranium and the type of oxygen defect.

In Chapter 7, the reactivity and reaction conditions to form lithium and sodium uranates are studied in an attempt to grope some useful head-end processes in nuclear fuel reprocessing. The solubility of products in a diluted acid is also examined.

In Chapter 8, the results and conclusions obtained in this study will be stated.

1.2 Review on ternary uranium oxides with alkaline earth metals

In this section, citing some of published reviews on ternary or polynary oxides of uranium [6-10], the present status of knowledge on ternary uranium oxides with alkaline earth metals will be reviewed. There are many compounds or oxide phases in ternary alkaline earth metal oxide-uranium oxide-oxygen systems. These are summarized in **Table 1-1**. The crystal structure and lattice parameters of these compounds are shown in **Table 1-2**.

(1) The Mg-U-O system

The ternary MgO-UO_2-O_2 phase diagram has not been published. Three compounds and one solid solution phase are identified in this system: These are MgU_3O_{10} [30, 31, 43, 45], $MgUO_4$ [31, 34, 35, 43, 45-49], MgU_2O_6 [19-22, 50] and $Mg_yU_{1-y}O_{2+x}$ solid solution [21, 50-52]. The crystal structure and lattice parameters of these three compounds are shown in **Table 1-2**.

The $Mg_yU_{1-y}O_{2+x}$ solid solution with a cubic fluorite type structure is obtained in the range $0 \leq y \leq 0.33$ [21]. The single phase region of the solid solution is shown in **Fig. 1-1**

[21]. The phase boundary of uranium rich side depends on the reaction temperatures. MgU_2O_6 of which crystal structure is the fluorite type is considered to be the limiting composition of the solid solution [20, 50]. The lattice parameter of the solid solution is given as a linear equation of x and y [21]:

$$a = 5.4704 - 0.1170x - 0.5677y \ (\text{Å}).$$

It is found from density measurements that magnesium ions substitute for uranium ions in the lattice points and that the defect structure of the solid solution is an oxygen interstitial type in the composition range $x \geq 0$ [50]. The thermodynamic properties of the solid solution have been measured using a solid electrolyte galvanic cell method and given as [51, 52]:

$$\Delta\bar{G}_{O_2}(Mg_yU_{1-y}O_{2+x}) = \Delta\bar{G}_{O_2}(UO_{2+x}) + 0.0035T\ln(1 + 0.07\frac{x}{y}) + 60y \ \text{(kcal/mol)},$$

$$\Delta\bar{H}_{O_2} = -5.735\ln(x + 5.755y) - 83.62 \ \text{(kcal/mol)},$$

$$\Delta\bar{S}_{O_2} = -10.03\ln(x + 2.985y) - 44.66 \ \text{(e.u./mol)}.$$

The crystal structure of $MgUO_4$ has been determined by X-ray diffraction method to be orthorthombic with space group Immа [34]. The projection of the structure on the b-c plane is shown in **Fig. 1-2**. The $(UO_2)O_4$ octahedra containing the uranyl group of U-$2O_I$, of which bond length is 1.92 Å, are chained endlessly along the c-axis by sharing edges of the O_{II} atoms.

Table 1-1 Compounds of oxide phases in the ternary system of alkaline earth metal oxides and uranium oxides

Compounds	Mg	Ca	Sr	Ba
MUO_3	X	?	O	O
M_2UO_4	X	?	?	?
M_3UO_5	X	X	O	O
MU_5O_{16-x}	X	O	X	X
MU_3O_9	X	O	X	X
MU_2O_6	O	O	O	O
$M_3U_5O_{16}$	X	O	X	X
$M_2U_3O_{10}$	X	X	X	O
$M_2U_2O_7$	X	X	X	O
$M_{2.67}U_{1.33}O_6$	X	O	O	O
MU_4O_{13}	X	O	O	X
MU_3O_{10}	O	X	X	X
MU_2O_7	X	O	?	O
$M_2U_3O_{11}$	X	O	O	?
MUO_4	O	O	O	O
$M_3U_2O_9$	X	X	?	X
M_2UO_5	X	O	O	?
M_3UO_6	X	O	O	O
$M_yU_{1-y}O_{2+x}$	O	O	O	?
$M_{1-x}U_{1+x}O_{4+2x}$	X	X	O	X

O: well established, ?: not well established, X: not formed.

Table 1-2 Crystal structure of ternary uranium oxides with alkaline earth metals

Compound	Symmetry	Space group	a (Å)	b (Å)	c (Å)	References
(1) MO - UO_2 systems						
$SrUO_3$	orthorhombic		6.101	8.61	6.17	[11]
			6.03	6.18	8.62	[12]
$BaUO_3$	cubic		4.40			[13]
	pseudo-cubic		4.387			[11,14]
	pseudo-cubic		4.411			[15]
Sr_3UO_5	orthorhombic	Pbnm	6.037	6.194	8.644	[16]
α-Ba_3UO_5	tetragonal	I4/mnc or P4/mnc	6.291		8.982	[16]
β-Ba_3UO_5	cubic	Fm3m	8.915			[16]
(2) MO - UO_{2+x} system						
$CaU_5O_{15.4}$	orthorhombic		6.647	4.015	4.143	[17]
CaU_3O_9	cubic		5.37			[18]
MgU_2O_6	cubic		5.284			[19]
			5.275			[20]
			5.281			[21]
CaU_2O_6	cubic		5.379			[22]
SrU_2O_6	cubic		5.452			[22]
BaU_2O_6	cubic		5.63			[23]
$Ca_3U_5O_{16}$	rhombohedral		6.391 $\alpha=35.02°$			[24]
$Ba_2U_3O_{10}$	pseudo-cubic		5.65			[25]
$Ba_2U_2O_7$	Pseudo-tetragonal		11.56	$\beta \fallingdotseq 90°$	11.31	[26]
$Ca_{2.5}U_{1.33}O_{5.83}$	monoclinic		5.767	5.974 $\beta=89.8°$	8.349	[27]
$Sr_{2.5}U_{1.33}O_{5.83}$	monoclinic		6.178	6.023 $\beta=89.8°$	8.629	[27]
$Ba_{2.67}U_{1.33}O_6$	cubic		8.901			[28]
(3) MO - UO_3 system						
CaU_4O_{13}	orthorhombic		6.656	4.161	4.030	[29]
SrU_4O_{13}	monoclinic		6.734	4.193 $\beta=90.16°$	4.063	[29]
MgU_3O_{10}	hexagonal		3.788		4.080	[30]
	hexagonal		7.57		16.32	[31]
BaU_2O_7	tetragonal		$I4_1/amd$	7.128	11.95	[32,33]
$Ca_2U_3O_{11}$	triclinic		6.186 $\alpha=37.12°$	6.212 $\beta=37.56°$	6.186 $\gamma=37.12°$	[29]
$Sr_2U_3O_{11}$	triclinic		6.484 $\alpha=35.44°$	6.523 $\beta=36.10°$	6.484 $\gamma=35.44°$	[29]
$MgUO_4$	orthorhombic	Imma	6.520	6.595	6.924	[34]
			6.499	6.592	6.921	[35]
$CaUO_4$	rhombohedral	$R\bar{3}m$	6.266 $\alpha=36.03°$			[36]
			6.2683 $\alpha=36.04°$			[37]
α-$SrUO_4$	rhombohedral	$R\bar{3}m$	6.54 $\alpha=35.53°$			[36]
			6.551 $\alpha=34.82°$			[38]
β-$SrUO_4$	orthorhombic	Pbcm	5.4896	7.9770	8.1297	[34,37,39]
$BaUO_4$	orthorhombic	Pbcm	5.751	8.135	8.236	[40,41]
			5.7553	8.1411	8.2335	[37]
Ca_2UO_5	monoclinic	$P2_1/c$	7.9137	5.4409 $\beta=108.803°$	11.4482	[37]
Sr_2UO_5	monoclinic	$P2_1/c$	8.1043	5.6614 $\beta=108.985°$	11.9185	[37]
Ca_3UO_6	monoclinic	$P2_1$	5.7275	5.5964 $\beta=90.568°$	8.2982	[37,42]
Sr_3UO_6	monoclinic	$P2_1$	5.9588	6.1795 $\beta=90.192°$	8.5535	[37,42]
Ba_3UO_6	cubic		8.922			[43]
			8.90			[41]
	tetragonal		6.825		8.943	[42]
	orthorhombic		44.63	44.31	8.973	[44]

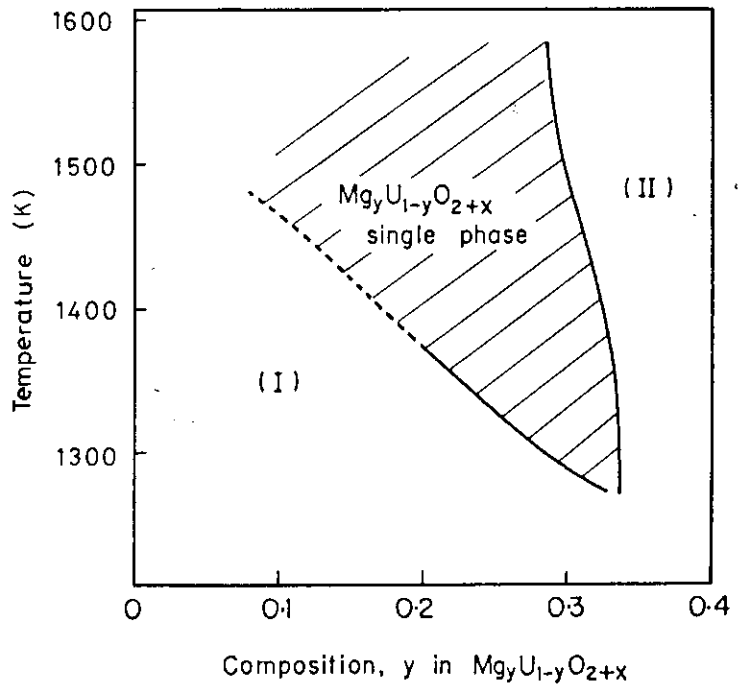

Fig. 1-1 An outline of phase diagram for $MgO\text{-}UO_{2+x}$ quasi-binary system [21]: Shaded area is the single phase region of cubic $Mg_yU_{1-y}O_{2+x}$. (I) Region of the mixture of cubic $Mg_yU_{1-y}O_{2+x}$, non-cubic magnesium uranates and U_3O_8. (II) Two-phase region of cubic $Mg_yU_{1-y}O_{2+x}$ and MgO.

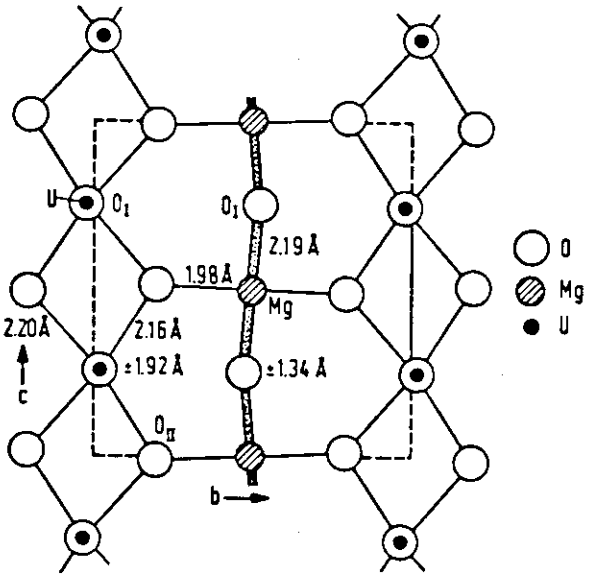

Fig. 1-2 Projection of the crystal structure of $MgUO_4$ on the b-c plane [34].

(2) The Ca-U-O system

The ternary $CaO\text{-}UO_2\text{-}O_2$ phase diagram has not been published yet. A quasi-binary $CaO\text{-}UO_{2+x}$ phase diagram is obtained in air [17], which is shown in **Fig. 1-3**. Ternary compounds formed in this system can be divided into two groups: compounds with uranium (IV) or uranium(V) and with uranium(VI). Compounds in the former group are $CaUO_3$ [18, 23, 53], Ca_2UO_4 [53], CaU_5O_{16-x} [17], CaU_3O_9 [18], CaU_2O_6 [22, 23, 54], $Ca_3U_5O_{16}$ [17, 24, 29] and $Ca_{2.67}U_{1.33}O_6$ [27]. Those in the latter group are CaU_4O_{13} [29], CaU_2O_7 [22, 23, 29, 55], $Ca_2U_3O_{11}$ [29], $CaUO_4$ [36, 37, 56-59], Ca_2UO_5 [29, 37, 55, 60] and Ca_3UO_6 [17, 37, 42-44, 49, 55, 59]. The crystal structure and lattice parameters of these compounds are summarized in **Table 1-2**. Although the lattice parameters of CaU_2O_7 have not been determined yet, the existence of this compound is confirmed [22, 23, 29, 53]. $CaUO_3$ and Ca_2UO_4 are not well established [18, 23, 53].

A cubic solid solution, $Ca_yU_{1-y}O_{2+x}$, with a fluorite type structure is obtained by the reaction of CaO and UO_{2+x} ($0 \leq x \leq 1$) [13, 17, 18, 22, 24, 25, 29, 53, 55, 61, 62]. The single phase region of the solid solution depends on reaction conditions: $0 \leq y \leq 0.47$ at 2353 K and $0 \leq y \leq 0.2$ at 1873 K in vacuum [53], $0 \leq y \leq 0.33$ at 1573 K in an inert atmostphere [24] and $0.3 \leq y \leq 0.33$ at 1273 K in air [17]. CaU_2O_6 which also has a fluorite type structure is described as the limiting composition of the solid solution [24]. The phase region of the solid solution at 1573 K is shown in **Fig. 1-4** [24]. The relation between lattice parameters and compositions of the solid solution has not been determined. No thermodynamic properties for the solid solution have been published.

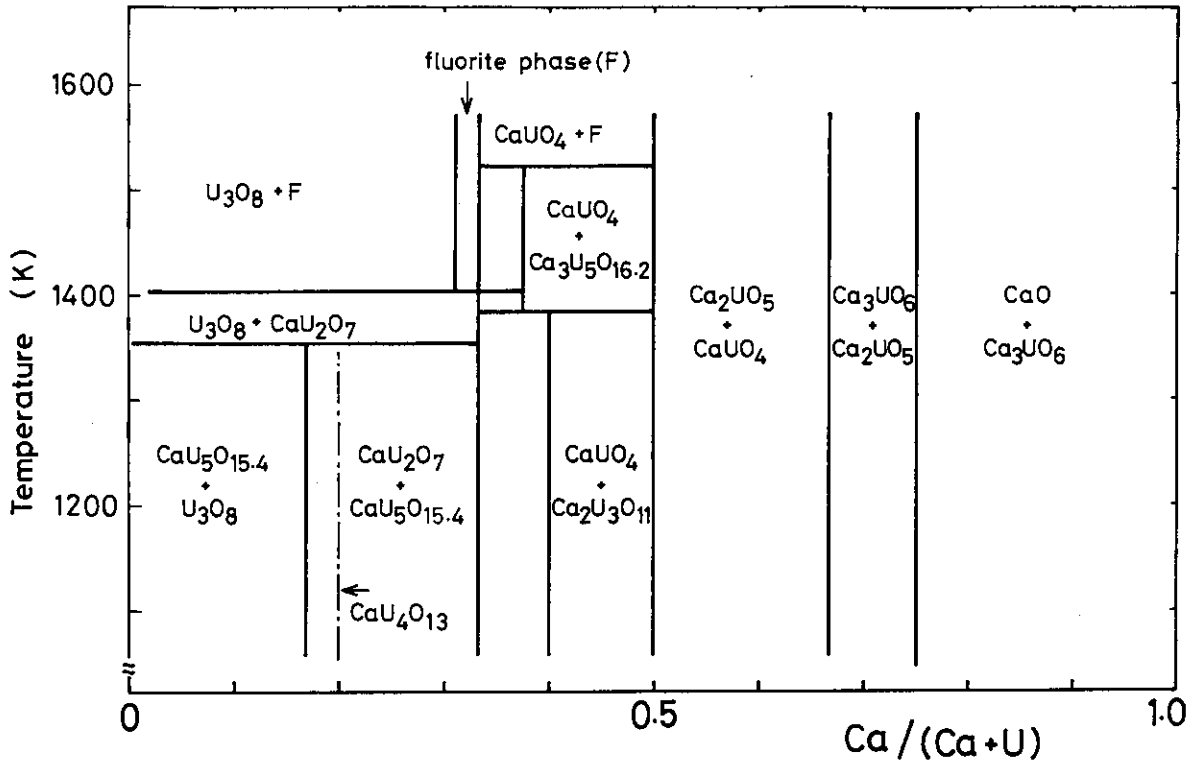

Fig. 1-3 The quasi-binary $CaO\text{-}UO_{2+x}$ phase diagram in air [17].

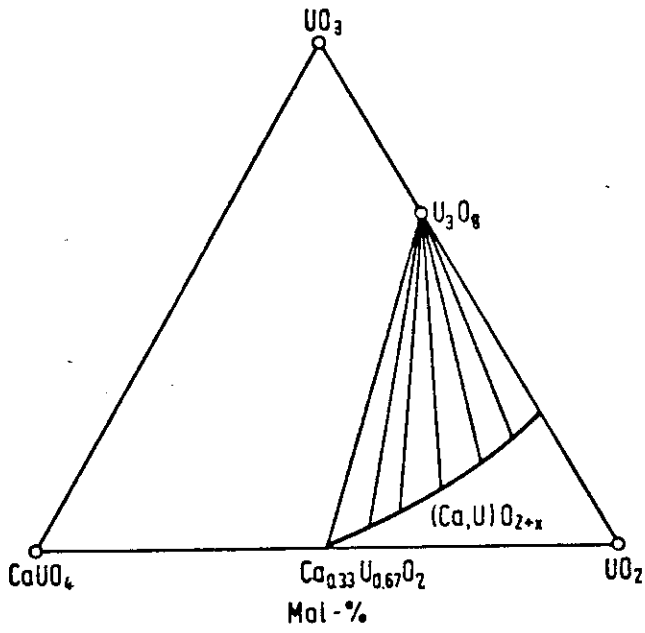

Fig. 1-4 The single phase region of $Ca_yU_{1-y}O_{2+x}$ solid solution at 1573 K [24].

(3) The Sr-U-O system

The ternary SrO-UO_2-O_2 phase diagram has not been published. The quasi-binary SrO-UO_2 phase is obtained in air [63] and shown in **Fig. 1-5**. An oxide phase designated as $Sr_{1-x}U_{1+x}O_{4+2x}$ in the figure is considered to be the solid solution of $SrUO_4$ and UO_3. Compounds with uranium(IV) or uranium(V) occurred in this system are $SrUO_3$ [11, 13], Sr_2UO_4 [13], Sr_3UO_5 [16], SrU_2O_6 [22, 23, 54, 64] and $Sr_{2.67}U_{1.33}O_6$ [27]. Compounds with uranium(VI) are SrU_4O_{13} [29], SrU_2O_7 [22, 23, 29, 31], $Sr_2U_3O_{11}$ [29], $SrUO_4$ [29, 34, 36-39, 49, 56, 64-66], $Sr_3U_2O_9$ [63], Sr_2UO_5 [19, 29, 37, 60] and Sr_3UO_6 [13, 29, 37, 42-44, 49, 67]. The crystal structure of these compounds are listed in **Table 1-2**. Among these compounds, Sr_2UO_4, SrU_2O_7 and $Sr_3U_2O_9$ have not been well established yet [13, 22, 23, 29, 31, 63].

A cubic solid solution, $Sr_yU_{1-y}O_{2+x}$, with a fluorite type structure has been obtained by the reaction of SrO and UO_{2+x} [25, 68-70]. Single phase solid solution is obtained in the composition range $0 \leq y \leq 0.107$ at 1773 K in wet hydrogen (the oxygen potential $\Delta\bar{G}_{O_2}$ = −110 kcal/mol) and its lattice parameter is expressed as [68]:

$$a = 5.4700 - 0.0046y \ (\text{Å}).$$

Recent results [70] show that the solid solution exists in the range $0 \leq y < \sim 0.3$ in an inert atmosphere at temperatures between 1423 and 1673 K and that the lattice parameter is expressed as a linear equation of x and y:

$$a = 5.4704 - 0.109x - 0.098y \ (\text{Å}).$$

Then, SrU_2O_6 which has a fluorite type structure is considered to be the limiting composition of the $Sr_yU_{1-y}O_{2+x}$ solid solution. No measurements on thermodynamic properties of the solid solution have been carried out.

The monouranate, $SrUO_4$, has three phases: α, β and γ phases. The phase transformation from α to β occurs at temperatures between 1003 K and 1133 K [43, 71] and the process is irreversible [71]. The phase transformation between β and γ, on the other hand, is reversible

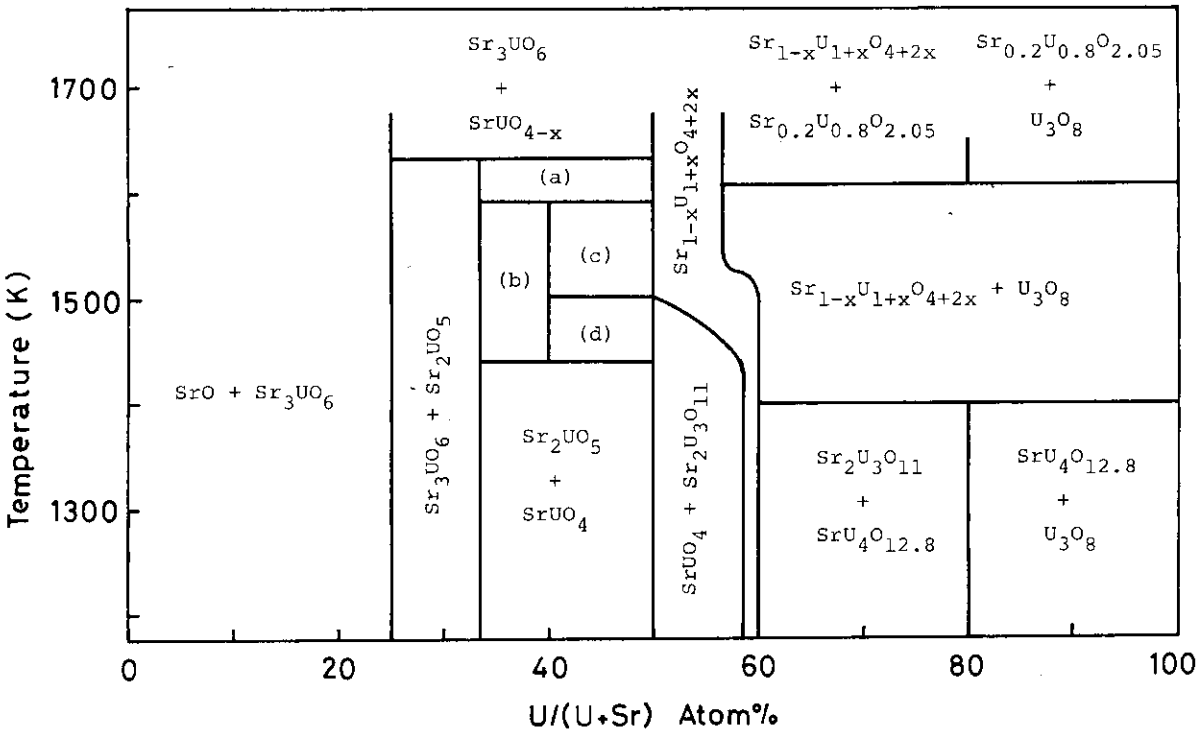

Fig. 1-5 The quasi-binary SrO-UO_{2+x} phase diagram in air [63]:
(a) $Sr_2UO_5 + SrUO_{4-x}$, (b) $Sr_2UO_5 + Sr_3U_2O_9$,
(c) $Sr_3U_2O_9 + SrUO_{4-x}$, (d) $Sr_3U_2O_9 + SrUO_4$.

and occurs at temperatures between 1500 and 1550 K [63, 72]. The crystal structure of α and γ phases is rhombohedral and the space group is $R\bar{3}m$, which is the same as that of $CaUO_4$. The β-$SrUO_4$ has a orthorhombic cell with space group Pbcm, which is the same as that of $BaUO_4$. Sketches of α and β-$SrUO_4$ structure are shown in **Fig. 1-6** [38, 65]. In α and γ-$SrUO_4$ as well as $CaUO_4$ crystals, each uranium atom is surrounded by six O_{II} atoms forming trigonal antiprism with two O_I stoms perpendicular to the trigonal planes. In β-$SrUO_4$ and $BaUO_4$ crystals, on the other hand, two O_I atoms and four O_{II} atoms are located around each uranium atom and form a distorted octahedron which share its corners to form infinite two-dimensional sheets in the plane with the b and c axes.

(4) The Ba-U-O system

The ternary BaO-UO_2-O_2 phase diagram has not yet been published. A sketch of quasi-binary BaO-UO_2 phase diagram has been given [73] as shown in **Fig. 1-7**. Ternary compounds with uranium (IV) or uranium (V) are $BaUO_3$ [11, 13-15], Ba_2UO_4 [13, 15], Ba_3UO_5 [15, 16, 19], BaU_2O_6 [13, 19, 22, 23, 54], $Ba_2U_3O_{10}$ [25], $Ba_2U_2O_7$ [20, 26] and $Ba_{2.67}U_{1.33}O_6$ [28]. Compound with uranium(VI) are BaU_2O_7 [22, 32, 33], $Ba_2U_3O_{11}$ [32], $BaUO_4$ [31, 37, 40, 41, 43], Ba_2UO_5 [13, 41] and Ba_3UO_6 [13, 41-44, 49]. Among these compounds, Ba_2UO_4, $Ba_2U_3O_{11}$ and Ba_2UO_5 are not well established [13, 15, 32]. The crystal structure and lattice parameters of these compounds are listed in **Table 1-2**.

Besides these compounds, there is a report that a cubic $Ba_yU_{1-y}O_{2+x}$ solid solution with a fluorite type structure has been obtained in the range $0 \leq y \leq 0.2$ by the reaction of BaO and UO_2 at 2073 to 2173 K [11]. No solubility of BaO into UO_2, however, has been observed since then [68, 74]. The relation between the lattice parameter and composition and thermodynamic properties of the solid solution have not been published.

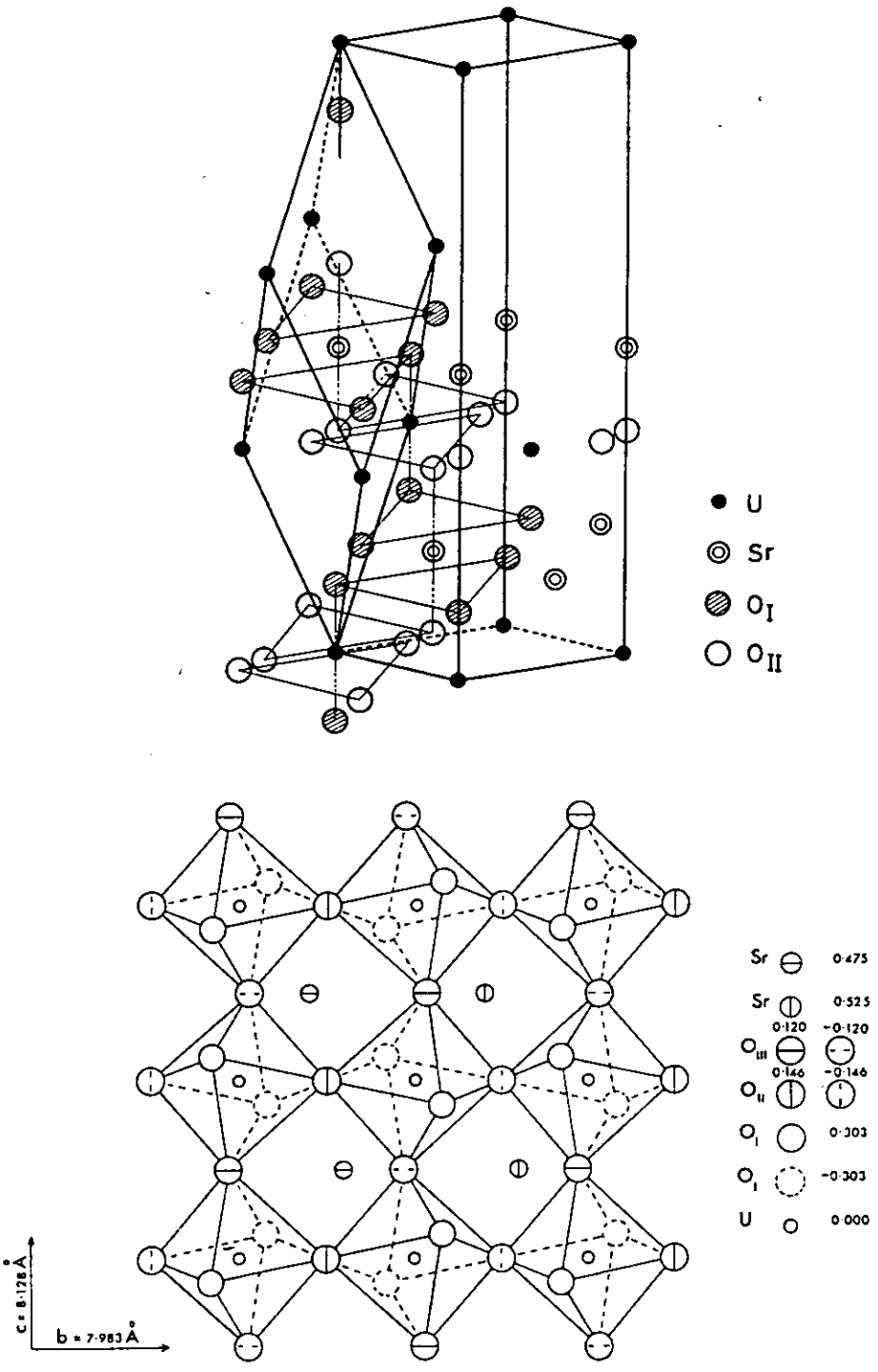

Fig. 1-6 The crystal structure of $SrUO_4$: (a) α-$SrUO_4$ [38], (b) β-$SrUO_4$ [65].

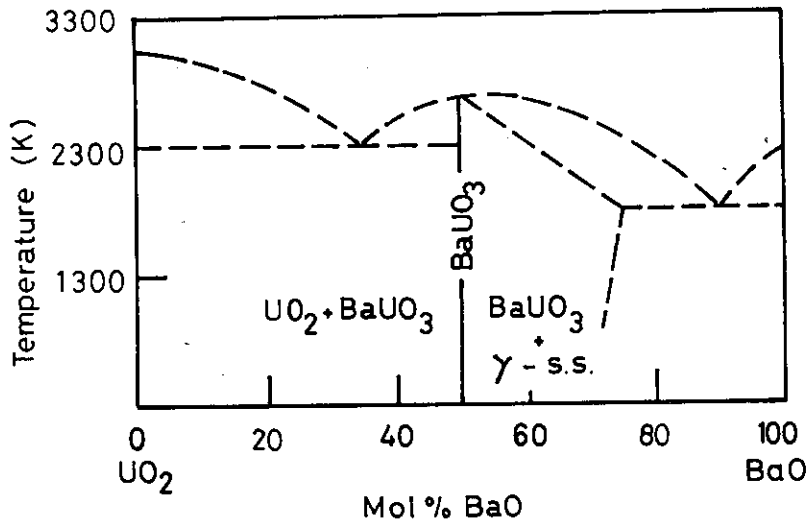

Fig. 1-7 Tentative phase diagram for the BaO-UO_2 system [73].

2. Study on analytical methods for the determination of the composition of ternary uranium oxides

2.1 Gravimetric method by addition of alkali or alkaline earth metal nitrates

2.1.1 Introduction

Nonstoichiometry occurs frequently in ternary uranium oxides, i.e., mixed oxides with uranium and another metal. The determination of oxygen in these oxides is of importance because their physical, chemical and/or thermodynamic properties vary considerably with the extent of the oxygen nonstoichiometry.

Many methods have been proposed, but only a few are currently used [75]. They can be classified as wet chemical methods and dry methods. The former will be discussed in section 2.2.1. The dry method most frequently encountered for analyzing uranium oxides takes the advantage of thermogravimetric techniques, in which the weight changes involved in the oxidation or reduction of the samples to a known O/M ratio (U_3O_8 or UO_2) are measured. If uranium oxides are heated in air between 973 and 1173 K, U_3O_8 is formed, but the compound has rather a wide range of nonstoichiometry, $U_3O_{8\pm x}$, where x may vary with history, amount and heating conditions of the samples [76, 77]. The problem of nonstoichiometry can be overcome practically by using UO_2 as a reference material: $UO_{2.000}$ is obtained by heating in a mixture of CO and CO_2 with a ratio of 10/1 at 1073-1123 K or in hydrogen at 1423 K [78]. The gravimetric method has been used for the determination of oxygen in plutonium-uranium mixed oxides. Markin et al.[79] determined O/M ratios of $Pu_yU_{1-y}O_{2+x}$ by reducing it to $MO_{2.00}$ with CO at 1123 K and by measuring the CO_2 produced using a gas handling apparatus, where M stands for Pu+U. They showed that the stoichiometric mixed oxides, $MO_{2.00}$, could be obtained by the reduction with CO at 1123 K citing their thermodynamic data on $Pu_yU_{1-y}O_{2+x}$ [80]. Accuracies of ±0.001 and ±0.002 have been reported for hyper-stoichiometric and hypostoichiometric plutonium-uranium mixed oxides, respectively. This method, however, is not applicable to the other ternary uranium oxide systems because it has not been ascertained whether the stoichiometric $MO_{2.00}$ is obtainable by the CO reduction of these oxides. In some ternary uranium oxides, in fact, uranium is not reduced to the tetravalent state even if these oxides are heated in hydrogen [27, 81]. The method of determining the O/M ratio through the lattice parameter obtained by X-ray diffraction is useful if the oxide sample is a well crystalline material. For the binary uranium oxide system, it is possible to measure the lattice parameter of the sample to ±0.0002 Å using the high angle diffraction lines, which corresponds to an error in the O/M ratio of ±0.005. Since the relation between the lattice parameter and the composition of ternary uranium oxides has been reported only for a few systems [21, 82-84], the application of the X-ray method is restricted.

A gravimetric method by addition of alkaline earth oxides or uranates has been developed for determining oxygen in ternary uranium oxides [85, 86]. This method is based on the fact that the valency of uranium is exactly +6 in alkaline earth uranates over certain continuous ranges of alkaline earth metal to uranium ratios [85, 87]. Under suitable conditions, uranium in the sample is oxidized to uranium(VI) on heating in air with alkaline earth oxide or uranate, and the oxygen content in the ternary uranium oxide can be determined from the increase

in weight. A precision between ±0.0008 and ±0.002 in the values for x in $M_yU_{1-y}O_{2+x}$ can be obtained by this method. However, grinding the samples intimately with alkaline earth oxide or the uranate is tedious and the reaction to form uranates with uranium(VI) requires a long heating period (50 h at 1073 K) because of rather slow rate in the solid-solid reaction.

In the present method described below, instead of solid additives a definite volume of lithium nitrate or calcium nitrate solution is pipetted on the sample of binary or ternary uranium oxides. The nitrate melts on heating in a stream of air or oxygen and reacts to form the uranium(VI) mixed oxides fast and completely. Analytical conditions were examined for test samples of UO_{2+x} and $Sr_yU_{1-y}O_{2+x}$, $Mg_yU_{1-y}O_{2+x}$ and $Th_yU_{1-y}O_{2+x}$ solid solutions.

2.1.2 Principle of the method

The present method is based on the fact [85, 86] that uranium is hexavalent in alkali and/or alkaline earth uranates formed in air at 973-1173 K. The main uranates with uranium (VI) are listed in **Table 2-1**. The hexavalency is conserved in continuous ranges of M/U ratios between certain discrete M/U values, where M indicates an alkali or alkaline earth metal. Thermodynamic considerations lead to the conclusion that two-phase mixture of the hexavalent uranates should exist in these continuous ranges [85]. The stability of the hexavalent uranium in the solid oxides increases in the presence of alkali or alkaline earth metal ions; for comparison, the mean valency of uranium in U_3O_8 which is stable in air at 973-1173 K is 5.333.

Table 2-1 Alkali or alkaline earth uranates formed by reaction at 1073 ~ 1373 K in air: $Li_2U_2O_7$ and SrU_2O_7 are not well established

M/U	1/4	1/3	1/2	2/3	1	2	3
Li	–	–	–	$Li_2U_3O_{10}$	$(Li_2U_2O_7)$	Li_2UO_4	–
Na	–	–	–	–	$Na_2U_2O_7$	Na_2UO_4	–
Mg	–	MgU_3O_{10}	–	–	$MgUO_4$	–	–
Ca	CaU_4O_{13}	–	CaU_2O_7	$Ca_2U_3O_{11}$	$CaUO_4$	Ca_2UO_5	Ca_3UO_6
Sr	SrU_4O_{13}	–	(SrU_2O_7)	$Sr_2U_3O_{11}$	$SrUO_4$	Sr_2UO_5	Sr_3UO_6
Ba	–	–	BaU_2O_7	$Ba_2U_3O_{11}$	$BaUO_4$	Ba_2UO_5	Ba_3UO_6

When a mixture of ternary uranium oxide $M_yU_{1-y}O_{2+x}$ and alkali or alkaline earth metal nitrate are heated in air, the following reaction occurs at a significant rate above the melting point of the nitrates evolving nitrogen dioxide:

$$M_y^{n+}U_{1-y}O_{2+x} + pA^{m+}(NO_3)_m + \frac{1}{2}\{1 - x + (\frac{n}{2} - 3)y - \frac{1}{2}mp\}O_2$$
$$= [A_p^{m+}M_y^{n+}U_{1-y}^{6+}O_{(1/2)\{mp + ny + 6(1-y)\}}] + mpNO_2$$

where p is the addition ratio, and $A^{m+}(NO_3)_m$ represents an alkali or alkaline earth metal nitrate. The square brackets indicate the bulk composition, which actually comprises two compounds, i.e., the alkali or alkaline earth metal oxide and the uranate, all the uranium being present as uranium (VI):

$$[A_p^{m+}M_y^{n+}U_{1-y}^{6+}O_{(1/2)\{mp + ny + 6(1-y)\}}]$$
$$= pA^{m+}O_{m/2} + M_y^{n+}U_{1-y}^{6+}O_{(1/2)\{ny + 6(1-y)\}}$$

The amount of the $A^{m+}O_{m/2}$ can be obtained by using a standard $UO_{2.000}$:

$$UO_{2.000} + pA^{m+}(NO_3)_m + \frac{1}{2}(1 - x - \frac{1}{2}mp)O_2$$
$$= [A_p^{m+}U^{6+}O_{(1/2)(mp+6)}] + mpNO_2$$
$$= [pA^{m+}O_{m/2} + UO_{3.000}] + mpNO_2$$

Since the amount of $UO_{3.000}$ can be calculated theoretically from the initial amount of $UO_{2.000}$, the weight of $A^{m+}O_{m/2}$ is obtained by subtracting the weight of $UO_{3.000}$ from that of the product. Therefore, the weight of the hypothetical uranates in which all the uranium are hexavalent:

$$M_y^{n+}U_{1-y}^{6+}O_{(1/2)\{ny+6(1-y)\}}$$

is obtained by subtracting the weight of $A^{m+}O_{m/2}$ from that of the product. The difference between the weights of this uranate and the initial uranate, $M_y^{n+}U_{1-y}O_{2+x}$, is due to the increase of oxygen in the compound accompanying the oxidation to uranium(VI). Thus, the x value of the sample can be derived from these weights.

2.1.3 Experimental

Apparatus and chemicals

The U_3O_8 was prepared by oxidizing high-purity uranium metal [88] at 1073 K in a silicon carbide muffle furnace with a 20x20x40-cm sample chamber [89]. Stoichiometric UO_2 used as the standard sample was obtained by reducing the U_3O_8 in a stream of purified hydrogen at 1273 K for 10 h in a silicon carbide tube furnace. The composition of the uranium dioxide used was checked to be $UO_{2.000}$ with an accuracy of ±0.003 by X-ray diffraction analysis [90]. For preparing solid solutions of $Sr_{0.1}U_{0.9}O_{2+x}$, $Sr_{0.2}U_{0.8}O_{2+x}$ and $Mg_{1/3}U_{2/3}O_{2+x}$, UO_2 was mixed with calculated amount of $SrUO_4$ $MgUO_4$ in an agate mortar and pressed into pellets. The pellets were then heated in a stream of helium at 1270-1570 K for 50 h. To prepare $Th_{0.5}U_{0.5}O_{2+x}$, a mixture of ThO_2 and UO_2 (Th/U = 1.000) was heated in a vacuum furnace at 1773 K for 15 h followed by reduction in a hydrogen stream at 1273 K in the tube furnace.

Lithium nitrate and $Ca(NO_3)_2 \cdot 4H_2O$ were both of analytical grade. The micropipette used was a Socorex type-821, of which the volume error was 0.46 μl (s.d.) at 200 μl.

Procedure

Weigh about 0.2 g of the sample on a microbalance (to ±0.005 mg) in a small quartz crucible which has been pre-heated at 1273 K to constant weight. Pipette a 200 μl aliquot of the nitrate solution into the crucible. Place several of these crucibles on a quartz boat and evaporate the water in an air bath at 340-360 K. Then, set the boat in the tube furnace and raise the temperature at a rate of 1-3 K/min with a flow of air or oxygen. Hold at the reaction temperature (923 K for lithium nitrate, 1073 K for calcium nitrate) for 3 h, and then switch off the furnace power. After the boat has cooled to 370-470 K, transfer it to a magnesium perchlorate desiccator. Weigh the crucible after it has cooled to room temperature.

Redox titration

Uranium oxide or the ternary uranium oxide sample (0.02-0.03 g) was dissolved in 5 ml of 0.07 M cerium(IV) sulfate solution in 1.5 M sulfuric acid. The excess of cerium(IV) was titrate with 0.05 M iron(II) ammonium sulfate in 1.5 M sulfuric acid using ferroin as indicator [91]. The cerium(IV) and iron(II) solutions were standardized by means of the stoichiometric UO_2.

2.1.4 Results and Discussion

Results for U_3O_8, $Sr_{0.1}U_{0.9}O_{2+x}$, $Sr_{0.2}U_{0.8}O_{2+x}$ and $Th_{0.5}U_{0.5}O_{2+x}$ are shown in **Table 2-2**; 7.045 M lithium nitrate solution was used. The weight increase shown is due to the formation of uranium(VI) with accompanying oxygen gain. The weight of the lithium oxide formed from the lithium nitrate added was obtained by using UO_2 standards which were heated together with the samples. The x values listed are in good agreement with the values obtained by titration, being within the standard deviations which vary from ±0.003 to ±0.007. Buoyancy errors in weighing were one order of magnitude less than the average standard deviation and were not corrected for. Correction for water absorbed during weighing was necessary because it caused significant systematic errors for uranates with large y values (e.g., $Th_{0.8}U_{0.2}O_{2+x}$). For these samples, 200 μl of the nitrate solution was too much, and the excess of lithium was converted into lithium oxide which is more hygroscopic than the uranates. Correction for moisture was done by weighing the sample several times and extrapolating to time zero. The weight increases in **Table 2-2** have been corrected for this molsture. Calcium nitrate was also tested as the addition compound; 200 μl of a 4.983 M calcium nitrate solution was pipetted onto the sample which was then heated at a rate of 3 K/min and at 1073 K for 3 h. For test sampels of UO_{2+x}, $Sr_{0.2}U_{0.8}O_{2+x}$ and $Mg_{1/3}U_{2/3}O_{2+x}$, the x values obtained agreed well with those from the titration method within the standard error of ±0.005.

The effect of metal-to-uranium atom ratio was examined with three times (x3) and five time (x5) diluted solutions. The results for UO_{2+x} and $Mg_{1/3}U_{2/3}O_{2+x}$ are shown in **Table 2-3**. The x values obtained with undiluted and 3-fold diluted solutions are consistent with the

Table 2-2 Determination of the x values of UO_{2+x}(U_3O_8 phase), $Sr_{0.1}U_{0.9}O_{2+x}$, $Sr_{0.2}U_{0.8}O_{2+x}$ and $Th_{0.5}U_{0.5}O_{2+x}$

Sample	Weight before heating (g)	Weight increase by heating* (g)	x value	x value by titration**
UO_{2+x} (U_3O_8 phase)	0.216660	0.004155	0.6636	
	0.192750	0.003590	0.6731	
	0.204165	0.004020	0.6548	
			x(av.)= 0.664 ± 0.007	0.664
$Sr_{0.1}U_{0.9}O_{2+x}$	0.204230	0.009940	0.0232	
	0.206170	0.010015	0.0246	
	0.205420	0.009855	0.0338	
			x(av.)= 0.027 ± 0.005	0.025
$Sr_{0.2}U_{0.8}O_{2+x}$	0.227275	0.009315	−0.0141	
	0.222175	0.009030	−0.0092	
	0.209895	0.008525	−0.0088	
			x(av.)= −0.011 ± 0.003	−0.008
$Th_{0.5}U_{0.5}O_{2+x}$	0.206495	0.006285	−0.0078	
	0.214250	0.007010	−0.0045	
	0.190675	0.005670	+0.0036	
			x(av.)= −0.003 ± 0.005	−0.001

(200 μl of 7.045 M $LiNO_3$ solution added, heating rate 3 K/min, heating temperature 923 K, holding time 3 h.)

* Corrected for moisture and Li_2O mass subtracted.

** Average of three determinations: standard deviation of ±0.003 [91].

Table 2-3 Effect of metal-to-uranium atom ratio on the x values of UO_{2+x}(U_3O_8 phase) and $Mg_{1/3}U_{2/3}O_{2+x}$ test samples

Solution	Cation concentration in solution (M)	Weight of Li_2O or CaO[a] (g)	M/U atom ratio (M = Li or Ca)[b]	x value for UO_{2+x} (U_3O_8 phase)[c]	x value for $Mg_{1/3}U_{2/3}O_{2+x}$[c]
Li (x1)	7.045	0.02105	1.98	0.664	−0.028
Li (x3)	2.218	0.00663	0.62	0.668	−0.028
Li (x5)	1.353	0.00404	0.38	0.670	−0.025
Ca (x1)	4.983	0.05608	1.40	0.663	−0.036
Ca (x3)	1.652	0.01853	0.46	0.665	−0.035
Ca (x5)	0.953	0.01069	0.27	0.670	−0.030
			x value by titration:	0.664[d]	−0.031[d]

(Sample weight ca. 0.2 g, heating rate 3 K/min, heating temperature 923 K for lithium nitrate and 1073 K for calcium nitrate, holding time 3 h.)

a) Volume of solutions 200 μl.

b) For 0.2 g sample of U_3O_8.

c) Average of three determinations: standard deviation of ±0.005.

d) Standard deviation of ±0.003.

values by titrimetry in all cases, but the values with 5-fold dilutions tend to show positive deviations, indicating that such solutions are inadequate for oxidizing uranium exactly to uranium(VI).

The heating rate had no significant effect on the values found but rapid temperature rise is not recommended in case unreacted nitrates bubble out of the crucibles. The heating temperature of 923 K for lithium nitrate was chosen so that the unreacted nitrate would decompose to the oxide [92], but lithium oxide would not volatilize. The equilibrium pressure of calcium oxide is low enough for its vaporization to be neglected below 1273 K [93], hence heating temperatures above 1073 K are possible.

The error in the determination is estimated as $x = \pm 0.005$. This error is considered to arise mainly from volumetric error in the addition of solution to the oxide samples. To minimize this error, the solution added was weighed using a microbalance. Results so obtained are shown in **Table 2-4**; the samples of UO_{2+x}, $Sr_{0.1}U_{0.9}O_{2+x}$ and $Sr_{0.2}U_{0.8}O_{2+x}$ were the same as in **Table 2-2**. In this procedure, 200 μl of the lithium nitrate solution was added to the precisely weighed sample in the crucible, which was immediately reweighed on the microbalance. Further treatment was as before. The nitrate solution was standardized with the standard UO_2; one gram of solution was equivalent to 30.43 ± 0.05 mg lithium oxide. **Table 2-4** shows that the x values can be determined with a standard deviation of ±0.002 by this procedure.

The present method is a convenient version of the earlier alkaline earth addition method because it requires neither tedious mixing nor long heating.

Table 2-4 Determination of the x values of UO_{2+x}(U_3O_8 phase), $Sr_{0.1}U_{0.9}O_{2+x}$ and $Sr_{0.2}U_{0.8}O_{2+x}$ with the solution weighing procedure

Sample	Sample weight (g)	Nitrate solution weight (g)	Weight after heating (g)	Weight increase due to uranium oxidation* (g)	x value
UO_{2+x} (U_3O_8 phase)	0.195775	0.218255	0.206175	0.003759	0.6632
	0.209245	0.216865	0.219825	0.003981	0.6662
	0.203165	0.219230	0.213705	0.003869	0.6659
					x(av.) = 0.665 ± 0.002
$Sr_{0.1}U_{0.9}O_{2+x}$	0.199470	0.215860	0.215695	0.009656	0.0272
	0.203240	0.217960	0.219720	0.009847	0.0266
	0.195780	0.218870	0.211965	0.009525	0.0235
					x(av.) = 0.026 ± 0.002
$Sr_{0.2}U_{0.8}O_{2+x}$	0.210135	0.219000	0.225310	0.008511	−0.0071
	0.202570	0.216670	0.217350	0.008187	−0.0059
	0.209015	0.218345	0.224160	0.008501	−0.0096
					x(av.) = −0.008 ± 0.002

(200 μl of 2.218 M $LiNO_3$ solution added: 30.43 ± 0.05 mg Li_2O in 1 g of solution.
Heating temperatures same as for **Table 2-2**.)
* For uranium oxidation after deduction of Li_2O added.

2.2 Cerium(IV)-Iron(II) back titration method

2.2.1 Introduction

Wet chemical methods for determining nonstoichiometry in uranium oxides involve the measurement of uranium(IV)/uranium(VI) ratios by titrimetry [91, 94-100], coulometry [101, 102], polarography [103-105] or spectrophotometry [106, 107] after dissolution of solid samples in a non-oxidizing acid. According to the colorimetric method by Kihara et al. [107], the samples are dissolved in phosphoric acid (at 453 K for about 2 h), and the amounts of uranium(IV) and uranium(VI) in the solution are determined by measuring the absorbance at 544 and between 280 and 350 nm, respectively, because there is no significant absorption band of uranium(IV) in the latter region. The precision of the method has been claimed to be ±0.0002 in O/M ratio for the samples having O/M ratios between 2.001 and 2.067 [107]. Although this method give high reproducibility, prevention of atmospheric oxidation of uranium(IV) and technical expertise are essential for satisfactory analyses. The precision of the coulometric titration or polarographic analysis is low: of the order of ±0.01-±0.04 as O/M ratio [101-105].

Many redox titration methods have been proposed and used for determining the composition of binary uranium oxides. This can be done by measuring the amount of either total uranium or uranium(IV) in the known weight of the sample. In general, the total uranium is determined by the titration with standard chromium(VI) or cerium(IV) solution after all the uranium ions are reduced to uranium(IV). Among many reactions adapted for this reduction process, the iron(II) reduction of uranium(VI) to uranium(IV) in concentrated phosphoric acid medium [94, 95] seems to be most widely used. Davies and Gray [96] oxidized the unreacted excess iron(II) with nitric acid in the presence of molybdenum(VI) as catalyst, and titrated uranium(IV) with potassium dichromate solution. The sluggishness of the reaction between uranium(IV) and chromium(VI) was overcome by the introduction of vanadyl sulfate

catalyst [97, 98].

The use of another non-oxidizing medium, sulfuric acid, is advantageous because of its handiness, though uranium(VI) can not be reduced to uranium(IV) by iron(II) in this medium. The reduction has been carried out by means of titanium(III) [99], Jones reductor [100] etc. Meanwhile, the oxygen content in the uranium oxide samples can also be obtained by determining the amount of uranium(IV). According to the titrimetric method by Dharwadkar and Chandrasekharaiah [91], uranium oxides are dissolved in dilute sulfuric acid in the presence of excess cerium(IV), and the amount of uranium(IV) is determined by back-titrating the remaining cerium(IV) with standard ammonium ferrous sulfate solution using ferroin as indicator. They have reported that the precision of ±0.003 can be attainable by this method. This method is simple and requires no elaborate apparatus.

Although these wet chemical methods are applicable to ternary uranium oxides, reports concerning them are meager [84, 108, 109]. Moreover, in these reports the metal-to-uranium atom ratio, M/(M + U), is determined separately by means of the other methods such as EDTA (ethylenediaminetetraacetic acid) titration analysis.

In the present work, a method for determining the composition, both x and y, of ternary uranium oxides was developed. The total uranium amount was determined by a pipetting technique of reduction with zinc amalgam after dissolution in sulfuric acid containing excess cerium(IV), while the uranium(IV) amount was determined by the back titration method of Dharwadkar and Chandrasekharaiah [91]. Applicability of the present method was examined for a solid solution, $Sr_yU_{1-y}O_{2+x}$, having known composition.

2.2.2 Theory

The composition of ternary uranium oxides can be derived if the amount of total uranium is known as well as that of uranium(IV) for known weight of the sample. The both quantities are determined by the cerium(IV)-iron(II) back titration method.

For obtaining the composition, x and y in $M_yU_{1-y}O_{2+x}$, following two equations in terms of x and y are considered:

i) The molecular weight of the sample, W, is given as

$$\begin{aligned} W &= y\underline{M} + (1-y)\underline{U} + (2+x)\underline{O} \\ &= x\underline{O} - y(\underline{U} - \underline{M}) + \underline{UO_2} \\ &= C_1x - C_2y + C_3 \end{aligned} \qquad (2\text{-}1)$$

where $\underline{M}$, $\underline{U}$ and $\underline{O}$ are the atomic weight of the foreign metal, uranium and oxygen, respectively, and $\underline{UO_2}$ is the molecular weight of uranium dioxide.

ii) The charge balance is maintained in the sample, then,

$$\begin{aligned} ny + v(1-y) &= 2(2+x) \\ 2x - (n-v)y &= v - 4 \end{aligned} \qquad (2\text{-}2)$$

where n and v are the valency of the foreign metal and the mean valency of uranium in the sample, respectively.

In equations (2-1) and (2-2), there are four unknowns, x, y, W and v, of which the latter two are obtained from the titration values for total uranium and uranium(IV).

From the titration of total uranium where all uranium are reduced to uranium(IV); the molecular weight W is given as

$$W = \frac{2w_1}{d_1} = C_4 \qquad (2\text{-}3)$$

where w_1 is the sample weight and d_1 is the amount of total uranium in the solution.

From the titration of uranium(IV), the mean valency of uranium, v, is given as

$$v = 6 - \frac{Wd_2}{w_2} = 6 - \frac{2w_1}{w_2}\frac{d_2}{d_1} = C_5 \tag{2-4}$$

where w_2 and d_2 are the sample weight and the amount of uranium(IV), respectively. By putting equations (2-3) and (2-4) into those (2-1) and (2-2), two equations which contain only two unknowns are obtained:

$$C_1x - C_2y = C_4 - C_3 \tag{2-5}$$

and

$$2x - (n - C_5)y = C_5 - 4 \tag{2-6}$$

Then,

$$x = \frac{(n - C_5)(C_4 - C_3) - C_2(C_5 - 4)}{C_1(n - C_5) - 2C_2} \tag{2-7}$$

and

$$y = \frac{2(C_4 - C_3) - C_1(C_5 - 4)}{C_1(n - C_5) - 2C_2} \tag{2-8}$$

where $C_1 = \underline{O}$,

$C_2 = \underline{U} - \underline{M}$,

$C_3 = \underline{UO_2}$,

$C_4 = \frac{2w_1}{d_1}$

$C_5 = 6 - \frac{2w_1}{w_2}\frac{d_2}{d_1}$.

In the limiting case of binary uranium oxides, i.e., $y = 0$, the x value can be obtained by determining the total uranium. Using equations (2-1) and (2-3), and putting $y = 0$ in the equation (2-1):

$$C_1x = C_3 - C_4.$$

Then,

$$x = \frac{C_3 - C_4}{C_1}. \tag{2-9}$$

2.2.3 Experimental

Reagents and samples

The reagents used were all of analytical grade. Cerium(IV) sulfate and iron(II) ammonium sulfate were dissolved in 1.5 M sulfuric acid to be ca. 0.07 and ca. 0.05 M solution, respectively. These were standardized just before each series of analysis by means of the stoichiometric uranium dioxide standard.

Zinc amalgam was prepared by adding 3 g of sandy zinc and small amount of dilute sulfuric acid to 100 g mercury followed by heating on a steam bath. After cooled to room temperature, undissolved residue was removed by decantation [110].

Ferroin indicator (0.025 M) was diluted in three times volume of 1 M sulfuric acid before use.

Triuranium octoxide, U_3O_8, was prepared by the air oxidation of high purity uranium

metal blocks [88] at 1073 K [89]. The standard uranium dioxide was obtained by the reduction of the U_3O_8 in a steam of purified hydrogen at 1273 K for 10 h. The O/M ratio of the standard UO_2 was analysed to be 2.000 ± 0.001 from the weight cahnge and the lattice parameter of the cubic cell [90]. Solid solution $Sr_{0.300}U_{0.700}O_{1.964}$ was prepared by heating the pellet of a mixture of $SrUO_4$ and UO_2 in a stream of helium at 1573 K for 50 h [86, 111].

Procedure

Two separate procedures are necessary for a sample, which will be designated as procedure (1) and (2) hereafter.

Procedure (1) is essentially the same as that of Dharwadkar and Chandrasekharaiah [91]. In a small glass crucible, 10-30 mg of the sample is weighed out and the sample powder is transferred to a titration vessel (50 ml beaker). 5 ml of cerium(IV) sulfate solution are pipetted into the beaker and several milliliter of 3 M H_2SO_4 are added. The beaker is warmed on a steam bath at 335-355 K until dissolution of the sample is completed. To the solution, one drop (ca. 0.06 ml) of ferroin indicator is added, and the excess cerium(IV) is titrated against standard iron(II) ammonium sulfate solution from a calibrated 10 ml micro-burette swirling the solution with magnetic stirrer.

Procedure (2) is the same as procedure (1) until dissolution. Then, the solution is transferred into a 20 ml glass bottle containing a few milliliter of zinc amalgam. This is done by using a fine-nozzled pipette of which the end is connected to a syringe with gum tube. The bottle should have a cap with polyethylene packing so as to prevent the leakage of solution on shaking. After the cap is tightened, the bottle is shaken vigorously for about one minute. Then, the solution is transferred back to the beaker by the same pipette. Several milliliter of 1.5 M H_2SO_4 are introduced into the bottle followed by shaking, and the solution is added to the solution of the reduced uranium by the pipette. This washing procedure is repeated twice. Subsequently, oxygen is passed through the solution from a fine nozzle of glass tubing at a rate of ca. 0.5 ml/s for 15 min to oxidize any traces of over-reduced uranium(III) to uranium(IV). 5 ml of cerium(IV) sulfate solution are pipetted into the beaker, and the remaining cerium(IV) is titrated against iron(II) after the addition of one drop of the ferroin solution.

2.2.4 Results and discussion

The effect of cerium(IV) in the reduction process of procedure (2) was examined by the blank test without uranium oxides. The results showed that the blank was 0.053 ml of the ammonium iron(II) sulfate solution as the average of three daterminations including indicator blank, 0.008 ml. On this basis, the accuracy of procedure (2) was checked with the $UO_{2.000}$ standard sample because the composition of binary uranium oxides can be determined by either of procedures (1) or (2). The results are shown in **Table 2-5**. The column 3 indicates the volume of the standard iron(II) solution corrected for the blank. The x value determined is shown in the column 4. The average of four determinations, -0.005 ± 0.01, is in good agreement with the value, 0.000 ± 0.001, determined by the gravimetric method [86] within the standard deviation. It may be noteworthy here that the error, ± 0.01, is taken place in the course of the calculation, since the titration error is amplified by about a factor of atomic weight quotient of uranium and oxygen if procedure (2) is used directly for determining the composition of binary uranium oxides (see equation (2-9) in section 2.2.2). As will be described below, this disadvantage can be eliminated by the combination of procedures (1) and (2) in the present method resulting in much smaller errors.

Table 2-6 shows the period of oxygen gas passage required for oxidizing uranium(III) to uranium(IV) [112]. This was examined using the $UO_{2.000}$ standard sample. The oxygen was bubbled through the solution with a flow rate of ca. 0.5 ml/s. As shown in the table, if oxygen

Table 2-5 Determination of uranium dioxide standard sample by procedure (2)

No.	sample weight (mg)	volume of iron(II)* (ml)	x value
1	28.520	2.045	−0.002
2	28.045	2.115	−0.009
3	29.485	1.903	+0.012
4	36.575	0.823	−0.022
		Av. = −0.005 ± 0.01	

O/U of the uranium dioxide: 2.000 ± 0.001
Concentrations of the standard solution: Cerium (IV) = 0.06233 ± 0.0001 M, Iron(II) = 0.04909 ± 0.0001 M.
Oxygen: 15 min at a flow rate of ca. 0.5 ml/s.
* Corrected for blank: 0.053 ml.

Table 2-6 Effect of oxygen gas passage through reduced uranium solutions

No.	sample weight (mg)	iron(II) solution[a] (ml)	period of gas passage[b] (min.)	x value
1	26.650	2.178	0	−0.605
2	28.055	1.870	0	−0.926
3			15	−0.005 ± 0.01[c]
4	27.700	2.166	30	−0.013
5	26.950	2.283	90	+0.003
6	30.305	1.1776	120	−0.001

Uranium oxide used: standard uranium dioxide with x = 0.000 ± 0.001
Concentrations of the standard solutions:
Cerium(IV) = 0.06233 ± 0.0001 M, Iron(II) = 0.04909 ± 0.0001 M.
a) Corrected for bland: 0.053 ml.
b) Flow rate of oxygen gas: ca. 0.5 ml/s.
c) Average value (See **Table 2-5**).

was not passed through, the x value of UO_{2+x} became −0.605 (No.1) or −0.926 (No.2) which is greatly deviated to negative side because the correct value of x is 0.000. On the other hand, the interference from uranium(III) was found to be completely removed by the passage of oxygen for 15 min. This result coincides with the observation by Lundell et al. [113]. The table also shows that more elongated bubbling period is not necessary for oxidizing uranium(III) to uranium(IV).

Applicability of the present method to ternary uranium oxides was studied for a solid solution, $Sr_yU_{1-y}O_{2+x}$, having known composition. The y value had been adjusted to 0.300 ± 0.001 on preparation by mixing $SrUO_4$ [111] and $UO_{2.000}$ in calculated ratio, while the x value was analyzed to be −0.036 ± 0.001 by gravimetric alkaline earth addition method [86]. In **Table 2-7**, the results of procedure (1) for this solid solution are exhibited. The x value in the column 4 was obtained by taking the y value as 0.300. Because the aim of this work is the simultaneous determination of x and y values, this calculation is somewhat trivial, but still useful to see that the value by procedure (1) is well in accord with the former gravimetric results.

Table 2-8 shows the x and y values of the $Sr_yU_{1-y}O_{2+x}$ which were obtained having no knowledge other than that the component elements were strontium, uranium and oxygen, and that the valencies of the strontium and oxygen were +2 and −2, respectively. These values were calculated by the combination of the titrated data of procedures (1) and (2) using equations (2-7) and (2-8) in section 2.2.2. As a way around the cumbersomeness of calculating all pairs of the data of procedures (1) and (2), the averaged values were used for procedure (1) which were taken from **Table 2-7**. The x and y values obtained are shown in the column 5 and 6, respectively. The average of five determinations of procedure (2) gives the following values: $x = -0.039$ and $y = 0.302$ which are in good agreement with the known composition for this test sample. From a number of titrations of this method, it may be reasonable to estimate that the volume error in titration is less than 0.006 ml which leads to the accuracies for x and y values to be ±0.006 and ±0.004, respectively. Direct calculation of standard deviations in **Table 2-8** give smaller errors.

Recent report [114] has described that cerium(IV) sulfate and potassium dichromate are equally suitable for precise determination of uranium. The present back-titration method using cerium(IV) has a sharp end point where 0.002 ml excess of titrant (iron(II)) rapidly makes the color of the solution change from pale blue to red. The redox reaction is fast enough to titrate in usual manner due to auto-catalytic action of iron ion.

Table 2-7 Application of procedure (1) to ternary uranium oxide, $Sr_{0.300}U_{0.700}O_{1.964}$

No.	sample weight (mg)	iron(II) solution* (ml)	x value
1	17.845	5.134	−0.0364
2	21.100	4.865	−0.0370
3	20.685	4.911	−0.0340
		Av. of x value	−0.036 ± 0.001

Concentrations of the standard solutions: Cerium(IV) = 0.06269 ± 0.0001 M, Iron(II) = 0.04753 ± 0.0001 M.
* Corrected for indicator blank: 0.008 ml.

Table 2-8 Determination of x and y values of $Sr_yU_{1-y}O_{2+x}$

No.	procedure	sample weight (mg)	iron(II) solution (ml)	x value	y value
	1	19.899[a)]	4.970[a)]		
1	2	20.435	3.921[b)]	−0.0371	0.3008
2	2	21.789	3.743[b)]	−0.0357	0.3000
3	2	18.855	4.127[b)]	−0.0357	0.3000
4	2	18.865	4.134[b)]	−0.0443	0.3052
5	2	18.850	4.133[b)]	−0.0413	0.3033
			Av. of x value =	−0.039 ± 0.004	
			Av. of y value =	0.302 ± 0.002	

Composition of the sample: $x = -0.036 \pm 0.001$, $y = 0.300 \pm 0.001$
Concentrations of the standard solutions:
Cerium(IV) = 0.06269 ± 0.0001 M, Iron(II) = 0.04753 ± 0.0001 M.
a) Averaged values of three determinations (See **Table 2-7**).
b) Corrected for blank: 0.053 ml.

3. Formation and some chemical properties of alkaline earth metal monouranates

3.1 Introduction

Alkaline earth metal uranates are usually produced in air by the reactions of uranium oxides with alkaline earth metal oxides or carbonates, nitrates, chlorides, etc. Among these uranates, the most common compound would be the monouranates(VI), which has a simple chemical formula MUO_4, where M is Mg, Ca, Sr or Ba [29, 36-38, 40, 41, 43, 55, 58, 59, 63-66, 71, 72, 115-121]. These monouranates are considered to be suited for use as staring materials to prepare the ternary uranium oxides containing these metals.

However, the stability of these monouranates has not fully been studied. Monouranates of $SrUO_4$ and $BaUO_4$ are reduced to MUO_3 (M = Sr, Ba) when heated in the stream of hydrogen at high temperatures [13, 15, 25, 53], while under more moderate reducing conditions $BaUO_4$ is admitted to form $Ba_2U_2O_7$ [122]. Moreover, $SrUO_4$ has three crystallographic modifications, i.e., α, β and γ-$SrUO_4$ [38]. The crystal structure of the low and high temperature modifications, α and γ-$SrUO_4$, is $CaUO_4$-type rhombohedral [29, 36, 38, 66, 72], and that of the middle temperature modification, β-$SrUO_4$, is $BaUO_4$-type orthorhombic [37, 65, 66]. In spite of these works, the relation between the composition of the monouranates and their preparing conditions are not well known.

In the present work, the formation of monouranates of calcium, strontium and barium by the reactions of their carbonates with U_3O_8 in various atmospheres of air, carbon dioxide and hydrogen and in vacuum was studied by means of thermogravimetry and X-ray diffraction analysis. The main purpose of this study is to establish preparation conditions of alkaline earth monouranates which are to be used as staring materials for sample preparations in the ternary uranium oxides. The chemical reactivity of the monouranates is also examined by means of thermogravimetry with attention to the change of the properties caused by varying alkaline earth elements.

3.2 Experimental

Materials

Alkaline earth metal carbonates and triuranium octoxide U_3O_8 were used as starting materials. Reagent grade, precipitated $CaCO_3$ was provided from Wako Pure Chemical Co. Ltd. $SrCO_3$ was prepared by adding aqueous solution of $Sr(NO_3)_2$ into ammoniacal solution of $(NH_4)_2CO_3$, similar to the procedure for producing the precipitated $CaCO_3$ [123]. $BaCO_3$ was obtained by the same way as $SrCO_3$ was prepared. U_3O_8 was prepared by heating ammonium diuranate in air at 1173 K for one day.

All reactions were performed with samples in the form of pressed pellets. An alkaline earth metal carbonate and U_3O_8 were thoroughly mixed in an agate mortar and compacted at 3×10^3 kg/cm^2 into cylindrical pellets of 10 mm in diameter and of about 2 mm in thickness. The weight of each pellet was about 800 mg.

Apparatus and procedure

The experimental apparatus consists of a Cahn RH-type automatic electrobalance, a

Kanthal resistance furnace, a pressure measurement system, and vacuum pumps. The balance was adjusted so as to have a maximum weight change of 500 mg and a sensitivity of 0.01 mg. A fused quartz crucible, 20 mm in height and 18 mm in outer diameter, was suspended from the balance, and then a quartz tube of 26 mm in outer diameter was connected to the vessel containing the balance. Then, the reaction system was evacuated to 1×10^{-5} mmHg or below, and the sample was weighed in vacuum. After that, the system was filled with air (or hydrogen in the reduction experiments). The weight changes due to buoyancy and the thermomolecular flow were corrected by using the platinum wire.

The temperature of the specimen was measured by means of a Pt/Pt + 13%Rh thermocouple placed close to the crucible inside the reaction tube. The temperature was automatically controlled to raise at a constant heating rate or to hold at a desired constant temperature. Most of the experiments were made at the heating rate of 2 K/min unless otherwise specified.

X-ray diffraction analysis

The sample were finely ground and loaded into capillaries, and then vacuum-sealed. The X-ray photographs were obtained with a Norelco 114.6 mm camera using the nickel-filtered copper Kα radiation.

3.3 Results and discussion

Formation of calcium monouranate

The reaction of $CaCO_3$ with U_3O_8, where the Ca/U atom ratio is unity, was examined by heating the mixture pellets in each of the atmospheres of air, carbon dioxide and hydrogen, and in vacuum. The oxygen partial pressures of these atmospheres are 2.1×10^4, 1.0, probably $<10^{-15}$ (at 1273 K) and 1.0 Pa, respectively. **Figure 3-1** shows typical thermogravimetric (TG) curves of the reactions from room temperature to 1273 K in hydrogen and to 1373 K in the other atmospheres. After the temperature was raised at 1273 or 1373 K, the sample was held at that temperature for 3 h, and then it was furnace-cooled. The figure also shows the decomposition curve of $CaCO_3$ in vacuum, which is normalized to the $CaCO_3$ content in the mixture of $CaCO_3$ and $UO_{8/3}$.

When heated in air, the weight loss of the sample began at 850 K, and it proceeded remarkably above 970 K. The weight loss finished at 1120 K. Above 1120 K, the sample weight increased slightly till 1230 K, and again decreased gradually up to 1373 K. The decomposition curve of $CaCO_3$ in air was on the same curve with the reaction of $CaCO_3$ with U_3O_8 in air. This is likely that $CaCO_3$ partly reacts with U_3O_8, and partly decomposes independently of proceeding the reaction. The CaO, which remains still as the unreacted material, may cause the subsequent reaction with U_3O_8 beyond the minimum point of the TG curve at 1123 K. When $CaUO_4$ is formed, the mixture takes up oxygen from the atmosphere as:

$$CaO + \frac{1}{3}U_3O_8 + \frac{1}{6}O_2 \rightarrow CaUO_4.$$

The composition of the peoduct was $CaUO_{3.969}$. Rigorously stoichiometric compound was not obtained. The color of the product was greeish-yellow.

In order to examine the reaction behavior of $CaCO_3$ with U_3O_8, the reaction in one atmospheric pressure of CO_2 was performed under the same condition as the reaction in air. $CaCO_3$ is not decomposed at least below 1171 K in one atmospheric pressure of CO_2. The reaction began at 920 K, and proceeded similarly as the reaction in air. Because the oxygen partial pressure of CO_2 is lower than that of air, the oxygen content of the product is expected to be lower than that formed in air: the composition was $CaUO_{3.65}$.

When heated in vacuum (curve 2), the weight loss of the sample occurred at a lower

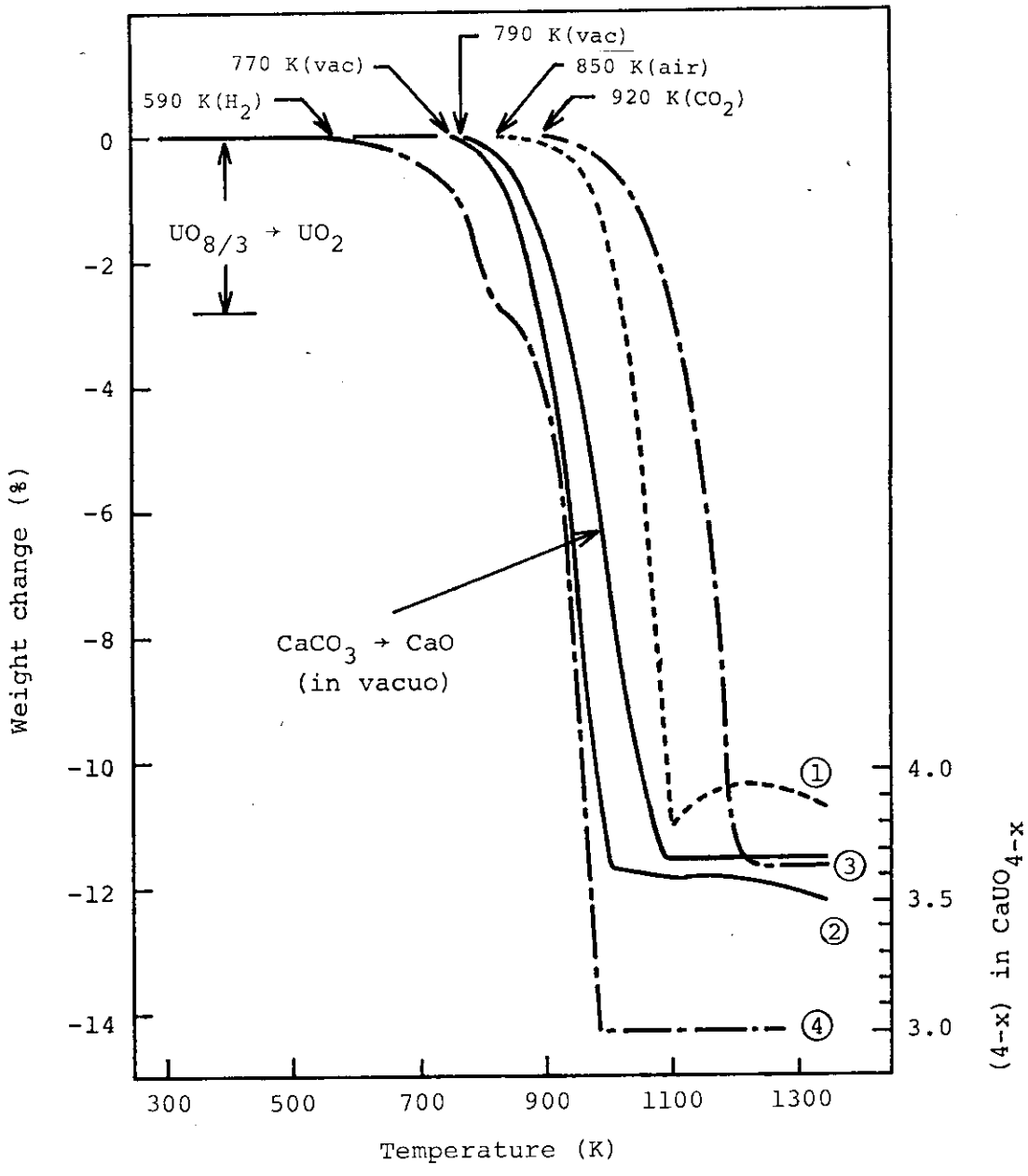

Fig. 3-1 TG curves for the reactions of $CaCO_3$ with U_3O_8 in various atmospheres: (1) in air, (2) in vacuum, (3) in CO_2, and (4) in H_2, Heating rate 2 K/min.

temperature than those in air and in CO_2. Above 1030 K, the curve became nearly flat but still showed small decrease with raising temperature. The weight loss in this portion is due to partial oxygen liberation from the monouranate produced.

In a hydrogen atmosphere, the weight loss proceeded stepwise. The first step is the reduction of U_3O_8 to UO_2 in the mixture. The fact is deduced because the same curve is obtained when U_3O_8 is reduced to UO_2 in hydrogen. The reaction of the second step proceeds at temperatures above 870 K, which is essentially the thermal decomposition of $CaCO_3$. The CO_2 produced from $CaCO_3$ may be partly converted into CO by the reaction:

$$CO_2 + H_2 \rightarrow CO + H_2O.$$

As water vapor is removed easily by the liquid nitrogen cold trap rather than CO_2, the oxygen

partial pressure around the sample is remarkably reduced. The composition of the product was $CaUO_{3.03}$. According to X-ray diffraction analysis, the product was not $CaUO_3$, but a mixture of CaO and UO_2. The existence of $CaUO_3$ has been reported [13, 53], but it has been denied [7, 25]. The present results also support the non-existence of $CaUO_3$. The lattice parameter of the UO_2 phase was $a = 5.4685 \pm 0.0005$ Å, which was slightly smaller than that for stoichiometric UO_2, $a = 5.4704$ Å [90]. The deviation is due to the formation of either non-stoichiometric UO_{2+x} or the solid solution $Ca_yU_{1-y}O_{2+x}$ with a very small y value. Although it is not clearly determined which case is actual in the present stage, the latter case is highly possible because the reaction was carried out in hydrogen where nonstoichiometric UO_{2+x} would be reduced into stoichiometric UO_2.

Formation of strontium monouranate

A typical heating curve for the reaction of $SrCO_3$ with U_3O_8 in air is shown in **Fig. 3-2**, curve 1. The weight loss by the reaction occurred stepwise In the figure, the results obtained

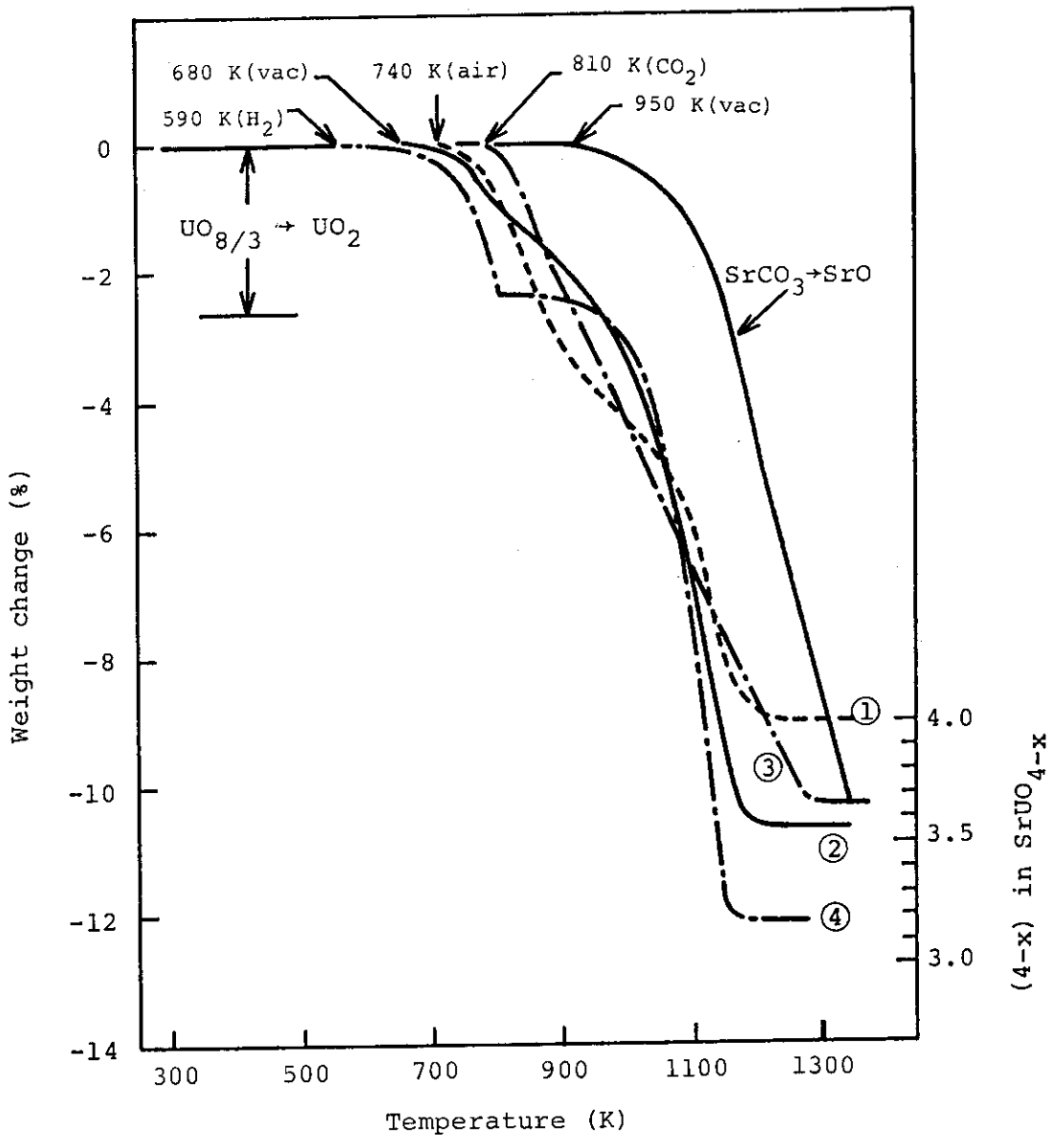

Fig. 3-2 TG curves for the reactions of $SrCO_3$ with U_3O_8 in various atmospheres: (1) in air, (2) in vacuum, (3) in CO_2, and (4) in H_2, Heating rate 2 K/min.

in the other atmospheres are also shown together with the decomposition curve of $SrCO_3$ which is normalized to the $SrCO_3$ content in the mixture of $SrCO_3 + (1/3)U_3O_8$. From the comparison of the heating curve of the mixture with the decomposition curve of $SrCO_3$, it is deduced that the first step is apparently due to the reaction of $SrCO_3$ with U_3O_8, and the second step is due to the reaction of SrO with U_3O_8 plus the reaction of the first step. The composition of the compound obtained was $SrUO_{3.997}$. The X-ray diffraction pattern of the product was identical with that of β-$SrUO_4$, which is orthorhombic and isomorphous with $BaUO_4$ with space group Pbcm, $Z=4$ [37, 65, 66]. The color of the product was yellow.

The initiation temperature of the reaction in CO_2 atmosphere was a little higher than that in air. The weight loss occurred nearly linearly with raising temperature. The reaction finished at 1323 K. $SrCO_3$ is stable during the reaction, since the decomposition temperature of $SrCO_3$ in one atmospheric pressure of CO_2 is 1443 K. The composition of the product was $SrUO_{3.673}$.

The weight loss of the reaction in vacuum proceeded at a large rate above 770 K. By comparing with the decomposition curve of $SrCO_3$, the rapid weight loss corresponds to the decomposition of $SrCO_3$. Therefore, it is thought that the monouranate is formed by the following successive reactions:

$$SrCO_3 \rightarrow SrO + CO_2,$$
$$SrO + \frac{1}{3}U_3O_8 \rightarrow SrUO_{4-x} + \delta O_2.$$

The composition of the product was $SrUO_{3.563}$ under the condition that the sample was held at 1373 K for 3 h. According to X-ray diffraction analysis, the crystal structure of the product was rhombohedral with space group $R\bar{3}m$, $z=1$, which is isomorphous with $CaUO_4$ [29, 36, 38, 66, 72]. The color of the product was dark green.

When heated in hydrogen, the reaction proceeded with destinct two step: the first step is the reduction of U_3O_8, and the second step is the reaction of $SrCO_3$ or SrO with UO_2. The bulk composition of the product was $SrUO_{3.175}$ and the color was dark gray.

Formation of barium monouranate

The reaction of a barium containing compound with uranium oxide in air yields orange $BaUO_4$, as reported by several investigators [37, 40, 41, 43, 59, 117]. **Figure 3-3** shows thermogravimetric curves of the reaction of $BaCO_3$ with U_3O_8 in various atmospheres, together with the decomposition curve of $BaCO_3$ in vacuum which is normalized to the $BaCO_3$ content in the mixture. The reaction in air proceeded stepwise. When the reaction curve is compared with the decomposition curve of $BaCO_3$, the first step is seen to be the reaction of $BaCO_3$ with U_3O_8. As the decomposition of $BaCO_3$ in vacuum occurred at 1023 K, the BaO produced may be added to the reaction of $BaCO_3$ with U_3O_8 above that temperature. The product was the stoichiometric monouranate, $BaUO_{4.000}$.

The initiation temperature of the reaction in one atmospheric pressure of CO_2 was 800 K, and the weight loss continued to 1373 K (curve 3). As the decomposition temperature of $BaCO_3$ at one atmospheric pressure of CO_2 is 1763 K [124], the TG curve shows the reaction of $BaCO_3$ with U_3O_8. The composition of the product of dark brown color was $BaUO_{3.794}$.

The TG curve in vacuum is seen to combine the first step of the reaction in air with the second step of the reaction in hydrogen. This shows that the reaction of BaO with U_3O_8 is predominant to the reaction of $BaCO_3$ with U_3O_8 with raising temperature. The composition of the product was $BaUO_{3.651}$.

The weight loss in hydrogen occurred atepwise. The first step is the reduction of U_3O_8, while the reaction of the second step is seen to be the reaction of $BaCO_3$ with UO_2. The product was $BaUO_{3.498}$.

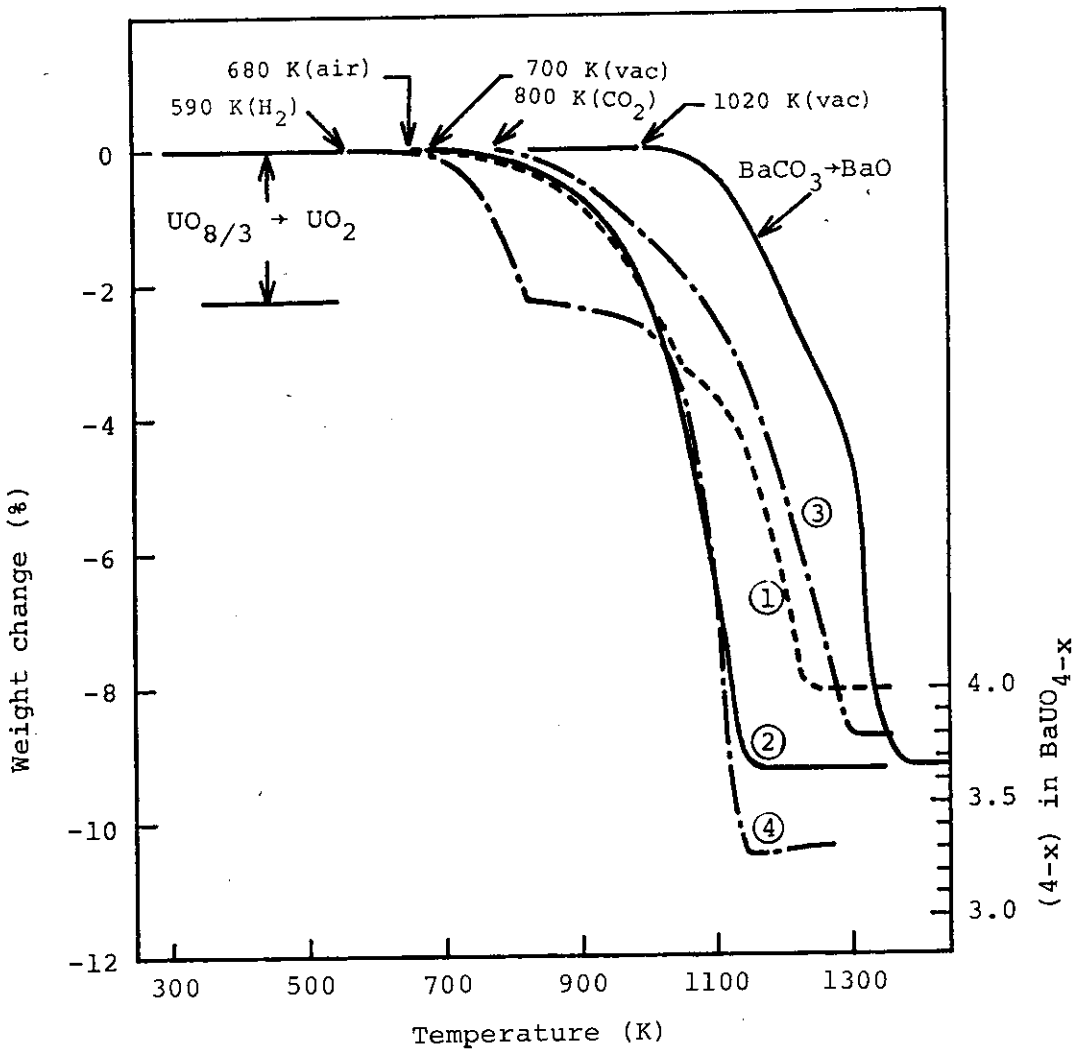

Fig. 3-3 TG curves for the reactions of $BaCO_3$ with U_3O_8 in various atmospheres: (1) in air, (2) in vacuum, (3) in CO_2, and (4) in H_2, Heating rate 2 K/min.

Comparison of the formation reaction of alkaline earth metal monouranate

As seen in **Figs. 3-1**, **3-2** and **3-3**, the behavior of the formation reactions of alkaline earth metal monouranates differs among the alkaline earth elements. The initiation temperatures of the reactions of $CaCO_3$, $SrCO_3$ and $BaCO_3$ with U_3O_8, for example, were 850, 740 and 680 K, respectively. This is in reverse order of the decomposition temperatures of alkaline earth metal carbonates.

The initiation temperature of the reaction can be used as a measure of the chemical reactivity although it merely means the temperature at which the reaction on the thermogravimetric curve occurs at a measurable rate and, thus, its applicability is limited. Then the reactivity of the carbonates is expressed as the following sequence:

$$BaCO_3 > SrCO_3 > CaCO_3.$$

For the reactions carried out in CO_2 for preventing the carbonates from decomposition, the initiation temperatures were changed into 920, 810 and 800 K for $CaCO_3$, $SrCO_3$ and $BaCO_3$, respectively, but the order of the temperature were not varied. From the fact it is deduced that the decomposition of the carbonates plays an importnat role in the reactions.

For understanding the difference in chemical reactivity of alkaline earth carbonates,

discussion by means of the Gibbs free energies for formation of alkaline earth monouranates (VI), ΔG°, may be meaningful because it is generally admitted that there exists a trend that the reactivity increases with decreasing the Gibbs energy. The direct reaction of alkaline earth metal carbonates, MCO_3, with U_3O_8 is expressed as:

$$MCO_3 + \frac{1}{3}U_3O_8 + \frac{1}{6}O_2 = MUO_4 + CO_2. \qquad (3\text{-}1)$$

If the reaction takes place through the alkaline earth metal oxide, MO, it can be expressed as:

$$MCO_3 = MO + CO_2 \qquad (3\text{-}2)$$

$$MO + \frac{1}{3}U_3O_8 + \frac{1}{6}O_2 = MUO_4 \qquad (3\text{-}3)$$

where alkaline earth monouranate, MUO_4, is treated as a stoichiometric compound. Thermodynamic functions of these reactions are calculated out in **Table 3-1** from the various literature values of the compounds [29, 118, 124-130]. Curves of ΔG_T as a function of temperature shown in **Fig. 3-4** are drawn if the equation,

$$\Delta G^\circ = \Delta H^\circ_{298} - T\Delta S^\circ_{298},$$

may be applied approximately, because the temperature dependence of enthalpies and entropies for the reactions (3-1) and (3-3) are not known. At temperatures as low as 670 K at which the reaction is initiated, ΔG° (reaction 3-3) is more negative than ΔG° (reaction 3-1). Therefore, it is deduced thermodynamically that the reaction (3-3) preferably occurs rather than the reaction (3-1).

Table 3-1 Thermodynamic quantities for formation of alkaline earth monouranates(VI) at 298.15 K

Reaction	$\Delta H^{\circ a)}$ kcal mol^{-1}	$\Delta S^{\circ b)}$ cal $K^{-1}mol^{-1}$	ΔG° kcal mol^{-1}
Reaction(1)			
$CaCO_3 + UO_{8/3} + \frac{1}{6}O_2 = CaUO_4 + CO_2$	0.73	34.04	−9.42
$SrCO_3 + UO_{8/3} + \frac{1}{6}O_2 = \beta\text{-}SrUO_4 + CO_2$	3.30	34.21	−6.90
$BaCO_3 + UO_{8/3} + \frac{1}{6}O_2 = BaUO_4 + CO_2$	6.26	36.39	−4.59
Reaction(2)			
$CaO + UO_{8/3} + \frac{1}{6}O_2 = CaUO_4$	−42.02	−5.67	−40.33
$SrO + UO_{8/3} + \frac{1}{6}O_2 = \beta\text{-}SrUO_4$	−52.70	−6.67	−50.71
$BaO + UO_{8/3} + \frac{1}{6}O_2 = BaUO_4$	−58.09	−6.17	−56.25
$CaO + \gamma\text{-}UO_3 = CaUO_4$	−34.32	2.21	−34.98
$SrO + \gamma\text{-}UO_3 = \beta\text{-}SrUO_4$	−45.00	1.06	−45.32
$BaO + \gamma\text{-}UO_3 = BaUO_4$	−50.39	1.72	−50.90

a) ΔH_f^0 for $CaUO_4$[118], $BaUO_4$[118], U_3O_8[125] and γ-UO_3[126] are −478.4, −475.2, −284.8 and −292.5 kcal mol^{-1}, respectively. ΔH_f^0 for β-$SrUO_4$, −479 kcal mol^{-1}, was estimated from ΔH_f^0 of molybdates(VI) and tungstates(VI) of Ca, Sr and Ba [124, 127], which have the same chemical formula (MXO_4; M = Ca, Sr, Ba, X = Mo or W) with alkaline earth uranates taking the difference of ΔH_f^0 in the sequence normalized by the ΔH_f^0 values. ΔH_f^0 for β-$SrUO_4$ measured by Cordfunke and Loopstra [29] and assessed by Cordfunke and O'Hare [130] are about 10 and 4 kcal larger than the value estimated here, respectively. Other ΔH_f^0 were taken from Refs. [124, 127].

b) S^0 for $CaUO_4$[118], $BaUO_4$[118], U_3O_8[128] and γ-UO_3[128] are 34.5, 41.7, 22.51 and 22.97 cal $K^{-1}mol^{-1}$, respectively. S^0 for β-$SrUO_4$, 37 cal $K^{-1}mol^{-1}$, was estimated using S^0 for molybdates(VI) and tungstates(VI) of Ca, Sr and Ba. Other S^0 were taken from Refs. [124, 127].

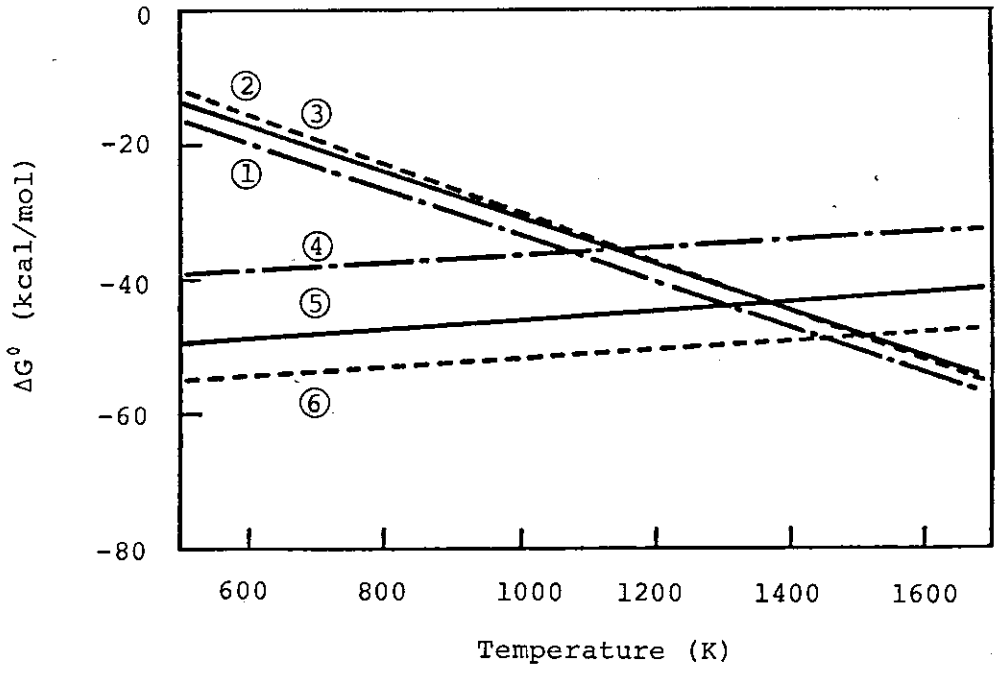

Fig. 3-4 Standard Gibbs free energies of the reactions:
(1), (2), (3) for $MCO_3 + \frac{1}{3}U_3O_8 + \frac{1}{6}O_2 = MUO_4 + CO_2$,
(4), (5), (6) for $MO + \frac{1}{3}U_3O_8 + \frac{1}{6}O_2 = MUO_4$, where M is Ca, Sr and Ba.

From the results of **Figs. 3-1**, **3-2** and **3-3**, it is seen that the reactions between MCO_3 and U_3O_8 in air occur apparently according to the reaction (3-1). Because the initiation temperature is changed by varying the atmosphere from air to CO_2, and the reactions in vacuum are seen to occur according to the reaction (3-3), the actual reactions of MCO_3 with U_3O_8 in air, however, are considered to proceed by the reaction (3-3). If $BaCO_3$, which is the most stable in alkaline earth metal carbonates, is used, for example, the equilibrium CO_2 pressure over $BaCO_3$ at 680 K is 10^{-7} Pa, which will be not so small as to hinder the reaction of BaO with U_3O_8. Therefore, it may be considered that one of reasons why the reactivity is varied by a sort of the carbonates comes from the difference of the Gibbs energy of the reaction (3-3).

Nonstoichiometry of alkaline earth monouranates

Among alkaline earth monouranates, the rhombohedral compounds, $CaUO_4$ and α-$SrUO_4$, have wide ranges of nonstoichiometry liberating oxygen at high temperatures even in air. **Figure 3-5** shows the heating curves of the nearly stoichiometric $CaUO_4$ and α-$SrUO_4$ of which the composition were $CaUO_{3.988}$ and $SrUO_{3.991}$. The figure also indicates the equilibrium compositions of these monouranates. The weight loss of $CaUO_4$ occurs above 1070 K. This oxygen liberation process is reversible. The filled circles show the relation between equilibrium compositon and oxygen pressure of $CaUO_4$, which is taken from the data obtained by Anderson and Barraclough [58].

The weight loss of α-$SrUO_4$ due to the release of oxygen occurs above 770 K. The weight loss continues to about 1050 K at which the minimum oxygen content is observed. The compound is still in the α phase, and the above process is reversible: when it is slowly cooled from the temperature of the minimum oxygen content, the oxygen content again increases on the same line with that of the heating process. On the other hand, if the sample is heated

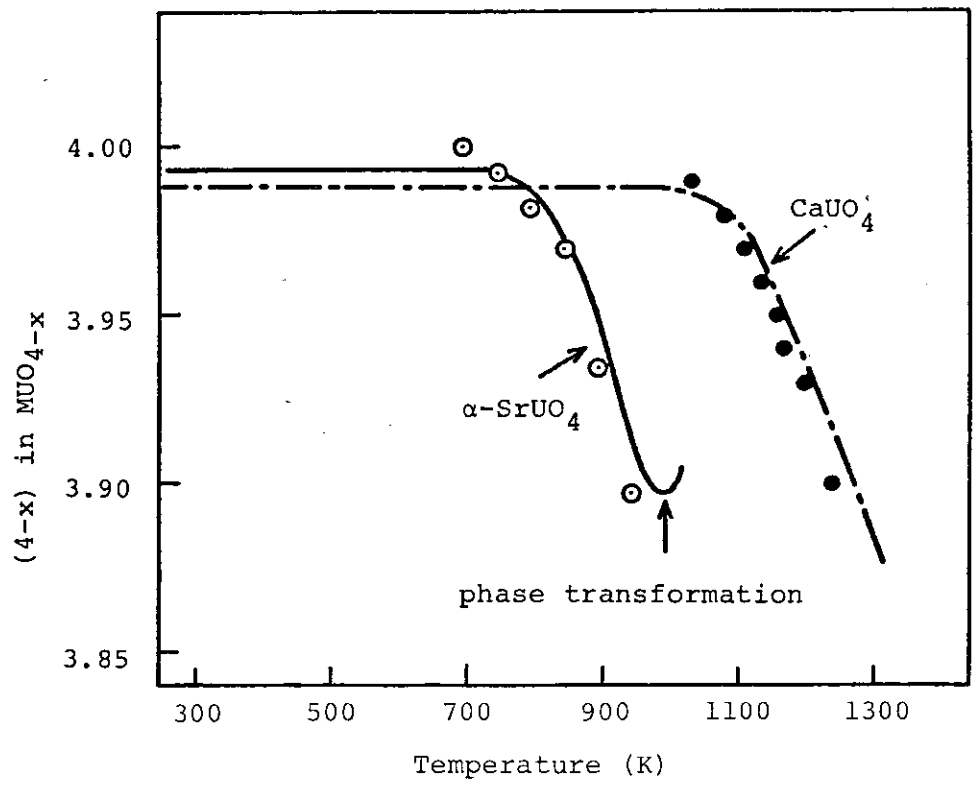

Fig. 3-5 Heating curves of $CaUO_4$ and α-$SrUO_4$ in air at 2 K/min and equilibrium composition of $CaUO_4$ ● (by Anderson and Barraclough [58]) and α-$SrUO_4$ ○. (The curves show that equilibrium is attained with the heating rate of 2 K/min in either case.)

above the temperature of the minimum oxygen content, the α phase transforms irreversibly into the β phase with accompanied oxidation. The transformation is finished at 1173 K in air and the composition of the β phase is $SrUO_{3.997}$. This transformation is not found in $CaUO_4$.

On the other hand, the orthorhombic monouranates, β-$SrUO_4$ and $BaUO_4$, show no detectable weight loss up to 1373 K when heated in air, and remain very nearly stoichiometric.

The crystal structure of orthorhombic $BaUO_4$ was determined by Samson and Sillén [40] and by Loopstra and Rietveld [37], and a refinement of the structure was made by Reis et al. [117] using a single crystal. In this structure there are infinite $\{(UO_2)O_2\}^{2-}$ layers, the oxygen atoms forming distorted octahedral array. The interatomic distances $U-O_I$ in β-$SrUO_4$ and $BaUO_4$ are 1.886 [37] and 1.872 Å [117], respectively. Infrared absorption spectra of both compounds show the stretching vibration of the uranyl bonds.

The structures of $CaUO_4$ and of the isostructural α-$SrUO_4$ are quite different from that of $BaUO_4$. According to Zachariasen [36], the rhombohedral $CaUO_4$-type structure may be considered as a slightly deformed fluorite structure. Each uranium is surrounded by eight oxygen atoms. The $U-O_I$ distances of $CaUO_4$ [37] and α-$SrUO_4$ [38] are 1.963 and 2.07 Å, respectively. As already reported elsewhere [38], the infrared absorption spectra showed that the absorption occurred at 620-650 cm^{-1} markedly shifted to longer wave side from the position of the absorption of the usual antisymmetric stretching vibration of the uranyl bond. A characteristic of uranates which are stable in air at high temperatures may be in the uranyl group, an indication of covalency, in their structures. When alkaline earth monouranates are examined from this point, the rhombohedral compounds are distinctly different from the orthorhombic compounds. The latter uranates are more stable than the former uranates.

Reduction of alkaline earth monouranates with hydrogen

Thermogravimetric curves of alkaline earth monouranates heated in hydrogen atmosphere are shown in **Fig. 3-6**. The reduction of $CaUO_4$ began at 550 K. The $CaUO_4$ was reduced first to $CaUO_{3.55}$ at 823 K, then stepwise to $CaUO_{3.50}$ above 1000 K. The reduction scheme was in agreement with the literature [7], though the composition of the first step at 823 K, $CaUO_{3.55}$, was different from the reported value, $CaUO_{3.66}$.

The weight loss of α-$SrUO_4$ by hydrogen reduction began at 500 K, and it proceeded continuously to $SrUO_{3.48}$. The reduction of α-$SrUO_4$ occurred at a slightly lower temperature than that of $CaUO_4$. This corresponds to the fact that when heated in air, the oxygen liberation from α-$SrUO_4$ takes place at a lower temperature than from $CaUO_4$, as shown in **Fig. 3-5**. The weight loss of β-$SrUO_4$ began at 650 K, which was about 150 K higher than the initiation temperature for α-$SrUO_4$. Both TG curves of α and β-$SrUO_4$, however, overlapped at the composition near $SrUO_{3.55}$. The difference of the reactivity by hydrogen reduction can be explained if it is considered that the weight loss of α-$SrUO_4$ occurs without the structure change, while the reduction of β-$SrUO_4$ needs the change of the orthorhombic structure to the rhombohedral structure. By reduction, the β-$SrUO_4$ phase, which is almost stoichiometric, changes into α-$SrUO_{4-x}$.

The reduction of $BaUO_4$ occurred at a higher temperature than that of β-$SrUO_4$. The monouranate becomes the composition of $BaUO_{3.50}$. The compound $BaUO_4$ changed into $Ba_2U_2O_7$ of which the structure was assigned to be pseudotetragonal [122] or monoclinic [26].

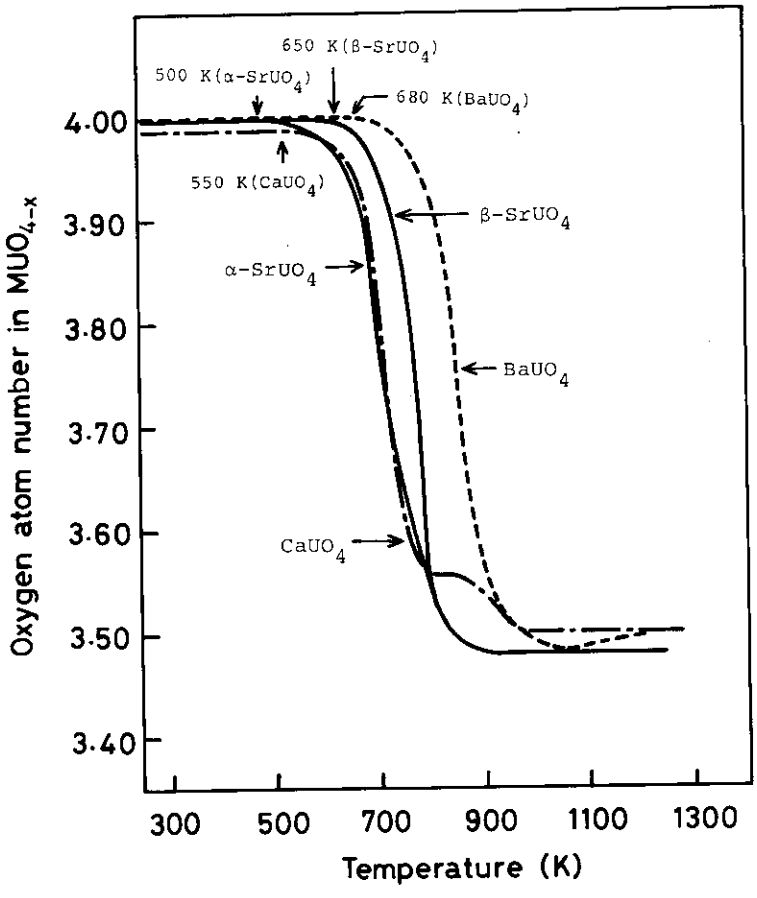

Fig. 3-6 TG curves for reduction of alkaline earth monouranates in 1 atm hydrogen: heating rate 2 K/min.

From the facts described above, the reactivity of alkaline earth monouranates with hydrogen is shown to decrease in the following order:

α-$SrUO_4$ > $CaUO_4$ > β-$SrUO_4$ > $BaUO_4$.

Although the thermodynamic functions of the reduced monouranates, $MUO_{3.5}$ (M = Ca, Sr, Ba) or $Ba_2U_2O_7$, are not known, if changes in Gibbs energy for the reduction of MUO_4 to $MUO_{3.5}$ are comparable, Gibbs energies of formation for the monouranates, $\Delta G_f^\circ(MUO_4)$, might be used instead of those for $MUO_{3.5}$. As given in **Table 3-1**, ΔG_f° of MUO_4 according to the reaction

$MO + \gamma\text{-}UO_3 = MUO_4$

increases negatively with the increase of atomic number. This is in agreement with the order of the initiation temperatures of hydrogen reduction.

The oxygen deficient alkaline earth monouranates, MUO_{4-x}, which were formed by the hydrogen reduction of the nearly stoichiometric monouranates, gradually took up oxygen into the crystal lattice even at room temperature when exposed to air: $CaUO_{3.50}$ to $CaUO_{3.69}$, $SrUO_{3.48}$ to $SrUO_{3.69}$ and $BaUO_{3.50}$ to $BaUO_{3.65}$.

4. The crystal structres of $CdUO_4$

4.1 Introduction

Cadmium monouranate(VI), $CaUO_4$, has been reported to have a polymorphism, i.e., α, β and γ phses, similar to strontium monouranate which has been described in section 1.2. According to Ippolitova et al. [131], the low temperature phase, α-$CaUO_4$, is formed by the reaction of cadmium oxide CdO and triuranium octoxide U_3O_8 with Cd to U atomic ratio of unity in air at 843 K, and this α phase transforms into β-$CdUO_4$ at 993 K, and the β phase decomposes into oxygen-deficient γ-$CdUO_{4-x}$ above 1198 K.

Ippolitove et al. also determined the lattice parameters of these cadmium monouranates by X-ray diffraction analysis. α-$CdUO_4$ is hexagonal, isomorphous with $CaUO_4$, and the lattice parameters are $a = 3.865 \pm 0.003$ and $c = 17.44 \pm 0.02$ Å. β-$CdUO_4$ is face centered orthorhombic with lattice parameters $a = 7.024 \pm 0.002$, $b = 6.850 \pm 0.003$ and $c = 3.526 \pm 0.005$ Å. γ-$CdUO_{4-x}$ has an oxygen-deficient structure of $CaUO_4$-type, of which lattice parameters are $a = 3.904 \pm 0.003$ and $c = 17.52 \pm 0.02$ Å in hexagonal indexing.

The crystal structure of the nonstoichiometric $CdUO_{4-x}$ has been determined by Reshetov and Kovba [132] by means of X-ray powder diffractometry. They used the sample having the composition of $CaUO_{3.63}$ and showed that it could be indexed also in a rhombohedral system with the space group $R\bar{3}m$ and that the oxygen parameters in $R\bar{3}m$ were given as $u = 0.110$ and $v = 0.335$.

The crystal structure of β-$CdUO_4$ has been studied by Kovba et al. [133] by X-ray diffraction using powder sample and single crystal. Their final proposed structure was a primitive orthorhombic structure with space group Pbam: The atomic positions were 2U in (a), 2Cd in (d), $4O_I$ in (g) with $x = 0.05$ and $y = 0.275$, and $4O_{II}$ in (h) with $x = -0.175$ and $y = 0.08$. However, the systematic absence of general (hkl) reflections was in conflict with the extinction rule for Pbam.

We have investigated the phase transformation of strontium monouranate from α to β where an anomalous oxygen nonstoichiometry change was observed around the transformation temperature [71, 121]. Since similar compositional anomaly has been recently observed also in the phase transformation of cadmium monouranate from α to β phse [134], comparison of the detailed structure of α and β-$CdUO_4$ to those of α and β-$SrUO_4$ would be meaningful.

In the present work, the crystal structures of α and β-$CdUO_4$ were determined by means of X-ray powder diffraction method in order to have an insight into the phase transformation of $CdUO_4$ from structural point of view.

4.2 Experimental

Samples

α-$CdUO_4$ was prepared by heating an intimate mixture of CdO and $UO_3 \cdot 2H_2O$ with Cd to U atomic ratio of unity at 793 K in air for 40 h. The product was orange-red and the composition was obtained to be $CdUO_{3.988}$ by thermogravimetric analysis. β-$CdUO_4$ was prepared by heating the mixture of CdO and U_3O_8 with $Cd/U = 1$ in air at 1123 K for 10 h. The yellow product had the composition of $CdUO_{3.983}$.

The X-ray diffraction study on these samples was performed with a Rigaku-Denki

Geigerflex 2182D1 type diffractometer using copper Kα radiation monochromatized with curved pyrolytic graphite placed in front of the NaI (Tl) scintillation detector. The integrated intensities of 42 and 47 reflections, in the range of 10 deg$\leq 2\theta \leq$ 120 deg, were recorded for α and β-$CdUO_4$, respectively. To eliminate systematic errors in obtained diffraction angles, the observed data were corrected with those of rhombohedral α-$SrUO_4$ as standard [38]. Lattice parameters were calculated by the least-squares method on a FACOM 230-75 computer for the diffraction angles in the range of 80 deg$\leq 2\theta \leq$ 120 deg.

The crystal data are tabulated in **Table 4-1** together with those by Ippolitove et al. [131], and Reshetov and Kovba [132]. In the table, lattice parameters of α-$SrUO_4$ [38] and β-$SrUO_4$ [65] are also given for comparison. The observed and calculated $Q(=1/d^2)$ for α-$CdUO_4$ are given in the second and the third columns of **Table 4-2**, respectively. The Q values for β-$CdUO_4$ are shown in **Table 4-3**.

Table 4-1 Crystal data

	α-$CdUO_4$			α-$SrUO_4$
	Ippolitova et al.[131]	Reshetov and Kovba [132]	Present work	Fujino et al.[38]
Composition	–	$CdUO_{3.63}$	$CdUO_{3.988}$	$SrUO_{3.948}$
a(hex) (Å)	3.865(3)	3.904(4)	3.864(3)	3.9207(10)
c(hex) (Å)	17.44(2)	17.54(1)	17.46(1)	18.443(5)
c/a (hex)	4.51(2)	4.49(1)	4.52(1)	4.704(2)
a(rhomb) (Å)	6.227(6)	6.266(3)	6.233(3)	6.551(3)
α(rhomb) (deg)	36.16(6)	36.30(3)	36.12(5)	34.82(2)
d(calc) (g/cm^3)	9.21	8.79	9.13	7.89

	β-$CdUO_4$		β-$SrUO_4$
	Ippolitova et al.[131]	Present work	Sawyer [65]
Composition	–	$CdUO_{3.983}$	$SrUO_{4.000}$
a (Å)	7.024(2)	7.023(4)	5.493
b (Å)	6.850(3)	6.849(3)	7.983
c (Å)	3.526(5)	3.514(2)	8.128
d(calc) (g/cm^3)	8.19	8.13	7.26

Table 4-2 Observed and calculated Q values and intensities for α-$CdUO_4$[a)]

hkl	Q_{obs}	Q_{calc}	I_{obs}	I_{calc}	hkl	Q_{obs}	Q_{calc}	I_{obs}	I_{calc}
111	0.0299	0.0295	12.05	11.16	442	0.6854	0.6852	3.55	2.95
100	0.0930	0.0296	9.58	7.66	320	0.7075	0.7070	0.695	0.633
110	0.1029	0.1024	60.89	64.18	554	0.7330	0.7322	3.22	2.78
222	0.1188	0.1181	20.80	20.09	555	0.7406	0.7381	5.21	5.32
211	0.1423	0.1418	27.86	27.00	543		0.7402		
221	0.1720	0.1713	2.31	1.51	533	0.7538	0.7541	0.634	0.531
322	0.2506	0.2500	1.52	1.21	421	0.7864	0.7858	0.720	0.625
333	0.2554	0.2657	0.959	1.29	$21\bar{1}$	0.8033	0.8036	2.97	3.19
$10\bar{1}$	0.2684	0.2679	21.42	23.48	$22\bar{1}$	0.8349	0.8331	6.50	6.29
210	0.2999	0.2974	21.04	20.61	300		0.8331		
332		0.2992			431		0.8350		
$11\bar{1}$	0.3616	0.3604	2.08	1.27	553	0.9213	0.9115	4.15	4.45
200	0.3706	0.3703	9.46	9.11	330		0.9217		
321	0.3865	0.3860	18.61	18.60	411		0.9217		
220	0.4101	0.4096	6.52	5.59	655	0.9299	0.9290	3.02	1.90
433	0.4180	0.4173	8.30	7.15	532	0.9528	0.9531	4.19	3.75
311	0.4396	0.4392	0.789	0.547	644	0.9999	1.0001	2.59	2.49
444	0.4731	0.4724	2.00	1.90	654		1.0059		
443	0.4870	0.4862	1.01	0.992	542	1.0218	1.0219	0.847	0.837
331	0.5189	0.5179	0.437	0.501	665	1.0383	1.0373	0.488	0.578
432	0.5339	0.5336	1.68	2.38	666	1.0633	1.0628	0.913	0.659
422	0.5674	0.5671	4.87	5.17	441	1.0707	1.0693	1.82	3.42
$20\bar{1}$	0.6289	0.6283	1.09	1.13	522		1.0693		
$21\bar{1}$	0.6382	0.6381	6.41	6.84	$20\bar{2}$		1.0715		
544	0.6475	0.6437	0.625	0.208	$31\bar{1}$	1.1000	1.1010	0.564	0.782
310	0.6776	0.6775	4.63	4.75					

a) I_{obs} are integrated observed intensities in arbitrary unit. $Q = 1/d^2$ are in $\mathring{A}^{-2}$.

Table 4-3 Observed and calculated Q values and intensities for β-$CdUO_4$[a)]

hkl	Q_{obs}	Q_{calc}	I_{obs}	I_{calc}
110	0.0420	0.0416	6.56	6.83
011	0.0815	0.0810	19.95	17.58
200		0.0811		
020	0.0857	0.0853	12.51	13.54
111	0.1229	0.1226	27.14	27.95
201	0.1626	0.1621	2.87	2.39
021	0.1670	0.1662	7.97	8.10
220		0.1664		
310	0.2046	0.2038	0.393	0.300
130	0.2128	0.2121	1.16	1.34
221	0.2480	0.2473	0.695	0.849
311	0.2855	0.2848	12.17	11.36
131	0.2938	0.2931	9.05	9.30
002	0.3243	0.3239	5.26	4.88
400		0.3244		
040	0.3417	0.3411	2.15	2.44
112	0.3659	0.3655	0.781	0.838
202		0.4050	8.33	8.37
401		0.4054		
022		0.4092		
420		0.4097		
		0.4053		
		0.4095		

Table 4-3 continued

hkl	Q_{obs}	Q_{calc}	I_{obs}	I_{calc}
041, 240	0.4228	0.4220, 0.4222	2.72	2.96
331	0.4559	0.4553	5.33	5.64
222, 421	0.4906	0.4903, 0.4907	3.28	3.58
241	0.5037	0.5031	0.703	0.705
312, 510	0.5278	0.5277, 0.5282	0.532	0.453
132	0.5364	0.5360	0.563	0.612
511	0.6098	0.6092	2.79	2.58
151	0.6347	0.6342	2.13	2.12
402	0.6486	0.6483	1.53	1.31
042, 440	0.6653	0.6650, 0.6655	2.74	2.72
332, 530	0.6986	0.6982, 0.6987	0.437	0.431
003, 600, 422	0.7310, 0.7340	0.7288, 0.7299, 0.7336	2.75	2.39
242, 441	0.7464	0.7461, 0.7467	2.20	2.55
060, 113	0.7702	0.7674, 0.7704	2.34	2.28
531	0.7803	0.7797	1.75	1.97
351	0.7967	0.7964	1.74	1.91
203, 601, 023, 620	0.8159	0.8099, 0.8109, 0.8140, 0.8152	1.38	1.28
061, 260, 512	0.8489	0.8484, 0.8485, 0.8521	0.921	1.08
261, 313	0.9323	0.9295, 0.9326	1.89	1.96
133	0.9406	0.9409	1.65	1.56
442	0.9895	0.9894	1.32	1.53
403, 602	1.0540	1.0532, 1.0538	1.08	1.10
170, 043, 640	1.0707	1.0648, 1.0698, 1.0710	1.07	1.17
062, 460, 711, 333	1.0916, 1.0963, 1.1028	1.0913, 1.0918, 1.0958, 1.1031	4.67	4.48
551	1.1212	1.1208	1.31	1.29
423, 622	1.1392	1.1384, 1.1391	1.65	1.69
171, 243, 641	1.1459	1.1458, 1.1509, 1.1520	2.30	2.08
262, 461	1.1724	1.1724, 1.1728	1.47	1.58

a) I_{obs} are integrated observed intensities in arbitrary unit.
$Q = 1/d^2$ are in $\mathring{A}^{-2}$.

4.3 Structure analysis

4.3.1 Structure of α-$CdUO_4$

All reflections of the combination of (hkl) were observed for rhombohedral α-$SrUO_4$ in the whole 2θ range of the experiments of which the diffraction pattern was closely related to that of the α-$SrUO_4$ [38]. Thus, we made the structure analysis on the basis of space group $R\bar{3}m$. The atomic positions were 1U in (000), 1Cd in (1/2 1/2 1/2), $2O_I$ in ±(uuu) and $2O_{II}$ in ±(vvv). To determine two unknown oxygen parameters, u and v, the peaks in two scans of different gains were recorded. One was for larger peaks and the other for smaller ones. The whole integrated intensities were collected by adjusting the former peak areas to the latter by means of several common peaks with middle height.

In order to know the initial value of the oxygen parameters, a difference Fourier synthesis was made along the body-diagonal axis using the equation

$$\rho(x) = \Sigma A_m \cos(2\pi m x)$$

where the sum was taken for $m = h + k + 1$ and x was the distance along the axis. The factor A_m is expressed as

$$A_m = c|F_{obs}| - |f_U + f_{Cd}\cos(\pi m)|$$

where c is the adjustable parameter expressed as

$$c = \Sigma|F_{calc}|/\Sigma|F_{obs}|$$

Atomic scattering factors for U^{6+} were those from International Tables for X-ray Crystallography [135], and the factors for Cd^{2+} were obtained from Cromer and Waber [136]. These were used with anomalous dispersion corrections [137]. The electron-density curve for oxygen with $0 \leq m \leq 18$ is shown in **Fig. 4-1**. The first maximum seen at $x = 0.114$ is assigned to O_I and the second one at $x = 0.356$ to O_{II}. Refinement was carried out by minimizing the reliability index R, which is expressed as

$$R = \Sigma w|I_{obs} - I_{calc}|/\Sigma w I_{obs},$$

as a function of the oxygen parameters and temperature factors for cadmium and uranium. The weight, w, was regarded as

$$w = (I_{obs})^{-1} \text{ for } I_{obs} \geq 10 \cdot I_{obs(min)}$$

and

$$w = 1 \text{ for } I_{obs} < 10 \cdot I_{obs(min)}.$$

Atomic scattering factors for O^{2-} were those from Tokonami [138], and as the initial u and v values for successive approximations of the least-squares calculations, those by the $\rho(x)$ synthesis were used. At first, the temperature effect was not taken into account. In this case, the minimum R was 0.102 at $u = 0.110$ and $v = 0.352$. However, if isotropic temperature factors for U^{6+} and Cd^{2+} were taken as the variables, the minimum R was reduced to 0.080 at $u = 0.113$ and $v = 0.350$; $B_U = 0.248$ and $B_{Cd} = 0.639$.

The integrated observed intensities, I_{obs}, and the calculated intensities, I_{calc}, at this minimum are shown in the fourth and the fifth columns of **Table 4-2**, respectively. In **Table 4-4**, the computed values of the oxygen prameters and isotropic temperature factors are tabulated together with the R value and the interatomic distances.

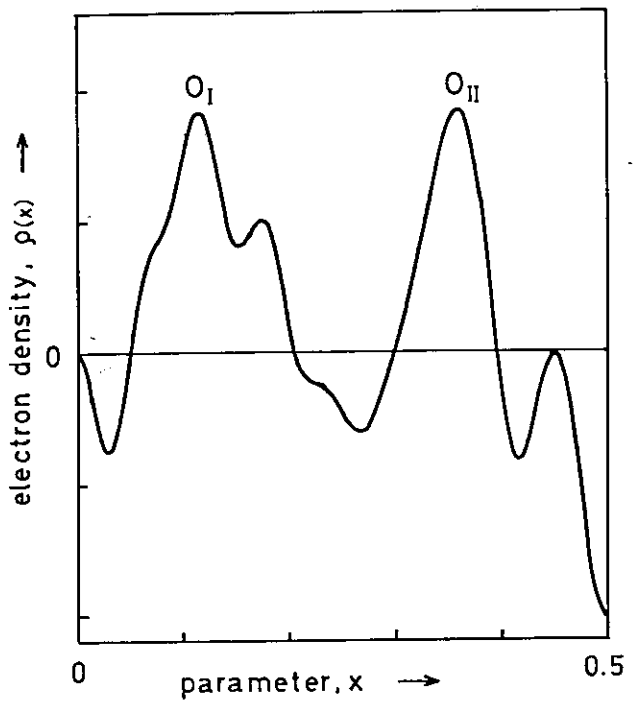

Fig. 4-1 The electron-density distribution along the body-diagonal axis due to oxygen atoms.

Table 4-4 Oxygen parameters, R factors, temperature factors and interatomic distances

	$CdUO_4$		$SrUO_4$	
	α	β	α	β
Composition	$CdUO_{3.988}$	$CdUO_{3.983}$	$SrUO_{3.948}$	$SrUO_{4.000}$
Space group	$R\bar{3}m$	Cmmm	$R\bar{3}m$	Pbcm
O_I	u = 0.113	y = 0.2778	u = 0.112	(a)
O_{II}	v = 0.350	x = 0.159	v = 0.357	
R factor	0.080	0.066	0.097	0.093
B_U (Å^2)	0.248	0.051	–	–
B_{Cd}	0.639	0.227	–	–
U-O_I (Å)	1.98	1.91	2.07	1.86
U-O_{II}	2.25	2.08	2.30	2.15
U-O_{III}	–	–	–	2.15
M-O_I	2.42	2.32	2.64	2.59, 2.83
M-O_{II}	2.61	2.40	2.48	2.75
M-O_{III}	–	–	–	2.61
O_I-O_I	2.91	3.04	3.03	
O_I-O_{II}	2.79	2.82	2.79	
O_{II}-O_{II}	2.31	2.23	2.42	

a) O_I : x = 0.697, y = 0.423, z = 0.068
O_{II} : x = 0.146, y = 0.250, z = 0.000
O_{III} : x = 0.880, y = 0.030, z = 0.250

4.3.2 Structure of β-$CdUO_4$

The observed peaks all satisfied the condition $h+k=2n$, which strongly suggests the C centered lattice. However, we first reexamined the space group Pbam of Kovba et al. [133], because it was thought that there might be the case that the intensities of diffraction peaks other than $h+k=2n$ were accidentally too weak to be observed. The minimization of the R index was carried out by setting the atomic position according to Kovba et al. [133], but the iterated computation of successive approximation did not converge. Moreover, I_{calc} obtained by using the oxygen parameters of Kovba et al. [133] showed that (211) and (120) reflections which were $h+k\neq 2n$ should be strong enough to be observed. From these results, the possibility of Pbam was ruled out.

Because of the limitation of the powder diffraction technique, we could not try two-dimensional Fourier synthesis. Then, the problem that has to be solved in this case, is to find out the atomic arrangement that conforms with C centered orthorhombic symmetry, under the guidance of the R index. The smallest R value was obtained for Cmmm with the atomic positions as follows:

2U in (000) and (1/2 1/2 0),

2Cd in (1/2 0 1/2) and (0 1/2 1/2),

$4O_I$ in (0 ±y 0) and (1/2 1/2±y 0),

$4O_{II}$ in (±x 0 1/2) and (1/2±x 0 1/2).

The space group Cmmm is the one that Kovba et al. [133] have reported as the possible alternative of the β-$CdUO_4$ structure. The oxygen parameters, x and y, and the isotropic temperature factors, B_U and B_{Cd}, were determined by minimizing the R index by the least squares calculations in a was similar with that for α-$CdUO_4$. The obtained minimum R value was 0.066 with the correction of the temperature effect.

The integrated observed intensities, I_{obs}, and the calculated intensities, I_{calc}, at the minimum R are indicated in the fourth and the fifth columns of **Table 4-3**, respectively. The computed values of the oxygen parameters and the isotropic temperature factors are shown in **Table 4-4** together with the R value and the interatomic distances. In the table, data for α and β-$SrUO_4$ reported by Fujino et al. [38] and by Sawyer [65], respectively, are also listed for comparison.

4.4 Discussion of the structure

The present lattice parameters on α-$CdUO_{3.988}$ are well in accord with those by Ippolitova et al. [131]. However, the present lattice parameter values a and c in hexagonal indexing are remarkably smaller than those by Reshetov and Kovba [132] on α-$CdUO_{3.63}$. The difference can be considered as caused from oxygen nonstoichiometry of the compound. The lattice parameters of α-$CdUO_{4-x}$ will be expressed as:

$$a = 3.863 + 0.1117\,x \ (\text{Å}),$$

and

$$c = 17.46 + 0.2235\,x \ (\text{Å})$$

provided that the dependence of lattice parameters on nonstoichiometry is linear.

The crystal structure of α-$CdUO_4$ is isomorphous with those of $CaUO_4$ [36, 37] and α and γ-$SrUO_4$ [38], where a uranium atom is surrounded by eight oxygen atoms which form a trigonal antiprism. Two of these oxygen atoms, O_I, which are on the body diagonal axis of the rhombohedral cell or along the c axis of the hexagonal cell one above and the other

below the uranium atom, are located closer to the uranium. Three of remaining six oxygen atoms, O_{II}, are on the plane 0.29 Å above and another three are on the plane 0.29 Å below the uranium atoms. These plance are normal to the body diagonal axis which is an inversion triad. Cadmium atoms are located between hexagonal layers binding them together. The oxygen around the cadmium atom is, however, made up of six O_I atoms and two O_{II} atoms. Arrangements are similar to those around the uranium atom if O_I and O_{II} are interchanged.

In $CaUO_4$ crystal which is typical of this structure, the U–O_I distance is known to be short enough to form so-called uranyl bond. However, the distance for α-$CdUO_4$ by the present data is 1.98 Å which is somewhat longer than the usual uranyl bond length which lies in the range of 1.7 to 1.9 Å. In this situation, infrared spectra were taken by the Nujol method. The data showed that the absorption peak was at 620 cm^{-1} which was shifted to the long wave side from the position of the antisymmetric stretching vibration of the uranyl bond, 700-900 cm^{-1}. From the equation relating the force constant K and the bond length R given by Ohwada [14],

$$K = (181.0/R)^{1/6},$$

the U–O_I distance was found to be 1.96 Å which is in good agreement with the X-ray results.

The isotropic temperature factors are 0.248 and 0.639 for uranium and cadmium atoms, respectively. These values may be compared with those of $CaUO_4$ where the factors are 0.297 for uranium atoms and 0.542 for calcium atoms which have been determined by means of the neutron powder diffraction analysis [37].

The crystal structure of β-$CdUO_4$ is determined to be orthorhombic with space group Cmmm. A three-dimensional view of the atomic arrangements is shown in **Fig. 4-2**. Around each uranium atom, two O_I atoms and four O_{II} atoms are situated forming a distorted octahedron. The four O_{II} atoms occupy a rectangular position on the plane normal to the b axis containing the uranium atom, and the two O_I atoms are located on the line normal to this plane forming the uranyl group. The collinearity of the uranyl group, O_I–U–O_I, is required from the space group symmetry.

The U–O_I bond length of the β-$CdUO_4$ is 1.91 Å. This value agrees well with the values of 1.92 and 1.91 Å for $MgUO_4$ [34] and $CaUO_4$ [36], respectively. The infrared spectra corresponding to the antisymmetric stretching vibration of the uranyl bond at 700 cm^{-1} led to the bond length of 1.88 Å which supports the X-ray value. The U–O_{II} distance by the present investigation is 2.08 Å. Since this distance is usually in the range of 2.2 to 2.3 Å in most monouranates, the U–O_{II} bond seems to be stronger in β-$CdUO_4$.

As is seen in **Fig. 4-2**, the $(UO_2)O_4$ octahedra in β-$CdUO_4$ are chained endlessly along the c axis by sharing edges of the O_{II} atoms. The shared O_{II}-O_{II} edge is 2.23 Å while the unshared O_{II}-O_{II} edge is 3.51 Å. Cadmium atoms are located at the center of the octahedra formed by four O_I atoms and two O_{II} atoms, and bind the uranyl chains together.

The arrangement of the $(UO_2)O_4$ octahedra in this crystal is similar to that of $MgUO_4$ [34] where the space group is Iman. The difference is that in β-$CdUO_4$ the shared O_{II}-O_{II} edge of $(UO_2)O_4$ octahedra is in the plane formed by a and b axes while in $MgUO_4$ it is not. As a result, c/2 of $MgUO_4$ becomes c of β-$CdUO_4$ forming a C centered lattice. The smaller lattice parameters in $MgUO_4$ [34] (a = 6.520, b = 6.595, c = 6.924 Å) may be because of the smaller ionic radius of Mg^{2+} than Cd^{2+}.

It is seen from **Table 4-4** that the interatomic distances between metal and oxygen atoms of β-$CdUO_4$ are shorter than those of α-$CdUO_4$. This fact shows that the metal-oxygen bonds of β-$CdUO_4$ are stronger than those of α-$CdUO_4$, which is in accord with the smaller temperature factors obtained for β-$CdUO_4$: $B_U = 0.051$ and $B_{Cd} = 0.227$.

Here, the results with $CdUO_4$ can be compared with those of $SrUO_4$ in which phase transformation from α to β phase is similar to that of $CdUO_4$ [134]. The crystal structure of α-$CdUO_4$ is isomorphous with that of α-$SrUO_4$, but the U–O_I distances are 1.98 and 2.07 Å for α-$CdUO_4$ and α-$SrUO_4$, respectively. It should be noted that the crystal structure of β-$CdUO_4$ is different from that of β-$SrUO_4$ where the space group is Pbcm [65]. Although the infinite chains of $(UO_2)O_4$ octahedra are parallel to each other along the c axis in β-$CdUO_4$, the distorted octahedra in β-$SrUO_4$ share the corners to form infinite two-dimensional sheets in the plane with the b and c axes. Because the U–O_I distance are 1.91 and 1.85 Å for β-$CdUO_4$ and β-$SrUO_4$ [65], respectively, these values are both regarded as forming the uranyl bond.

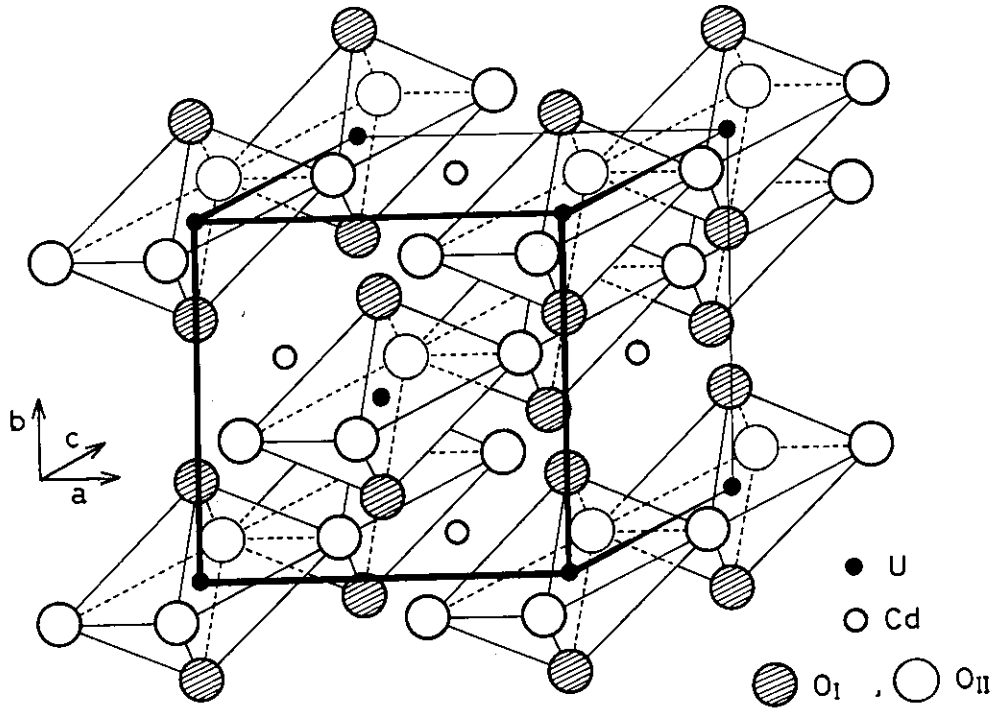

Fig. 4-2 Structure of β-$CdUO_4$.

5. Study on the phase behavior of $Ca_yU_{1-y}O_{2+x}$ solid solution

5.1 Introduction

It is known that some metal oxides are dissolved in UO_2 at high temperatures forming substitutional solid solutions, $M_yU_{1-y}O_{2+x}$, where M is a foreign metal ion. The physical, chemical and/or thermodynamic properties of such solid solutions are usually different considerably from those of UO_2. The knowledge of these solid solutions is, therefore, of basic importance for clarifying the nonstoichiometric nature of the UO_2 oxide fuel in relation to the irradiation behavior.

In the calcium-uranium-oxygen system, the preparative conditions, thermal stabilities and crystal structures of calcium uranates have been investigated in some detail [6, 7, 9], but little is known for the fluorite type solid solution, $Ca_yU_{1-y}O_{2+x}$ [24, 25, 53]. Moreover, these data seem to be not in good agreement. As for the single phase region of the solid solution, Alberman et al. [53] have reported it to be $0 \leq y \leq 0.47$ at 2353 K and $0 \leq y \leq 0.2$ at 1873 K, whereas according to Brisi et al. [24], the region is $0 \leq y \leq 0.33$ at 1573 K. The lattice parameter change of the solid solution with y, da/dy, does not coincide in these reports. The values of da/dy are 0.115, 0.283 and 0.33 Å for the specimens prepared at about 2200 K [25, 53], 1273 K [25] and 1573 K [24], respectively. Although no data about oxygen nonstoichiometry have been given in these reports, the properties above would be affected not only by calcium content but also by the oxygen nonstoichiometry of the solid solution.

In the present work, the phase behavior of $Ca_yU_{1-y}O_{2+x}$ solid solution was studied in the temperature range between 1473 and 1673 K for the samples heated in a stream of helium of which oxygen partial pressure was 8 Pa. By means of X-ray diffractometry and chemical analysis, the relation between lattice parameter and composition of the fluorite solid solution was determined together with the phase behavior. The oxidation state of uranium was discussed using a simple ionic model. Using these results, the partial molar enthalpy of oxygen for the solid solution was estimated.

5.2 Experimental

Samples were prepared from triuranium octoxide U_3O_8, uranium dioxide UO_2 and calcium monouranate $CaUO_4$. U_3O_8 was prepared by heating high purity uranium metal [88] in air at 973 K for one day [89]. UO_2 was prepared by reducing the U_3O_8 in a stream of purified hydrogen at 1273 K for 10 h. $CaUO_4$ was prepared by heating an intimate mixutre of precipitated $CaCO_3$ (reagent grade, provided from Wako Pure Chemical Co. Ltd.) and U_3O_8 with the Ca/U atom ratio of unity in air at 1273 K. Mixing and heating process was repeated three times until obtaining a homogeneous product. The temperature at the final heating was 973 K in order to have nearly stoichiometric $CaUO_4$ as described in Chapter 3. The X-ray powder diffraction pattern of the product agreed well with the literature [37].

All reactions forming the solid solutions were performed in the form of pellets. The weighed amounts of UO_2, U_3O_8 and $CaUO_4$ were intimately mixed in an agate mortar and compacted at 2000 kg/cm^2 into cylindrical pellets of 7 mm in diameter and of about 2 mm in

thickness. The over all composition of these pellets was $Ca_yU_{1-y}O_{2.10}$. The weight of each pellet was about 700 mg. Nine or ten pellets with various Ca/(Ca + U) (= y) ratios were placed together on a platinum plate in an alumina boat, and were heated in an SiC resistance tube furnace. Heating conditions are summarized in **Table 5-1**. The oxygen partial pressure in a stream of helium was checked by the change of electrical resistance of $Co_{1-x}O$. The method has been described elsewhere [140]. After the reaction, the specimens were cooled in the furnace. The cooling rate just after stopping the power supply was about 100 K/min.

Debye-Scherrer patterns of powdered specimens in vacuum sealed capillaries were taken with a Norelco 114.6 mm camera using the nickel-filtered copper Kα radiation. Lattice parameter of the cubic solid solutions was determined by the least squares calculation for eight diffraction peaks higher than 90 degrees (2θ). For the specimens showing broad peaks, patterns were also taken with a Philips PW-1390 diffractometer using copper Kα radiation monochromatized with curved pyrolytic graphite. The slit system used was 1/2 deg-0.1 mm-1/2 deg.

Chemical analysis was carried out to determine x and y in $Ca_yU_{1-y}O_{2+x}$ using cerium(IV)-iron(II) back titration method described in section 2.2. After the y value was ascertained to be unchanged by heating, only x value was determined by the titration. The error in x is estimated to be less than ±0.003.

Table 5-1 Experimental conditions taken for sample preparation

Atmosphere	Temperature (K)	Series	Time (h)	$\Delta\bar{G}_{O_2}$ (kJ/mol)
purified helium[a)]	1473	1	80	−115
	1473	2	194	−115
	1473	3	60[b)]	−115
	1573	4	125	−123
	1623	5	90	−127
	1623	6	30[c)]	−131

a) Oxygen partial pressure, 8 Pa.
b) Series 1 products were regrinded, compacted and heated.
c) Series 2 products were regrinded, compacted and heated.

5.3 Results and discussion

The mean valency of uranium and the O/M ratio (=2+x) in the specimens prepared in the present study were calculated assuming the valencies of calcium and oxygen in the specimen to be +2 and −2, respectively. **Figure 5-1** shows the plots of the mean valency of uranium against the calcium contents (= y) for the specimen heated at 1473 and 1673 K. The uranium valency increases with increasing y, but the rate of increase is so small in the range $0 \leq y \leq 0.1$ that the mean valency of uranium in the specimen may be regarded to be nearly constant in this range. The slope of the curves becomes steeper over y = 0.1. Then, they intersect the horizontal line of mean valency 5.0 at y = 0.33. This calcium concentration accords with that of a phase boundary between a face centered cubic (fcc) solid solution single phase and a two-phase mixture of the fcc solid solution and a rhombohedral phase determined from the break in the lattice parameter of the fcc solid solution (**Fig. 5-3**). Therefore, the mean valency of uranium

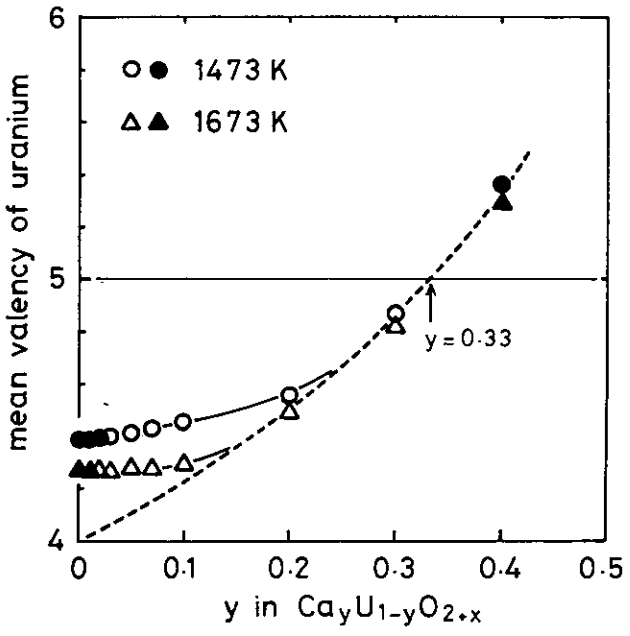

Fig. 5-1 Mean valency of uranium as a function of y in $Ca_yU_{1-y}O_{2+x}$ solid solution: Open marks indicate single phase and filled marks two-phase mixture. Broken line shows the mean valency of uranium calculated theoretically for the case where no change occurs in the O/M ratios of the solid solution by the incorporation of calcium.

in the fcc solid solution is between four and five, which is quite different from the cases of solid solutions of rare earth oxides and uranium oxides where all uranium atoms can be oxidized to U^{6+} state [82, 141-144].

The plots of the O/M ratios as a function of y are shown in **Fig. 5-2**. The O/M ratios decrease linearly with increasing y up to about $y = 0.1$ and then the curves are flattened around the O/M ratio of two.

When Ca^{2+} substitutes for U^{4+} in the UO_2 crystal lattice, the condition of electrical neutrality requires the formation of oxygen vacancy or oxidation of some of U^{4+} atoms to U^{5+} or U^{6+} state. In the present system, these two types of the charge compensation were observed: In the range $0 \leq y \leq 0.1$, because the uranium valency is remained unchanged (**Fig. 5-1**), the O/M ratio decreases with increasing y (**Fig. 5-2**). In the range $\sim 0.2 < y \leq 0.33$, on the other hand, U^{4+} atoms in the solid solution are oxidized to the higher states. **Figure 5-2** shows that there is no significant decrease of O/M ratio in this range. A broken line in **Fig. 5-1** is a theoretical curve for the case where no change occurs in the O/M ratio of the solid solution by the incorporation of calcium. The agreement between the experimental curves and the theoretical one is satisfactory in the range $y > 0.2$.

X-ray diffraction analyses were performed to identify the phases in the products obtained by heating at temperature from 1473 to 1673 K in helium and to determine the lattice parameter by the least squares method. All specimens showed diffraction lines of an fcc structure either in a single phase or in two phase mixture. **Figure 5-3** shows the variation of lattice parameter of the specimens heated at 1473 and 1673 K as a function of calcium contents, y in $Ca_yU_{1-y}O_{2+x}$, together with the literature values [24, 25, 53]. Because the lattice parameters for the specimens heated at 1573 and 1623 K were between those for 1473 and 1673 K, these are not shown in the figure. It can be seen that the lattice parameter becomes larger as the heating temperature is higher, which is caused by the liberation of oxygen from the specimens when heated at higher temperatures.

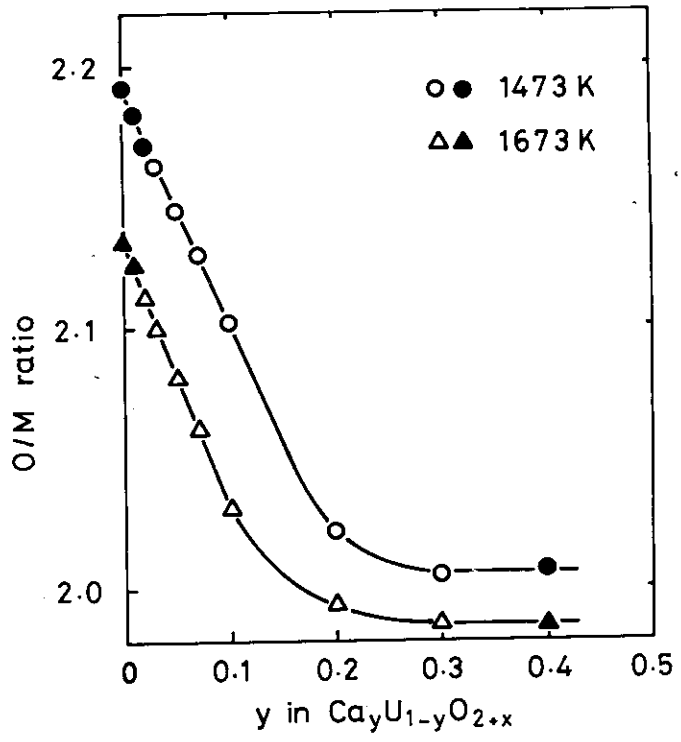

Fig. 5-2 Oxygen to metal atom ratios as a function of y in $Ca_yU_{1-y}O_{2+x}$ solid solution: Open marks indicate single phase and filled marks two-phase mixture.

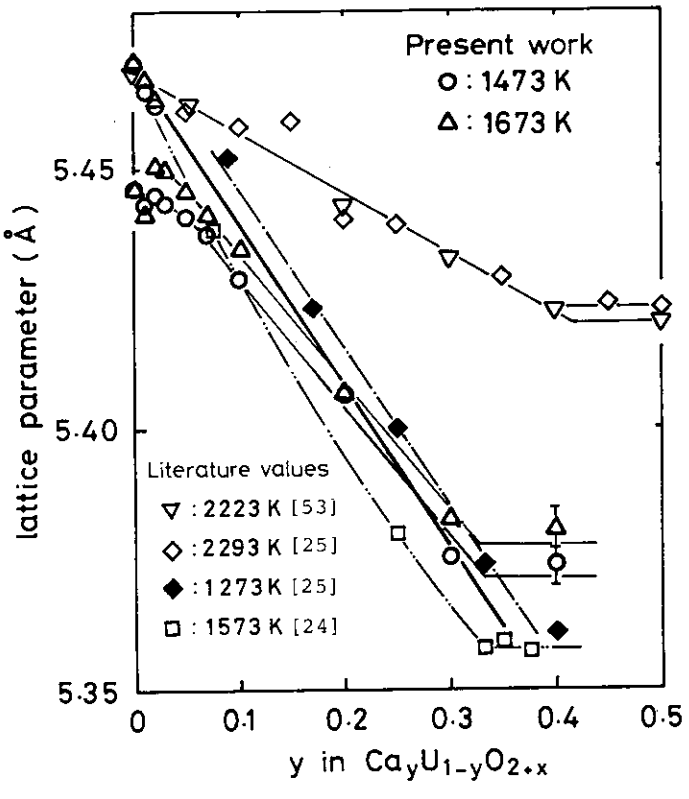

Fig. 5-3 Lattice parameter change of cubic solid solutions: The bold line shows the change of the lattice parameter for stoichiometric $Ca_yU_{1-y}O_{2.00}$.

Results of X-ray diffraction analysis show that the phase behavior of this system could be discussed in three regions.

(1) The first region is $0 \leq y < 0.03$, where two fcc phases exist and the lattice parameter of both the phases seems to decrease with increasing y.

(2) In the range $0.03 \leq y \leq 0.33$, the fcc solid solution exists in a single phase the lattice parameter of which decreases linealy with increasing y.

(3) Above $y = 0.33$, there exists a mixture of the fcc phase and a rhombohedral phase.

The lattice parameters of the rhombohedral phase were found to be $a = 6.273 \pm 0.006$ Å and $\alpha = 35.99 \pm 0.03$ deg. According to the literatures, six compounds having Ca/U atom ratio less than unity have been found. These are $CaU_5O_{15.4}$ [17], $Ca_3U_5O_{16}$ [24], CaU_4O_{13} [29, 145], CaU_2O_7 [29], $Ca_2U_3O_{11}$ [29], and $CaUO_4$ [35-37, 72, 146]. Inspection of the lattice parameters of these compounds revealed that those of $CaUO_4$, $a = 6.267 \pm 0.001$ Å and $\alpha = 36.03 \pm 0.01$ deg [36, 72, 146] are good accordance with the present values. Therefore, the rhombohedral phase is considered to be $CaUO_{4(-x)}$.

According to the phase rule, the lattice parameters of the condensed phases should remain unchanged in ternary oxide systems, if one gas phase and two condensed phases are in equilibrium under the condition of fixed temperature and oxygen partial pressure. The horizontal line shown in **Fig. 5-3** represents the two-phase mixture region. The phase boundary of the fcc single phase is at $y = 0.33$, which well accords with the literature value [24]. As mentioned in **Fig. 5-1**, the valency of uranium in the solid solution is +5 at this y value. This coincidence suggests that the mean valency of uranium of +5 is a major factor which determines the single phase limit of the fcc solid solution. As indicated in **Fig. 5-3**, the samples heated at high temperatures and/or in reducing atmospheres show the extended solubility ranges up to $y = 0.4$ [25] or 0.47 [53]. This fact is, however, not discrepant with the consideration above. Under these heating conditions, the oxygen deficient solid solution would be formed, and the mean valency of uranium would be below +5 until $y = 0.4$ or 0.47 although the authors [25, 53] did not describe about the oxygen nonstoichiometry of these phases. In the study on the solid solution $Pr_yU_{1-y}O_{2+x}$, it has been observed that the solubility limit of $PrO_{1.5}$ into UO_{2+x} increases from $y = 0.667$ to 0.77 by decreasing O/M from 2.00 to 1.80 [144].

In the region $y < 0.03$, two fcc phases with different lattice parameters exist in the products and both the parameters seem to decrease with increasing y. This fact is, at first sight, not very reasonable from the point of the phase rule which predicts that the lattice parameters of both phases should remain unchanged. One possible explanation for the phase behavior in question is a disproportionation of a hyperstoichiometric $Ca_yU_{1-y}O_{2+x1}$ into $Ca_yU_{1-y}O_{2+x2}$ and $Ca_yU_{1-y}O_{2.25-x3}$ during furnace cooling. The phase separation of UO_{2+x1} into UO_{2+x2} and $UO_{2.25-x3}$ has been well known and is, in fact, observed in the present system at $y = 0$. The compositions of both the phases were obtained to be $UO_{2.000 \pm 0.005}$ and $UO_{2.24 \pm 0.01}$ from their lattice parameters, 5.470 ± 0.001 Å and 5.446 ± 0.002 Å, respectively. The phase separation in this system would not express equilibrium states. By analogy to the UO_2-O_2 system, the solid solution would be in a single phase at the heating temperatures of 1473 and 1673 K whereas would be separated afterwards on cooling. In other words, the crystals obtained are those in equilibrium with lower temperature than the heating temperatures. Although there can exist several thermodynamical routes to attain to this state, a postulation that the y values for the separated phases are the same as that for the phase before separation would be reasonable because the rate of cooling was not so low as to allow the inter-diffusion between calcium and uranium to change y value and because the inter-diffusion between these metals is regarded to be much slower than oxygen diffusion. Therefore, the y values of $Ca_yU_{1-y}O_{2+x2}$ and $Ca_yU_{1-y}O_{2.25-x3}$ changes with bulky y value, and the lattice

parameters vary even in the two-phase region according to the change of y in each phase. The bold line in **Figure 5-3** represents the variation of the lattice parameter of $Ca_yU_{1-y}O_{2.00}$ which was calculated by use of eq. (5-1) setting $x=0$. As seen from the figure, the lattice parameters of the phase with smaller oxygen content seem to be on the line. The very small x values in the present ternary system are coincident with those of the separated UO_{2+x} phase in the UO_2-O_2 system. It should be noted that the solid solutions in a single phase can be regarded to be in equilibrium with the respective heating temperatures because they hardly take up oxygen from the gas phase during rather short cooling periods.

In the region $0.03 \leq y \leq 0.33$, the fcc solid solution existed in a single phase. The lattice parameter of the fcc solid solution decreased linearly at rates of −0.255 and −0.262 Å per y unit for the specimens heated at 1673 and 1473 K, respectively. However, the rate of change of lattice parameter with y, da/dy, contains implicitly the effect of oxygen nonstoichiometry (= x). To examine the effect of x, the lattice parameter of the fcc solid solution was plotted against the O/M ratio (= 2 + x) in **Fig. 5-4**, where M is Ca + U. The lattice parameters of the specimens containing the same calcium content are represented by a straight line. Then, by using these parameters and O/M ratios, a calculation by the least squares method was performed to express the change of the lattice parameter as a linear equation of x and y under the condition that the lattice parameter is 5.4704 Å [90] for both x and y being zero. The results is:

$$a = 5.4704 - 0.102x - 0.310y \ (\text{Å}). \qquad (5\text{-}1)$$

This equation shows that the lattice parameter decreases with increasing x and y, while the effect of y is about three times larger than that of x. The observed change rates of the lattice parameter with y, −0.255 and −0.262, are smaller than the coefficient of y. This means that x decreases monotonously with increasing y. The coefficient of x in equation (5-1), −0.102, is well comparable with −0.094, −0.117 and −0.109, for UO_{2+x} [90], $Mg_yU_{1-y}O_{2+x}$ [21] and $Sr_yU_{1-y}O_{2+x}$ [70], respectively. Since the defect structure in these solid solutions are found to be oxygen interstitials from density measurements [50, 147], these coefficients

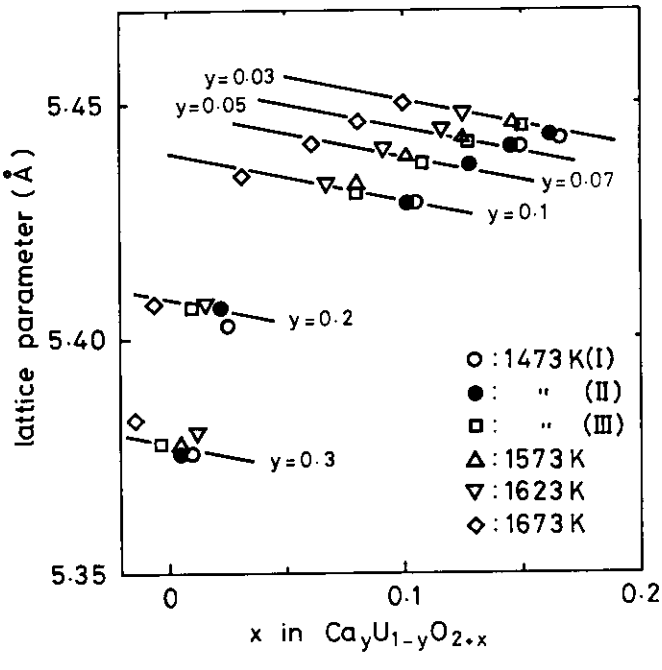

Fig. 5-4 Effect of excess oxygen content (= x) on the lattice parameter of the $Ca_yU_{1-y}O_{2+x}$ solid solution.

of x are considered to express the effect of oxygen interstitials on the lattice parameter. Therefore, the defect type of oxygen in the present solid solution can be considered to be the same as that in UO_{2+x}, i.e., oxygen interstitials.

Using a simple ionic model, Ohmichi et al. [84] explained the rate of change of lattice parameter with y in $RE_yU_{1-y}O_{2+x}$ solid solutions (RE = rare earth elements), and found that the oxidation state of uranium is U^{5+} rather than U^{6+} in the low concentration range of rare earth elements ($y < 0.15$). By applying the model to the present case, the following two equations were derived according to the resultant oxidation states of uranium, U^{5+} and U^{6+}, by the incorporation of Ca^{2+}. In the case of U^{5+}, the chemical form of the solid solution is described as

$$Ca^{2+}{}_yU^{4+}{}_{1-2x-3y}U^{5+}{}_{2x+2y}O^{2-}{}_{2+x}.$$

The lattice parameter is given as

$$a = \frac{4}{\sqrt{3}}[yr_{Ca^{2+}} + (1-2x-3y)r_{U^{4+}} + (2x+2y)r_{U^{5+}} + r_O{}^*].$$

By differentiating the lattice parameter with y,

$$\frac{\partial a}{\partial y} = \frac{4}{\sqrt{3}}(r_{Ca^{2+}} - 3r_{U^{4+}} + 2r_{U^{5+}}). \tag{5-2}$$

In the case of U^{6+}, the chemical form is

$$Ca^{2+}{}_yU^{4+}{}_{1-x-2y}U^{6+}{}_{x+y}O^{2-}{}_{2+x},$$

then

$$\frac{\partial a}{\partial y} = \frac{4}{\sqrt{3}}(r_{Ca^{2+}} - 2r_{U^{4+}} + r_{U^{6+}}). \tag{5-3}$$

In these equations, $r_{Ca^{2+}}$, $r_{U^{4+}}$, $r_{U^{5+}}$ and $r_{U^{6+}}$ are the ionic radii of respective ions for eight-coordination and $r_O{}^*$, which is not a function of y, is an effective radius of oxygen. Calculation of $\partial a/\partial y$ was carried out using the ionic radii given by Shannon [148] for Ca^{2+}, U^{4+} and U^{6+} and the estimated ionic radius of U^{5+} by Ohmichi et al. [84]. The results are -0.277 and -0.046 for the cases of U^{5+} and U^{6+}, respectively. The experimental value, -0.310, is in good accordance with the one for U^{5+}, which indicates that U^{5+} exists in preference to U^{6+} in the present solid solutions.

Equation (5-1) can be used to estimate the x value for the specimens reported earlier [24, 25] where the lattice parameters and Ca/(Ca + U) ratios were given but the x values not. The results of calculation shows that the specimens of Brisi et al. heated at 1573 K [24] were hyperstoichiometric, for example, the O/M ratio is estimated to be 2.126 at $y = 0.25$, and those of Voronov et al. heated at 1473 K [25] were hypostoichiometric. Since equation (5-1) can be applied for $x \geq 0$ only, another equation between the lattice parameter and composition, x and y, is needed for $x < 0$. In the present work, highly reductive reaction conditions have not been taken to produce the solid solutions with $x < 0$. However, the samples prepared by Alberman et al. [53] and Voronov et al. [25] should be the solid solutions of CaO and $UO_{2.00}$, i.e., $Ca_yU_{1-y}O_{2-y}$, from their experimental conditions where the oxygen potential ($\Delta\bar{G}_{O_2}$) is deduced to be well below -300 kJ/mol. A coefficient of x was calculated using their lattice parameters and y value, assuming that the coefficient of y was the same as that in the case of $x \geq 0$. The value of -0.19 ± 0.02 was obtained for the coefficient of x in the region $x < 0$. The equation is, therefore

$$a = 5.470 - 0.19x - 0.31y \ (\text{Å}), \text{ for } x < 0. \tag{5-4}$$

The coefficient of x in the region $x < 0$, -0.19, is about twice as large as that in the region $x \geq 0$. For the solid solutions containing trivalent rare earth element, it has been reported that the lattice parameter dependence on x changes at $x = 0$ and that the rate of the change

of the lattice parameter by x in the region $x<0$ is twice or three times larger than that in the region $x\geq 0$ [82, 83, 142-144]. The present result is in accordance with the changes in these systems.

The partial molar enthalpy of oxygen $\Delta\bar{H}_{O_2}$ for the single phase $Ca_yU_{1-y}O_{2+x}$ solid solution was estimated using an equation for the partial molar entropy of oxygen $\Delta\bar{S}_{O_2}$ derived by Fujino and Naito [21]:

$$\Delta\bar{S}_{O_2} = -2R\ln\left(\frac{x}{1-x}\right) - 4R\ln\left(\frac{2x+2y}{1-2x-3y}\right) + Q, \qquad (5\text{-}5)$$

where the first and second terms of equation (5-5) are due to the configurational entropy change and the factor Q includes the vibrational term which does not vary greatly with the composition [149, 150]. Due to the lack of the Q value for the present solid solution, the averaged value of those reported earlier [149, 150], −167 J/K·mol, was used as the Q value in the present estimation. The partial molar free energy of oxygen $\Delta\bar{G}_{O_2}$ was calculated from the experimental conditions and the values are given in the last column of **Table 5-1**. The values of $\Delta\bar{H}_{O_2}$ were obtained by

$$\Delta\bar{H}_{O_2} = \Delta\bar{G}_{O_2} + T\Delta\bar{S}_{O_2}, \qquad (5\text{-}6)$$

which are shown in **Fig. 5-5** as a function of x in $Ca_yU_{1-y}O_{2+x}$. Since none of the specimens having the same y value covers the whole range of x in the figure, the variation of $\Delta\bar{H}_{O_2}$ with x and y can not be discussed precisely. However, the general trends of $\Delta\bar{H}_{O_2}$ with x can be seen from the figure. A sharp increase of $\Delta\bar{H}_{O_2}$ near $x=0$, maximum in the vicinity of $x=0.01$ and slow decrease of $\Delta\bar{H}_{O_2}$ over $x=0.1$ were observed. The phenomenon giving maximum of $\Delta\bar{H}_{O_2}$ has been observed also in the other systems: $x=0.01$ [151] and $x=0.002$ [152, 153] for UO_{2+x} and near $x=0$ for $Gd_yU_{1-y}O_{2+x}$ [150]. In the figure, the $\Delta\bar{H}_{O_2}$ values for $Mg_{0.05}U_{0.95}O_{2+x}$ [51] are also shown. These values are about −25 kJ/mol smaller than the present ones in the range $x\geq 0.1$. The difference is due to the smaller Q values, −188 to −196 J/K·mol, in the solid solutions of magnesium.

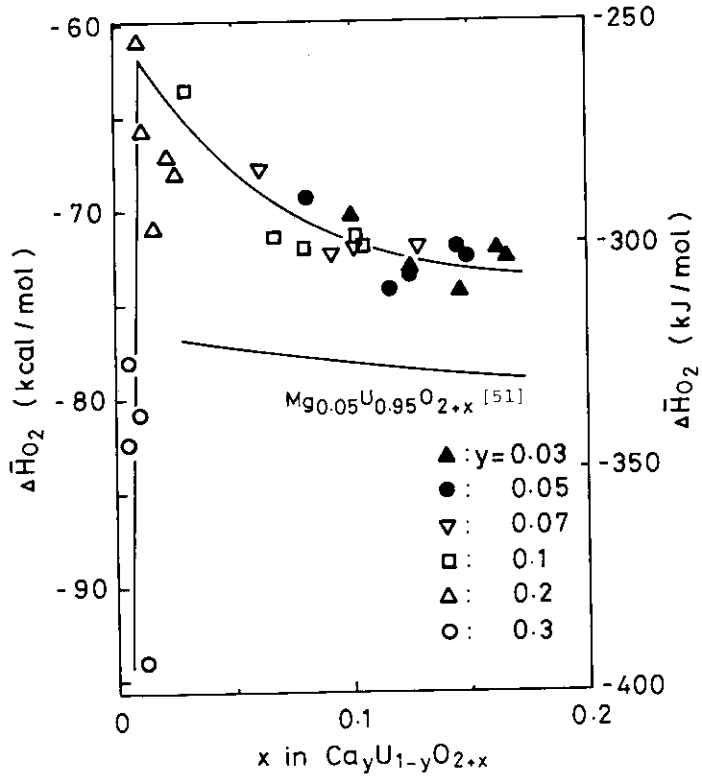

Fig. 5-5 The partial molar enthalpy of oxygen as a function of excess oxygen content (=x).

6. Phase relations and crystal chemistry in the ternary $PrO_{1.5}$-UO_2-O_2 system

6.1 Introduction

Rare earth elements (RE's) are known to be produced in nuclear fuel as fission products with high yields. **Table 6-1** shows the yields of main fission products in light water reactor fuel with a burnup of 33, 000 MWd/t [154]. The total amount of rare earth elements reaches to about 30 weight per cent of total fission products. The knowledge of phase relations and thermodynamic properties for RE–U–O ternary systems is, therefore, of basic importance for discussing the irradiation behavior of uranium dioxide fuel. Although there have been a relatively large number of works concerned with the RE–U–O systems [155], the studies on Pr–U–O ternary system are meager [156-160] and the phase relations have not been well resolved. These reports show that a homogeneous region of solid solution having the fluorite structure exists in the Pr–U–O system. Hund and Peetz [156] studied the solid solution of praseodymium oxide and uranium oxide in air at 1523 K and showed that the region of the

Table 6-1 Main fission product yields in LWR fuel with a burnup of 33,000 MWd/t [154]: yields in weight-ppm at shut down

Element	Atomic No.	yield
Krypton	36	370
Xenon	54	5420
Rubidium	37	331
Cesium	55	2720
Strontium	38	887
Barium	56	1397
Yttrium	39	466
Lanthanum	57	1260
Cerium	58	2706
Praseodymium	59	1193
Neodymium	60	3870
Promethium	61	101
Samarium	62	809
Europium	63	185
Gadolinium	64	110
Zirconium	40	3647
Molybdenum	42	3434
Technetium	43	837
Ruthenium	44	2270
Rhodium	45	379
Palladium	46	1310
Tellurium	52	565
Iodine	53	269
	Total	34536

fluorite solid solution was divided into two parts from the difference in dependence of the cubic lattice parameter on praseodymium content. They also found from density measurements that the cation sublattice rather than anion one is intact in the solid solution. Recently, the solubility of $PrO_{1.5}$ in uranium oxudes was more extensively studied by KFK researchers [157, 158]. A ternary UO–PrO–$(1/2)O_2$ phase diagram at 1523 K has been published [158] which is shown in **Fig. 6-1**. As seen from the figure, three single phase regions exist in this system: These are an extended fluorite phase, a rhombohedral phase with a nominal composition of Pr_6UO_{12} and a C-type rare earth oxide phase. Aitken et al. [159] worked out the cell parameters of this rhombohedral Pr_6UO_{12} to be a = 10.301 and c = 9.800 Å in hexagonal indexing.

However, the agreement of phase relations among them seems to be unsatisfactory and crystal chemical properties in reducing atmospheres are almost unknown. In the present work, therefore, efforts were paid for determining the phase regions and for knowing the defect characteristics in this system using X-ray diffraction and precise chemical analysis techniques. Reactions were performed in the temperature range from 1473 to 1773 K under the atmospheres of air, helium stream and high vacuum. The relations between lattice parameters and compositions of the fluorite solid solution were determined. Discussion was made on the phase regions of this system in term of the oxidation state of uranium and the type of oxygen defect.

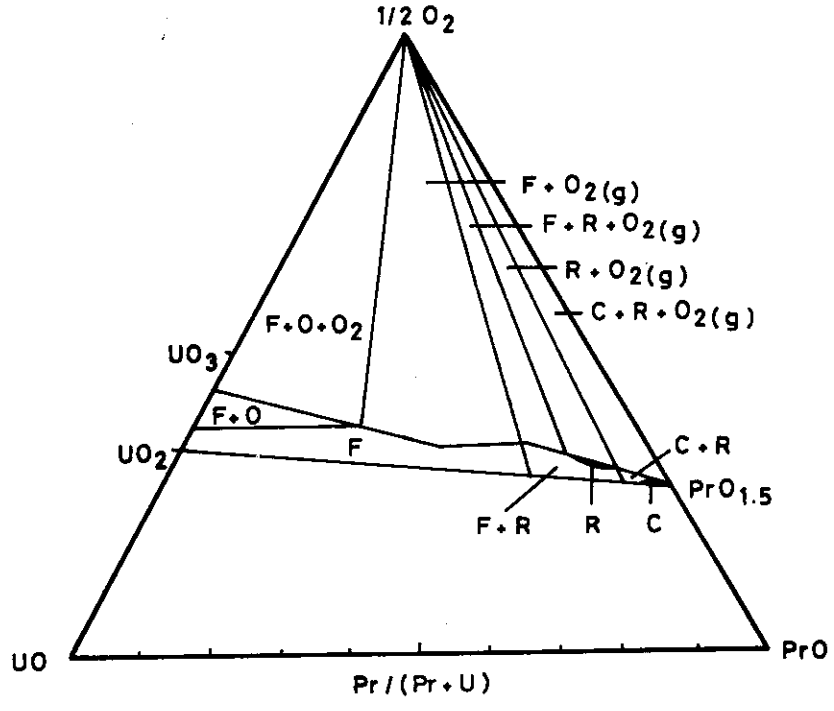

Fig. 6-1 Ternary phase diagram for the PrO-UO_2-O_2 system at 1523 K [158]: F = fluorite phase ($Pr_yU_{1-y}O_{2+x}$), O = β-U_3O_8 phase, R = rhombohedral phase (Pr_6UO_{12}), and C = C-type $PrO_{1.5}$ phase.

6.2 Experimental

Uranium peroxide, which was precipitated from uranyl nitrate solution, was washed with distilled water and dried in an air bath. This material was heated in air at 1173 K to form U_3O_8. Praseodymium oxide, $PrO_{1.833}$. (99.99% metallic purity) was provided from Shin-Etsu Chemical Co. Ltd. The U_3O_8 and $PrO_{1.833}$ were reduced to UO_2 and $PrO_{1.5}$, respectively, in

a stream of purified hydrogen at 1273 K for 10 h. The weighed amounts of UO_2 and $PrO_{1.5}$ were intimately mixed in an agate mortar and heated in air at 1073 K for 15 h. The content of praseodymium in the mixture ranged from $y=0.1$ to 0.9 with 0.1 increment. Composition will be designated by x and y in $Pr_yU_{1-y}O_{2+x}$ hereafter irrespective of single compound, that is, if mixture, these indicate bulk composition. The oxidized mixture were pressed at 2 t/cm^2 into pellets of 7 mm in diameter and 2 mm in height, the weight being ca. 600 mg. The pellets were heated in air, in a stream of helium or in vacuo. In the cases of the first two, the pellets were placed together on a platinum plate in an alumina boat, and were heated in an SiC resistance tube furnace. The reactions in vacuum were carried out on a molybdenum boat in a high-vacuum-furnace. Heating conditions are summarized in **Table 6-2**. The oxygen partial pressure in a stream of helium shown in the table was obtained from the electrical resistivity of oxydized cobalt wire, which has been described elsewhere [140].

Debye-Scherrer patterns of powdered specimens in vacuum sealed capillaries were taken with a Norelco 114.6 mm camera using copper Kα radiation filtered through nickel foil. Lattice parameters of cubic solid solutions were obtained by least squares calculation for eight diffraction peaks higher than 90 degrees (2θ). For the specimens showing broad peaks, patterns were also taken with a Philips PW-1390 diffractometer using copper Kα radiation monochromatized with curved pyrolytic graphite.

Chemical analysis was carried out to determine x and y in $Pr_yU_{1-y}O_{2+x}$ using the cerium (IV)-iron (II) back titration method described in section 2.2. After the y value or Pr/(Pr+U) atom ratio was ascertained to be unchanged by heating, only x value was determined by the titration. The error in x is estimated to be less than ±0.003 at high uranium contents but increases to ±0.03 at $y=0.9$.

Table 6-2 Experimental conditions adopted

Atmosphere	P_{O_2} (Pa)	Temperature (K)	Heating period (h)
air	1.2×10^{4}	1473	60
		1623	60
helium	1.0	1473	60
		1623	69
vacuum	1.0×10^{-4}	1473	28
		1623	25
		1773	6

6.3 Results and Discussion

6.3.1 X-ray diffraction

By X-ray diffraction analyses, three phases were found to exist under the present experimental conditions, i.e., a face centered cubic (fcc) solid solution, a rhombohedral phase with a narrow range of composition and an A-type rare earth sesquioxide phase. The fcc phase covers considerably wide ranges of y in $Pr_yU_{1-y}O_{2+x}$. The phases and lattice parameters for specimens prepared at 1623 K in air, helium and vacuum are summarized in **Table 6-3**.

The variation of cubic lattice parameter with y for the specimens heated in air is shown in **Fig. 6-2** together with literature values [156, 157, 160]. The data are able to be connected by three straight lines with different slopes. The present values are in good accordance with those of Hund and Peetz [156], whereas somewhat different from those of Jocher [157]. The values of Lowe [160] scatter considerably. No significant differences were observed between the present values for samples heated at 1573 and 1623 K. At y = 0, X-ray diffraction pattern revealed an existence of β-U_3O_8 with orthorhombic lattice parameters of a = 7.070, b = 11.45 and c = 8.302 Å, and of small amount of α-U_3O_8 with a = 6.73, b = 11.95 and c = 4.15 Å. Coexistence of α-U_3O_8 in β-U_3O_8 may be caused by rather rapid cooling (cooling rate, 100 K/min or higher at the first stage) since β-U_3O_8 was obtained only by slow cooling (100 K per day) [161]. It is seen from the figure, breaks occur on the line (curve 1) at y = 0.32 and 0.60. Below y = 0.32, the lattice parameter of the fcc phase remained unchanged at 5.443 Å, and α and β-U_3O_8 lines were also detected: Two-phase mixture exists in this range. From y = 0.32 to 0.60, the lattice parameter increases linearly with y. The value reaches 5.4727 Å at y = 0.60. Above y = 0.60, the lattice parameter increases with a steeper slope, which is consistent with literatures [156, 157]. The extrapolated value of the lattice parameters to y = 1.0, 5,540 Å, is close to the half-cell value of 5.530 Å for nonstoichiometric C-type rare earth sesquioxide quenched from 1523 K [157].

At y = 0.8, the diffraction lines corresponding to another fcc phase with smaller lattice parameter became distinct, and they grew clearer and stronger with the increase of y value. The lattice parameter change of this phase is shown in **Fig. 6-2** as curve 3. The parameter diminishes with increasing y and comes to that of $PrO_{1.833}$ at y = 1.0. This curve coincides with the former fcc line (curve 1) at about y = 0.7, which suggests that the new phase ($PrO_{1.833}$)

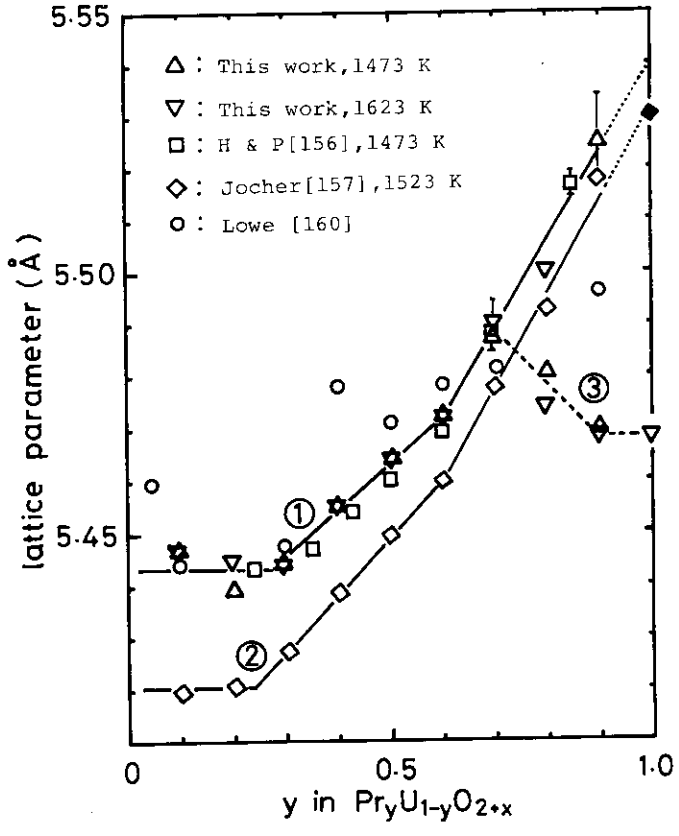

Fig. 6-2 Lattice parameter change of cubic solid solutions obtained by heating in air: ♦ = half of the lattice parameter of the body centered cubic cell of C-type $PrO_{1.5}$ heated at 1523 K [157].

exists in the range $0.7 < y \leq 1.0$. There is no available explanation for the change of the lattice parameters of the two fcc phases in the coexistence region, but similar behavior has been reported also in Gd–U–O system [142].

A rhombohedral phase known as Pr_6UO_{12} [157-159] coexisted with $PrO_{1.833}$ at $y = 0.9$ when heated at 1623 K. The lattice parameters obtained were $a = 10.24$ and $c = 9.570$ Å in hexagonal indexing. By heating at 1473 K, however, this rhombohedral phase was not formed. The product was a mixture of the fcc solid solution and the $PrO_{1.833}$ phase. It may be noteworthy here that the super-structure lines due to C-type rare earth sesquioxide structure could not be detected in the diffraction patterns for either the solid solution with high y value or the $PrO_{1.833}$ phase. This may due to the rather short reaction period of ~60 h, because according to Burnham and Eyring [162] the annealing period of about 100 days was required for well developed crystals that produce the super-structure lines.

The variation of the fcc lattice parameter with composition for the samples heated in helium is shown in **Fig. 6-3**, where the broken line is that for samples heated in air at 1623 K for comparison. It is seen from **Fig. 6-3** that the lattice parameter of the samples heated in helium can be followed by two straight lines with different slopes. The difference between the lattice parameters heated in helium and those in air is that the parameter increases with y almost linearly from $y = \sim 0$ to 0.52. In the range $0.52 < y \leq 0.77$, the lattice parameter increases with a steeper slope. An extrapolated value to $y = 1.0$ is near the half of the C-type $PrO_{1.5}$ lattice parameter, 5.576 Å [163], shown by an open star mark. This parameter is larger than that of $PrO_{1.65}$ ($a/2 = 5.535$ Å) [163] shown by the filled star mark because of lower O/Pr ratio.

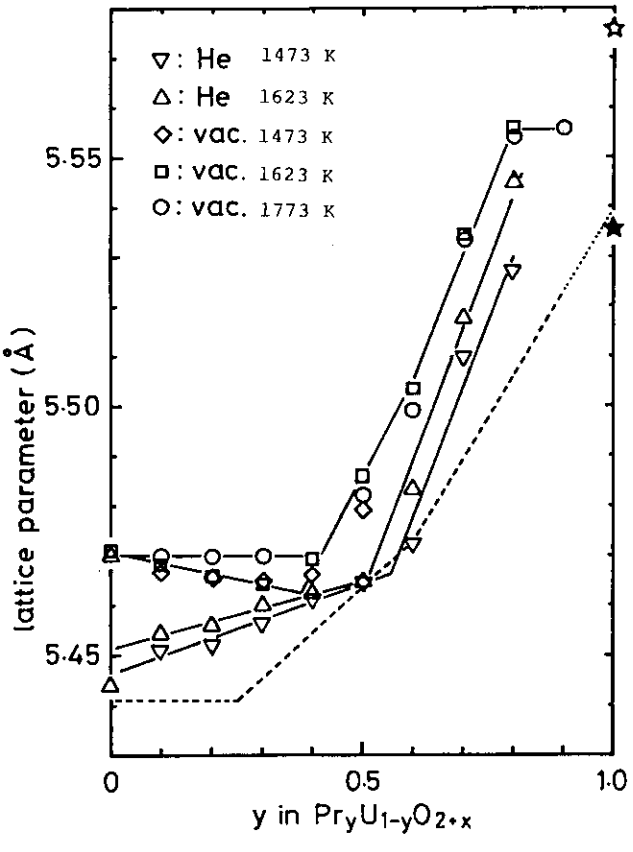

Fig. 6-3 Lattice parameter change of cubic solid solutions obtained by heating in helium or in vacuum: ☆, ★ = half of the lattice parameters of the body centered cubic cell of C-type $PrO_{1.5}$ and $PrO_{1.65}$ [163]. Broken line indicates the lattice parameters for those heated in air at 1623 K.

The rhombohedral phase appeared both at $y=0.8$ and 0.9 when heated in helium at 1473 or 1623 K. At $y=0.8$, it coexisted with the cubic solid solution, and at $y=0.9$, on the other hand, with A-type (hexagonal) rare earth sesquioxide phase. Because of weak and overlapping peaks in diffraction patterns from the two phases, the lattice parameters of the rhombohedral phase could not be obtained precisely. The values were $a=10.3$ and $c=9.80$ Å, which are in good agreement with those reported, i.e., $a=10.301$ and $c=9.800$ Å [157-159].

The lattice parameter change for the fcc solid solutions of the specimens heated in vacuum is also shown in **Fig. 6-3**. In this case, the lattice parameter decreases with increasing y in the range $0 \leq y \leq 0.38$ when heated at 1473 or 1623 K. On the other hand, when heated at 1773 K, the lattice parameter does not change at $y \leq 0.38$ but increases steeply with y at $y > 0.38$.

It was the same as in the series of heating in helium that the rhombohedral phase was observed at $y=0.8$ and 0.9 provided that the heating temperature was either 1473 or 1623 K. This phase, however, did not appear at 1773 K, where only the diffraction lines of the fcc solid solution and the A-type $PrO_{1.5}$ phase were detected. On the other hand, Jocher [157] has reported the existence of the rhombohedral phase under one atmospheric pressure of oxygen at 1773 K. The present result suggests that this phase is unstable in a reducing atmosphere.

Oxygen partial pressure shows significant effects also in Pr-O binary system. There have been many papers, concerning the stability of C and A-type rare earth sesquioxides. One distinct point is that C-type phase has fairly wide O/RE (RE = rare earth elements) ranges of existence over $O/RE \geq 1.5$, whereas A-type phase can be seen only in narrow ranges around $O/RE=1.5$. These trends have been observed also in americium sesquioxides [164] and uranium sesquinitrides [165]. The formation of the A-type phase instead of the C-type phase at $y=1.0$ in the present system could be caused by almost complete reduction to $O/Pr=1.5$ in helium and vacuum as will be shown in the following section. Another feature of these phases is seen in the solubility of uranium oxides into A or C-type phase. C-type $REO_{1.5}$ (RE = Pr, Dy to Lu) phases take up small smount of uranium oxides into their crystal lattice: the solubility limit is usually less than a few per cent [157, 158, 166]. A-type $REO_{1.5}$ (RE = La, Nd) phases, on the other hand, shows no detectable solubility of uranium oxides [109, 141]. The fact that the lattice parameters of the A-type $PrO_{1.5}$ phase at $y=0.9$ are the same as those for $y=1.0$ in the present system shows that it does not take up any uranium oxides in its lattice, which is in agreement with the general trend of the solubility above.

6.3.2 Chemical analysis and thermogravimetry

Figure 6-4 shows the thermogravimetric curves for $PrO_{1.833}$ heated at a rate of 2 K/min in air and in vacuum. When heated in air, the O/Pr ratio reached to 1.65 at 1373 K while it lowered to 1.50 by heating in vacuum (0.4 Pa) at 1223 K. On cooling to room temperature at a rate of 2 K/min, the O/Pr ratio was restored to 1.833 at 723 K in air. On the other hand, it remained 1.50 down to room temperature if cooled in vacuum.

The O/M ratio obtained by chemical analysis for the present system is tabulated in **Table 6-3**, where M indicates Pr + U. The variation of the O/M ratio with y is shown in **Fig. 6-5**. These curves are for the specimens heated at 1623 K.

The O/M ratio for the samples heated in air at 1623 K is seen to decrease rapidly from 2.651 to 2.00 at $y=\sim 0.6$. The ratio further decreases to 1.65 at $y=0.9$ and then increases forming $PrO_{1.833}$ at $y=1.0$.

The O/M ratio for the samples heated in helium stream was smaller than that for those heated in air but larger than that for those heated in vacuum. After passed through O/M =

Table 6-3 Mean valency of uranium, O/M ratio, phases and lattice parameters for the products heated at 1623 K

Pr content (y)	mean valency of uranium	O/M ratio (2+x)	phase	lattice parameter (Å)
(1) heated in air at 1623 K				
0	5.302	2.651	α-U_3O_8	a = 6.73, b = 11.95, c = 4.15
			β-U_3O_8	a = 7.070, b = 11.45, c = 8.302
0.1	5.202	2.491	α, β-U_3O_8 + fcc	(a) + 5.447
0.2	5.048	2.319	α, β-U_3O_8 + fcc	(a) + 5.445
0.3	4.954	2.184	fcc	5.4454
0.4	5.013	2.104	fcc	5.4554
0.5	5.156	2.039	fcc	5.4647
0.6	5.465	1.993	fcc	5.4727
0.7	5.980	1.947	fcc	5.4909
0.8	5.87	1.79	fcc + fcc (b)	5.500 + 5.474 (weak)
0.9	5.72	1.64	rhom. + fcc (b)	a_{hex} = 10.24, c_{hex} = 9.57 + 5.468 (weak)
1.0	–	1.833 (c)	fcc (b)	5.468
(2) heated in helium at 1623 K				
0	4.330	2.165	fcc + fcc	5.4440 + 5.4702
0.1	4.351	2.108	fcc	5.4546
0.2	4.443	2.077	fcc	5.4561
0.3	4.503	2.026	fcc	5.4603
0.4	4.643	1.993	fcc	5.4627
0.5	4.960	1.990	fcc	5.4647
0.6	5.290	1.958	fcc	5.4833
0.7	5.573	1.886	fcc	5.5180
0.8	5.62	1.76	fcc + rhom.	5.545 + a_{hex} = 10.3, c_{hex} = 9.80
0.9	5.86	1.64	rhom. + hex.	(d) + (e)
1.0	–	1.50 (c)	hex.	a = 3.857, c = 6.013
(3) heated in vacuum at 1623 K				
0	4.000	2.000	fcc	5.4709
0.1	4.116	2.002	fcc	5.4682
0.2	4.248	1.999	fcc	5.4660
0.3	4.414	1.995	fcc	5.4653
0.4	4.620	1.986	fcc	5.4693
0.5	4.764	1.941	fcc	5.4869
0.6	5.055	1.911	fcc	5.5036
0.7	5.053	1.808	fcc	5.5348
0.8	5.03	1.70	fcc + rhom.	5.556 + (d)
0.9	5.24	1.61	rhom. + hex.	(d) + (f)
1.0	–	1.50 (c)	hex.	a = 3.861, c = 6.014

fcc = face centered cubic phase,
rhom. = rhombohedral phase,
hex. = hexagonal $PrO_{1.5}$ phase,
(a) the same as those for y = 0, (b) $PrO_{1.833}$ phase, (c) obtained from thermogravimetric analyses,
(d) the same as those for y = 0.8 heated in helium, (e)(f) the same as those for y = 1.0.

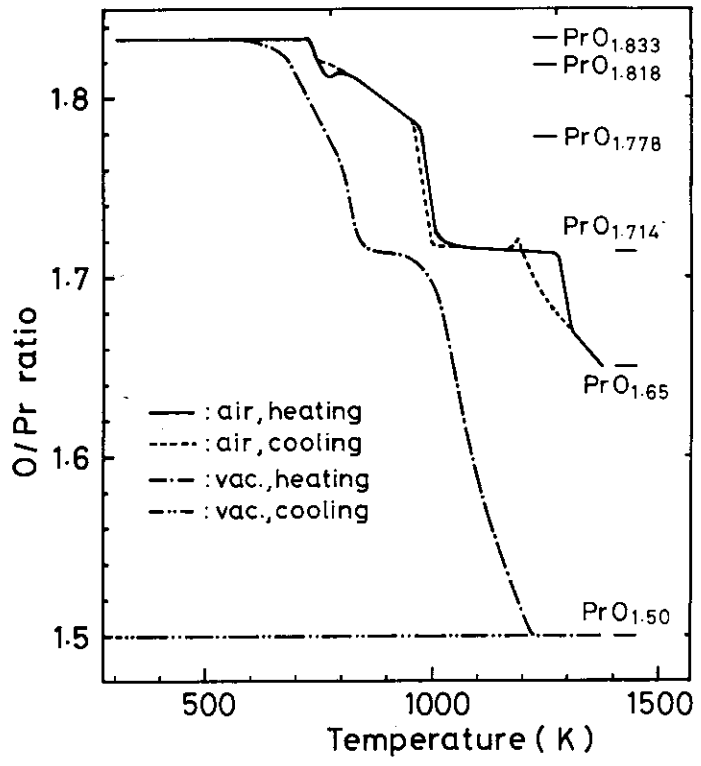

Fig. 6-4 Thermogravimetric curves for $PrO_{1.833}$ heated in air and in vacuum: heating rate 2 K/min.

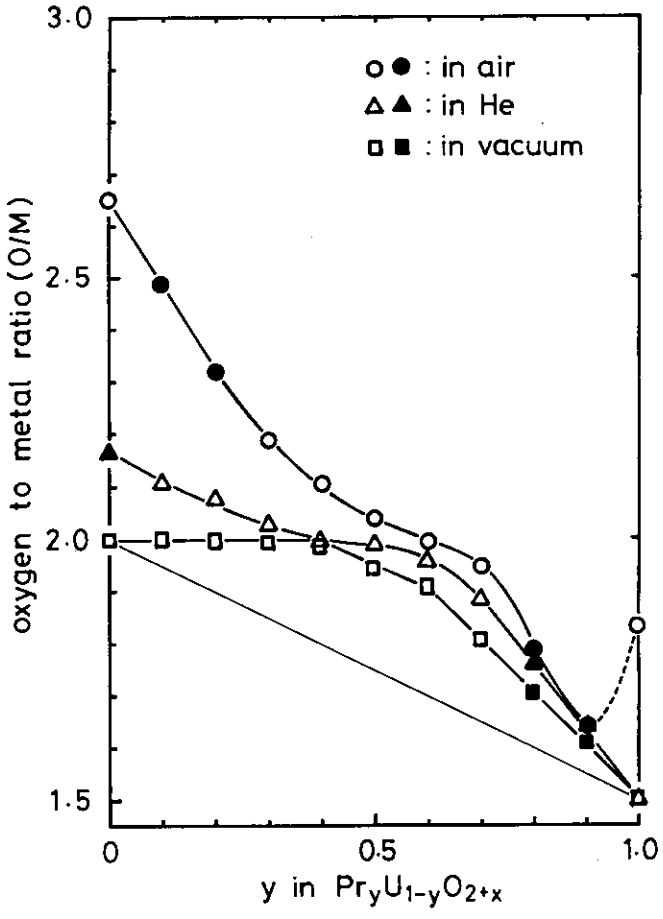

Fig. 6-5 Oxygen to metal atom ratios of the products obtained by heating at 1623 K in air, helium and vacuum: Open marks indicate single phase and filled marks two-phase mixture.

2.0 at y = 0.38, the curve was not lowered greatly until y = 0.6. Over that y value, then, the curve was lowered almost linearly down to O/M = 1.5 at y = 1.0.

When heated in vacuum, the O/M ratio did not vary until y = 0.38. Similar behavior has been reported also in the other systems between rare earth oxides and uranium oxide [82, 142, 143]. At y = 0.4, the ratio was 1.986, and decreases to 1.911 at y = 0.6. Further increase in y was accompanied by a more rapid decrease of the ratio down to 1.50 at y = 1.0.

6.3.3 Lattice parameter change by nonstoichiometry

In the change of the lattice parameter with y shown in **Figs. 6-2** and **6-3**, the effect of oxygen nonstoichiometry, x, is implicitly contained. The lattice parameter of the fluorite single phase is plotted as a function of O/M (= 2 + x) in **Fig. 6-6**. It is seen that the fluorite lattice contracts with increasing x. The data can be followed by two straight lines of which slope changes of O/M = 2.00. Similar sharp breaks at the stoichiometric $MO_{2.00}$ point have been noted in the systems La–U–O [82], Gd–U–O [142] and Nd–U–O [83, 143].

By using the observed lattice parameters in the cubic single phase region, least squares calculations were performed to express the change of lattice parameter as linear equations of x and y under the condition that the parameter is 5.4704 Å [90] for both x and y being zero. The results are:

$$a = 5.4704 - 0.127x - 0.007y \text{ (Å)}, \text{ for } x \geq 0 \qquad (6\text{-}1)$$

and

$$a = 5.4704 - 0.397x - 0.007y \text{ (Å)}, \text{ for } x < 0. \qquad (6\text{-}2)$$

These equations show that the lattice parameter diminishes with increasing x and y. Because the effect of y is much smaller than that of x, the experimental values shown in **Fig. 6-6** may be represented by two straight lines. The coefficient of x in equation (6-1), which expresses the effect of oxygen on lattice parameter in O/M ≥ 2 region, is −0.127. This value is

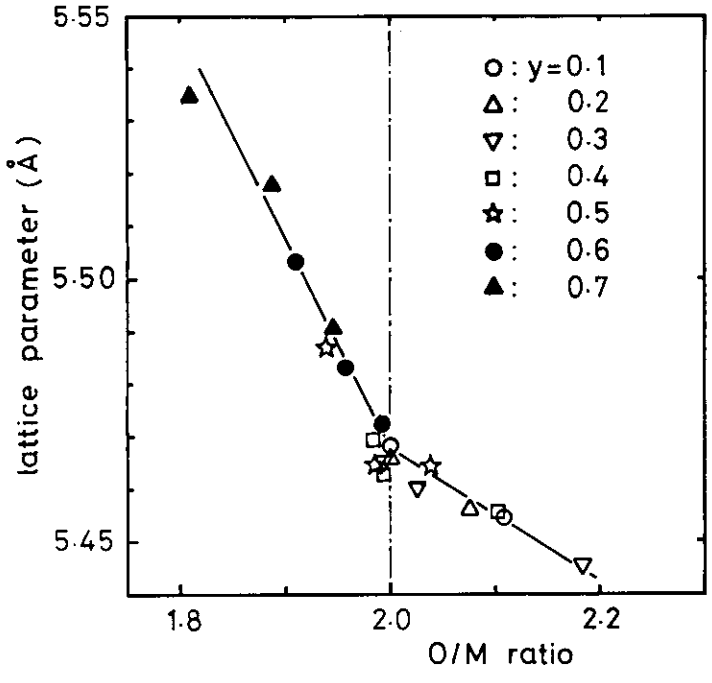

Fig. 6-6 Effect of oxygen to metal atom ratios on the lattice parameter of cubic solid solutions with praseodymium oxide and uranium oxide.

well comparable with −0.10, −0.117 and −0.094 for $Nd_yU_{1-y}O_{2+x}$ [83], $Mg_yU_{1-y}O_{2+x}$ [21] and UO_{2+x} [90], respectively. Since these coefficients have been verified to correspond to the defect structure with oxygen interstitial type [50, 147], the present result can be considered to give a strong support that the "x" oxygen atoms are in interstitial sites in the range $O/M \geq 2$ in this system.

For the range of O/M less than two, the coefficient of x seems to be about three times greater than that for $O/M \geq 2$. The values of −0.30, −0.24 and −0.28 have been reported for $Nd_yU_{1-y}O_{2+x}$ [83], $Gd_yU_{1-y}O_{2+x}$ [84] and $La_yU_{1-y}O_{2+x}$ [82], respectively. Although the present coefficient, −0.397, is slightly larger than these values, the ratio of coefficient of x for $O/M < 2$ to that for $O/M \geq 2$ is near to three. In this region, oxygen vacancies are assumed to be formed.

The coefficient of y, which is equivalent to $\partial a/\partial y$, indicates the rate of change of lattice parameter with the content of rare earth elements. The present value is shown as a star mark in **Fig. 6-7** together with literature data [82-84, 109, 141-143, 148, 166-171]. The figure shows that $\partial a/\partial y$ changes linearly with ionic radius. These results suggest that the lattice parameter change with y in the solid solutions of $RE_yU_{1-y}O_{2+x}$ depends only on the trivalent ion size of rare earth elements which substitute for uranium.

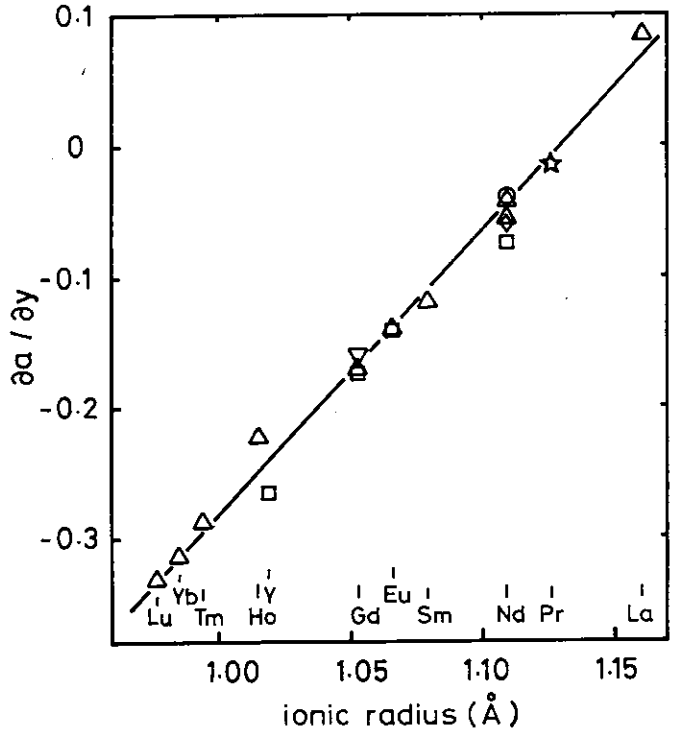

Fig. 6-7 Partial derivative of lattice parameter with y as a function of ionic radius of RE^{3+} [148]: □ [84], ◇ [83], ▽ [142], ○ [143], △= calculated from the lattice parameters of $RE_{0.5}U_{0.5}O_{2.00}$ [82, 109, 141, 166-171] assuming that linear relationships hold between the lattice parameters of UO_2 and these phases.

6.3.4 Valency of uranium in the solid solution

The O/M ratio enables us to calculate the valency of uranium if praseodymium is regarded to be trivalent in the solid solutions. This is not confirmed, but the fact that the present value of $\partial a/\partial y$ for praseodymium was on the line connecting those for the other $RE_yU_{1-y}O_{2+x}$

with trivalent rare earth elements (**Fig. 6-7**) is a support for this hypothesis. **Figure 6-8** shows that for the samples heated in air at 1623 K, the mean valency of uranium decreases with increasing y until y = 0.32, and then it increases steeply up to y = ~0.70. The valency decreases with y in the region above y = ~0.70. The points of y = 0.32 and ~0.70 can be considered to express the phase boundaries.

For samples heated in helium, the mean valency increases from y = 0 to ~0.6 with increasing slope. The curve crosses the horizontal line of mean valency of 5.0 at y = 0.52. Above y = ~0.70, the points scatter.

When heated in vacuum, the curve crosses the line of mean valency of 5.0 at y = 0.62. At $y \geq 0.70$, the valency fluctuates along the curve with smaller increasing rate. There may be a phase boundary around this concentration of y.

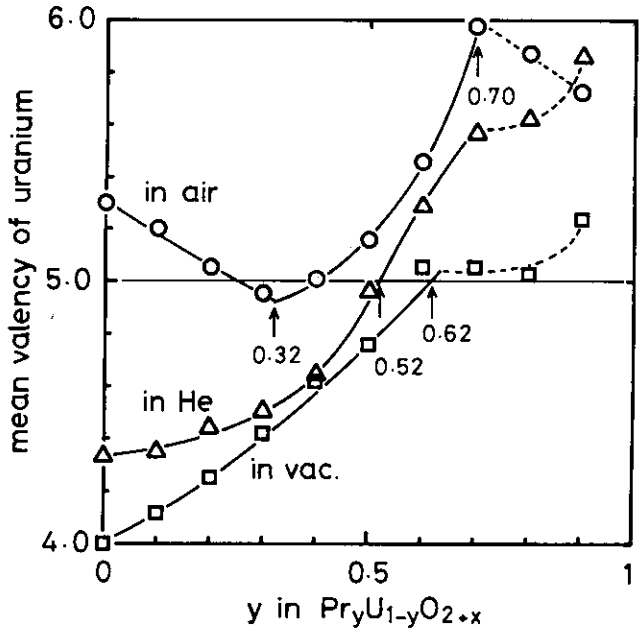

Fig. 6-8 Mean valency of uranium of the products obtained by heating at 1623 K in air, helium and vacuum.

6.3.5 Phase relations and types of defect

According to Ohmichi et al. [84], the lattice parameter change with y in $Gd_yU_{1-y}O_{2+x}$ can be interpreted by considering that the accommodation of one atom Gd^{3+} causes oxidation of one atom U^{4+} in the crystal to U^{5+} in the composition range where the mean valency of uranium is between +4 and +5. If this holds also for the present $Pr_yU_{1-y}O_{2+x}$ solid solutions, the uranium atoms will be oxidized first to U^{5+} from U^{4+} and then to U^{6+} from U^{5+} by introducing praseodymium atoms in the mean valency ranges $U^{4+} \sim U^{5+}$ and $U^{5+} \sim U^{6+}$, respectively.

Phase relations and lattice parameter change in the present system could be classified by the uranium valency and the type of oxygen nonstoichiometry. These are shown in **Table 6-4**. For determining y ranges, the results of chemical analysis (O/M ratio) and X-ray diffraction were used. For example, as seen in **Table 6-3**, the sample with y = 0.9 heated in helium is a mixture of hexagonal $PrO_{1.50}$ and rhombohedral Pr_6UO_{12-z}. The z value was calculated to be 0.07 from the O/M ratio observed. Since this $Pr_6UO_{11.93}$ coexisted with the fcc phase at y = 0.8, the composition of phase boundary of the latter phase was obtained to be $Pr_{0.77}U_{0.23}O_{1.80}$. For the heating condition of air and vacuum, the limiting compositions of the fcc solution

Table 6-4 Phases in relation to uranium valency and oxygen nonstoichiometry

region	phase	uranium valency and type of defect
(1) in air at 1623 K		
$0 < y \leqq 0.32$	fcc s.s. + α, β-U_3O_8	
$0.32 < y \leqq 0.38$	fcc s.s.	$U^{4+} \sim U^{5+}$ oxygen interstitial
$0.38 < y \leqq 0.60$	fcc s.s.	$U^{5+} \sim U^{6+}$ oxygen interstitial
$0.60 < y \leqq 0.71$	fcc s.s.	$U^{5+} \sim U^{6+}$ oxygen vacancy
$0.71 < y < 1.0$	fcc s.s. + Pr_6UO_{12} or $PrO_{1.833}$ phase	
(2) in helium at 1623 K		
$0 < y \leqq 0.38$	fcc s.s.	$U^{4+} \sim U^{5+}$ oxygen interstitial
$0.38 < y \leqq 0.52$	fcc s.s.	$U^{4+} \sim U^{5+}$ oxygen vacancy
$0.52 < y \leqq 0.77$	fcc s.s.	$U^{5+} \sim U^{6+}$ oxygen vacancy
$0.77 < y < 1.0$	fcc s.s. + Pr_6UO_{12} or A-$PrO_{1.5}$ phase	
(3) in vacuum at 1623 K		
$0 < y \leqq 0.38$	fcc s.s.	$U^{4+} \sim U^{5+}$ no oxygen defect
$0.38 < y \leqq 0.62$	fcc s.s.	$U^{4+} \sim U^{5+}$ oxygen vacancy
$0.62 < y \leqq 0.70$	fcc s.s.	$U^{5+} \sim U^{6+}$ oxygen vacancy
$0.70 < y < 1.0$	fcc s.s. + Pr_6UO_{12} or A-$PrO_{1.5}$ phase	

were $Pr_{0.71}U_{0.29}O_{1.91}$ and $Pr_{0.70}U_{0.30}O_{1.77}$, respectively. These are well in accord with the literature values [157, 158].

Table 6-4 shows that when heated in air at 1623 K, the fcc solid solution having fluorite type structure is formed as a mixture with U_3O_8 in the range $0 < y \leq 0.32$. At y values of $0.32 < y \leq 0.38$, the uranium valencies of the fcc phase are $U^{4+} \sim U^{5+}$ with excess oxygen atoms on interstitial sites, while those in the range $0.38 < y \leq 0.60$ are $U^{5+} \sim U^{6+}$. In the range $0.60 < y \leq 0.71$, oxygen vacancies are formed instead of interstitials. The change of slope in lattice parameter was seen at $y = 0.6$ in **Fig. 6-2**. Above 0.71, the solid solution phase does not exist in single phase.

When heated in helium, the fcc solid solution was in a single phase even below $y = 0.1$, which is in contrast with the case of heating in air. The uranium valencies of the fcc phase in the range of $0 < y \leq 0.38$ are $U^{4+} \sim U^{5+}$ with interstitial oxygen, and it has oxygen vacancies in the range $0.38 < y \leq 0.52$. As seen from **Fig. 6-3**, the lattice parameter increases with a slope of 0.027 per y in these ranges. The uranium valencies change from $U^{4+} \sim U^{5+}$ to $U^{5+} \sim U^{6+}$ at $y = 0.52$. In the range $0.52 < y \leq 0.77$, the fcc phase is in the region $U^{5+} \sim U^{6+}$ and has oxygen vacancies. The lattice parameter increases more repidly in this range. Above $y = 0.77$, the fcc phase exists as a mixture with Pr_6UO_{12} phase or A-$PrO_{1.5}$ phase.

Let us calculate the slope in the range $0 < y \leq 0.38$ theoretically. Since partial molar entropy of oxygen, $\Delta\bar{S}_{O_2}$, will be expressed by the following equation as discussed previously [21],

$$\Delta\bar{S}_{O_2} = -2R\ln\frac{x}{1-x} - 4R\ln\frac{2x+y}{1-2x-2y} + Q, \tag{6-3}$$

and partial molar free energy, $\Delta\bar{G}_{O_2}$, is given by

$$\begin{aligned}\Delta\bar{G}_{O_2} &= RT\ln(P_{O_2}) \\ &= \Delta\bar{H}_{O_2} - T(-2R\ln\frac{x}{1-x} - 4R\ln\frac{2x+y}{1-2x-2y} + Q).\end{aligned} \tag{6-4}$$

Since the values of $\Delta\bar{H}_{O_2}$, and Q do not change greatly with composition and temperature except near $x=0$ [150], let these put constants. The total derivative of $\Delta\bar{G}_{O_2}$ with y is expressed as:

$$d(\Delta\bar{G}_{O_2}) = \frac{\partial(\Delta\bar{G}_{O_2})}{\partial x}dx + \frac{\partial(\Delta\bar{G}_{O_2})}{\partial y}dy. \tag{6-5}$$

Under the condition of constant oxygen partial pressure,

$$d(\Delta\bar{G}_{O_2}) = 0.$$

Then,

$$\frac{dx}{dy} = -\frac{2x(1-x)(1+2x)}{4x^2y-8x^2-10xy-2y^2+6x+y} \tag{6-6}$$

and from equation (6-1)

$$\frac{da}{dy} = -0.127\frac{dx}{dy} - 0.007. \tag{6-7}$$

The dx/dy values were calculated to be −0.441, −0.426 and −0.275 for $y=0.1$, 0.2 and 0.3, respectively, with equation (6-6). Therefore, by substituting these values in equation (6-7), da/dy values of 0.0490, 0.0471 and 0.0279 were obtained for $y=0.1$, 0.2 and 0.3, respectively. These are in reasonable agreement with the observed slopes.

In the case of vacuum heating, uranium valencies of the fcc phase in the range $0 \leq y \leq 0.38$ are $U^{4+} \sim U^{5+}$ with no oxygen nonstoichiometry. The absence of oxygen nonstoichiometry causes the slight decrease of lattice parameter in this range of y. Above $y=0.38$, the oxygen vacancies are produced. In the range $0.38 < y \leq 0.62$, the uranium valencies of the fcc phase are $U^{4+} \sim U^{5+}$, while in $0.62 < y \leq 0.70$ they are in $U^{5+} \sim U^{6+}$. In the range $0.70 < y < 1.0$, the fcc phase exists as a mixture with either Pr_6UO_{12} phase or A-type $PrO_{1.5}$ phase.

As Pr^{3+} substitutes for U^{4+} in the cubic lattice of the solid solution, an oxygen deficiency is created. The oxidation of some of the remaining U^{4+} to higher states will balance the valence deficiency. At $y=0.667$, all of the uranium ions would be in U^{6+} state for an intact anion sublattice. Further increases in $PrO_{1.5}$ content bring about the oxygen vacancies in the lattice. However, in the real cases of the present system, oxygen vacancies are formed below $y=0.667$, as seen in **Table 6-4**. This tendency becomes more enhanced if samples are heated under low oxygen partial pressures. Above $y=0.38$, the defect type is oxygen vacancy in the heating experiments at 1623 K in both helium and vacuum, although mean valency of uranium is less than +5. Such a vacancy formation may be motivated by the adjacent C-type rare earth sesquioxide phase which has a structure closely related to the fluorite type structure with ordered oxygen vacancies. However, the formation of vacancy brings about large distortion of the crystal lattice around the defects, which results in significant broadening in X-ray diffraction lines. The larger effect of vacancies on the lattice parameter compared with interstitials can be seen in equation (6-2).

Figure 6-9 shows oxygen partial pressures as a function of x in $Pr_yU_{1-y}O_{2+x}$ at 1623 K, where the oxygen partial pressures used were those determined experimentally. It is seen from the figure that $\log(P_{O_2})$ changes greatly with x around $x=0$ for $y=0.4$ or 0.5, which conversely

means that x value does not change materially with P_{O_2} around x = 0 for y = 0.4 or 0.5. In fact, as seen in **Fig. 6-3**, the lattice parameters for the specimens heated in air and in helium almost overlap at y = 0.5, and the same can be said for the specimens heated in helium and in vacuum at y = 0.4. These results would suggest a possibility of stabilization of the solid solution or compound formation at these y values. The y value of 0.5 is corresponding to $REUO_4$ reported earlier [109, 141, 166-173].

The composition of the rhombohedral compound Pr_6UO_{12-z} was obtained to be $Pr_6UO_{11.93}$ and $Pr_6UO_{11.62}$ for helium and vacuum heated specimens, respectively, using the observed O/M ratios in **Table 6-3** on the basis that Pr/U ratio of six does not change with oxygen partial pressure. The existence of reduced Pr_6UO_{12} phase, which is suggested in the literature [157, 158], is confirmed in the present experiment under a low oxygen partial pressure.

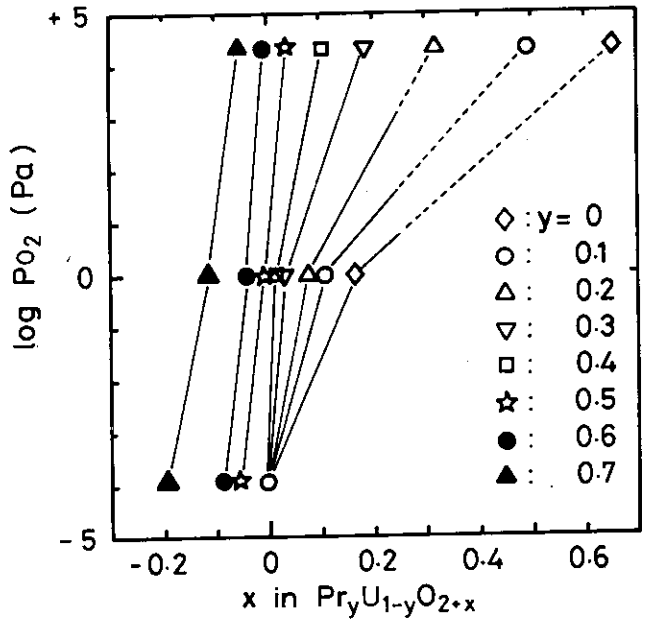

Fig. 6-9 Oxygen partial pressure as a function of x in $Pr_yU_{1-y}O_{2+x}$ at 1623 K.

7. Reaction of lithium and sodium nitrates and carbonates with uranium oxides

7.1 Introduction

The intention of the voloxidation which consists of heating spent fuel oxides in oxygen or air at 773-973 K after the fuel rods are sheared into pieces is to disintegrate the fuel into fine powder during oxidation as well as to remove tritium from it before dissolution in nitric acid [174]. This head-end process in nuclear fuel reprocessing has been studied by many researchers. A typical result on the removal of volatile fission products by voloxidation [175] is shown in **Table 7-1**. As seen from the table, the evolution of tritium is quantitative although that of ^{14}C-oxides, ^{85}Kr and ^{129}I is insufficient [175, 176]. The removal of tritium prior to dissolution in acid is especially important because extensive isotopic dilution by nontritiated water can be avoided by adopting the process.

For liquid metal-cooled fast breeder reactor fuels, however, it has been pointed out that uranium-plutonium mixed oxides with the plutonium amount more than 25 mole per cent could not be oxidized to O/M (M = U + Pu) ratios greater than about 2.36 (M_4O_9 phase) and did not fragment even at temperatures as high as 1123 K [175, 177]. **Figure 7-1** shows the effect of voloxidation and burnup on the amount of insoluble residue [175]. The voloxidation causes to increase the amount of insoluble residue on dissolution by roughly a factor of two. It has been also observed that the voloxidation increased the amount of plutonium in the residue by a factor between 4 and 5 [175].

Under these circumstances, it seems to be worth consideration to use fused salts for digesting the spent fuels. There have been several reports concerning the problem. The fuels were treated with $NaNO_3$ or $NaNO_3$-NaOH fused salt at 623-723 K and with $NaNO_3$-$NaCO_3$ at 1123-1173 K [178]. Milner et al. [179] used Na_2O_2-NaOH or NH_4HSO_4 at 673 K, while Maurice et al. [180] examined $Na_2S_2O_7$-$K_2S_2O_7$. Avogadro et al. [181, 182] studied the reaction of UO_2 in molten alkali metal nitrates at 723-773 K, and found that the compounds formed were $Na_{2-x}M_xU_2O_7$ where M were Li, K and Cs. They have reviewed that PuO_2 should react with the nitrates to form plutonates and that tritium could be eliminated during the process. However, the molten salt method leaves a large amount of excess salts unreacted which increase the amount of high level wastes.

In this work, the reaction of UO_2 with various amounts of lithium and sodium nitrates and carbonates was studied with an aim to know the minimum amounts of alkali metal salts which are required to form uranates as well as their reactivities. Although many kinds of uranates are known to be formed not only in the fused salts but also by the reaction with alkali metal nitrates, carbonates, chlorides etc. by heating at 773-1073 K [9, 183], there have only been a few experimental data reported on the uranates with least alkali metal to uranium atom ratio, the use of which, nevertheless, may confine the increase of the high level wastes to a necessary minimum. The reaction products were examined by means of X-ray diffraction analysis and thermogravimetry.

Table 7-1 Removal of volatile fission products by voloxidation [175]

Fuel[a)]	Source	Quantity of Isotope Removal, % ^{3}H	^{14}C	^{85}Kr	^{129}I
Saxton	Voloxidizer off-gas	>99.9	39	10	8
	Dissolver off-gas	<0.1	61	90	92
	Dissolver solution	<0.1	–	–	<1
Big Rock Point	Voloxidizer off-gas	99.5	11	9	3
	Dissolver off-gas	<0.1	89	91	97
	Dissolver solution	0.5	–	–	<1
Quad Cities	Voloxidezer off-gas	99.4	31	<30	5
	Dissolver off-gas	<0.1	69	>60	95
	Dissolver solution	0.6	–	–	<1

a) Burnup of the fuel: Saxton 40,000 MWd/t
Big Rock Point 25,000 MWd/t
Quad Cities 9,450 MWd/t

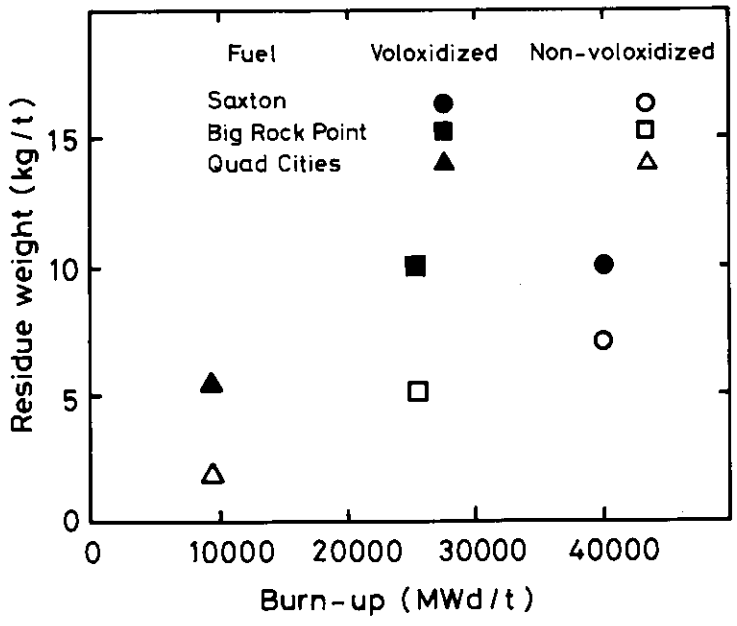

Fig. 7-1 Effect of voloxidation on the amount of insoluble residue [175].

7.2 Experimental

7.2.1 Materials

$LiNO_3$, Li_2CO_3, $NaNO_3$ and Na_2CO_3 used were all of reagent grade. U_3O_8 was prepared by heating high purity uranium metal in air at 1073 K [89]. UO_2 was prepared by hydrogen reduction of the U_3O_8 at 1273 K for 5 h.

7.2.2 Apparatus and procedure

A seried of experiments on the reaction between lithium and sodium nitrates was carried out in a horizontal SiC tube furnace. In a fused quartz crucible of 15 mm outer diameter and 10 mm height, UO_2 powder or pieces of sintered pellet were weighed. The weighed amount of lithium nitrate powder was added to the UO_2. A number of such crucibles containing the UO_2 and lithium nitrate in various ratios were placed on a quartz boat, and heated in the furnace in a stream of oxygen. For the reactions with sodium nitrate, an aliquot of solution of the nitrate was pipetted on the UO_2 in the crucible with a Socorex-821 micropipette because sodium nitrate was markedly hygroscopic. The samples were dried in air bath, and heated as in the case of lithium nitrate.

The reactions of U_3O_8 with lithium and sodium carbonates were studied as a function of temperature by a Cahn-RH electrobalance. The balance was adjusted so as to have a maximum weight change of 500 mg, and a sensitivity 0.01 mg. A fused quartz crucible in which the weighed amount of the sample mixture of around one gram had been loaded was suspended from the balance. The temperature of the specimen was measured by a Pt/Pt + 13%Rh thermocouple placed close to the crucible inside the reaction tube.

7.2.3 X-ray measurements

The X-ray diffraction patterns were taken with a Philips PW-1390 diffractometer. The copper Kα radiation was monochromatized with a curved pyrolytic graphite monochromator placed between a specimen and an NaI(Tl) detector. The slit system used was 1/2 deg-0.1 mm-1/2 deg.

7.3 Results and discussion

7.3.1 Formation of several lithium and sodium uranates from carbonates and U_3O_8 and their X-ray patterns

Although crystal structures have been determined for most of the lithium and sodium uranates, the relative intensities of the X-ray diffraction peaks for these compounds were not all reported. Moreover, we found out no available data on the compounds with various M/U ratios (M = Li, Na) prepared under the same reaction conditions. Then, the uranates with established M/U ratios [9, 183] were prepared, and their X-ray patterns were taken in order that the reaction products might be identified in the following reactivity experiments.

Calculated amounts of Li_2CO_3 and U_3O_8 were intimately mixed in an agate mortar. The mixtures of Li/U atom ratios 0.333, 0.667, 1.205, 2, 4 and 6 corresponding to the uranates $Li_2U_6O_{19}$ [184], $Li_2U_3O_{10}$ [185], $LiU_{0.83}O_3$ [186], Li_2UO_4 [187], Li_4UO_5 [132], and Li_6UO_6 [188], respectively, were heated in the quartz crucibles in air at 923 K for 5 h. After having been cooled to room temperature, the products were ground in the agate mortar, and they were re-heated at 923 K for 5 h. X-ray diffraction analysis was performed for these products. Then, they were ground again, and heated in air at 1073 K for 48 h. The X-ray diffraction patterns for these products are shown in **Fig. 7-2**, which are nearly the same as

those for the products heated up to 923 K except that the peaks were somewhat sharper in the patterns of the 1073 K heated samples. These facts show that the reactions were almost finished during heating at 923 K.

It is seen from the Li/U=0.333 pattern in **Fig. 7-2** that the product is a mixture of the L/U=0.667 compound and U_3O_8. Peaks at $2\theta = 21.41$, 25.91, 26.52, 34.21 and 34.31 deg are from α-U_3O_8 [89]. It is not clear that our Li/U=0.667 compound is monoclinic as reported by Kovba [185] for $Li_2U_3O_{10}$ because too many calculated lines should be derived from this

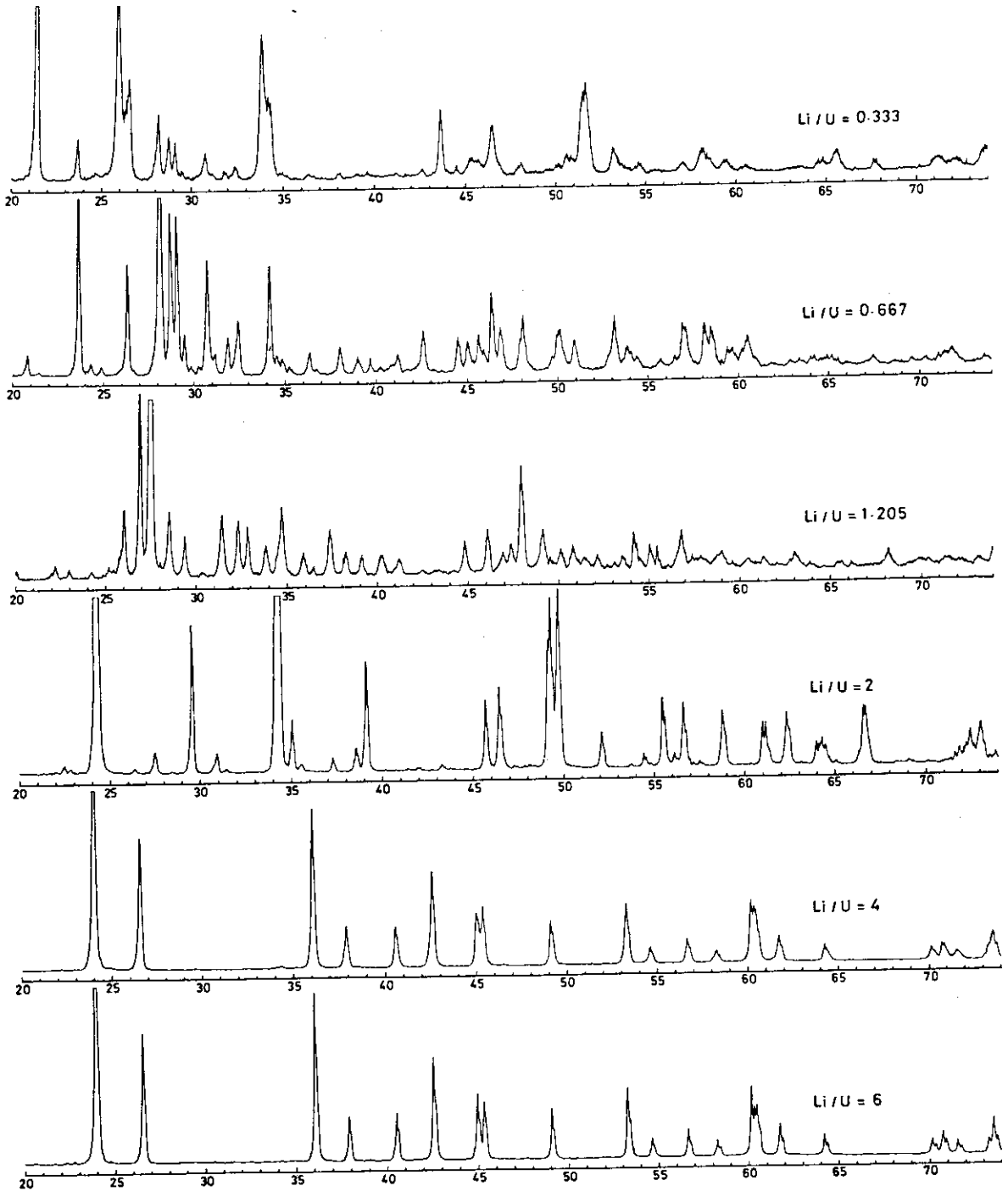

Fig. 7-2 X-ray diffraction patterns of the lithium uranates formed by the reactions between lithium carbonate and U_3O_8. Mixtures were heated in air at 1073 K for 48 h. Diffraction angle is given in 2θ.

$P2_1/c$ structure. The peak positions and intensity ratios for the Li/U = 1.205 compound agreed very well with the experimental data of Toussaint and Avogadro [192] for "$Li_2U_2O_7$", while the observed peak positions could be explained with an orthorhombic indexing a = 20.382, b = 11.511 and c = 11.417 Å for "$Li_{22}U_{18}O_{65}$" [185]. The diffraction peaks of our Li/U = 2 compound were very well in agreement with the experimental values of Toussaint and Avogadro [182], which were also well consistent with the calculated values for Li_2UO_4 with an orthorhombic system a = 10.547, b = 6.065 and c = 5.134 Å with space group Pnma [187, 189]. The peak positions observed for the Li/U = 4 specimen were in complete agreement with the calculated ones for tetragonal I4/m with lattice parameters a = 6.720 and c = 4.451 Å [190]. It was found that the patterns for the Li/U = 4 and Li/U = 6 specimens were the same in this experiments. This fact does not accord with the results reported that α-Li_6UO_6 is hexagonal with a = 8.338 and c = 7.352 Å [188]. The discrepancy may be caused by the reaction conditions. According to Hauck [188], Li_6UO_6 decomposes to Li_4UO_5 with the sublimation of Li_2O at temperatures above 1123 K.

The method of preparation of sodium uranates was the same as the lithium compounds. The Na/U atom ratios studied were 0.5, 0.8, 0.857, 1, 2 and 4. The ratio 0.5 was taken to know whether the sodium uranate of this composition exists under the present reaction conditions. The mixing ratios 0.8, 0.857, 1, 2 and 4 correspond to the uranates Na_2O $2.5UO_3$ [191], $Na_6U_7O_{24}$ [192], $Na_2U_2O_7$ [191, 193], Na_2UO_4 [194] and Na_4UO_5 [190], respectively. As in the case of the lithium compounds, the X-ray patterns of the sodium compounds formed at 923 and 1073 K were almost the same, which shows that the reaction is finished at 923 K. **Figure 7-3** shows the X-ray patterns for the specimens heated at 1073 K. In general, peaks for sodium compounds are broader compared with those for lithium compounds. The pattern for the Na/U = 4 compound is not given in **Fig. 7-3** because it was hygroscopic and the peaks changed during the X-ray experiment. It is shown from the figure that the Na/U = 0.5 specimen is a mixture of the Na/U = 0.8 compound and α-U_3O_8. The patterns also show that the Na/U = 0.8 and 0.857 compounds are the same. This is consistent with the reported observations [192], but α-U_3O_8 does not exist in these specimens or if it exists the amount is extremely small because the peaks around 34 deg(2θ) can hardly be found in the Na/U = 0.8 and 0.857 charts. The peak positions and intensities for the Na/U = 1 specimen are well in accord with those of Toussaint and Avogadro [182]. There are no α-U_3O_8 peaks mingled. Some similarities exist in the interplanar spacings of the Na/U = 0.8 (and/or 0.857) and Na/U = 1 compounds, but these are clearly not the same compound. The Na/U = 2 product obtained under our reaction condition was found to be a mixture of α-Na_2UO_4 and $Na_2U_2O_7$ (Na/U = 1 compound). The larger peaks were well assigned to the orthorhombic system with a = 9.74, b = 5.72 and c = 3.49 Å [194], whereas the smaller peaks were all in common with the Na/U = 1 peaks observed in this study. This result may be explained by the fact reported [195, 196] that the uranate first formed is $Na_2U_2O_7$ which changes to Na_2UO_4 on continued heating. It may be noteworthy that for the samples heated at 923 K no basic difference was seen between the Na/U = 2 and 4 patterns, which would show that Na_4UO_5 was not formed under the present reaction conditions.

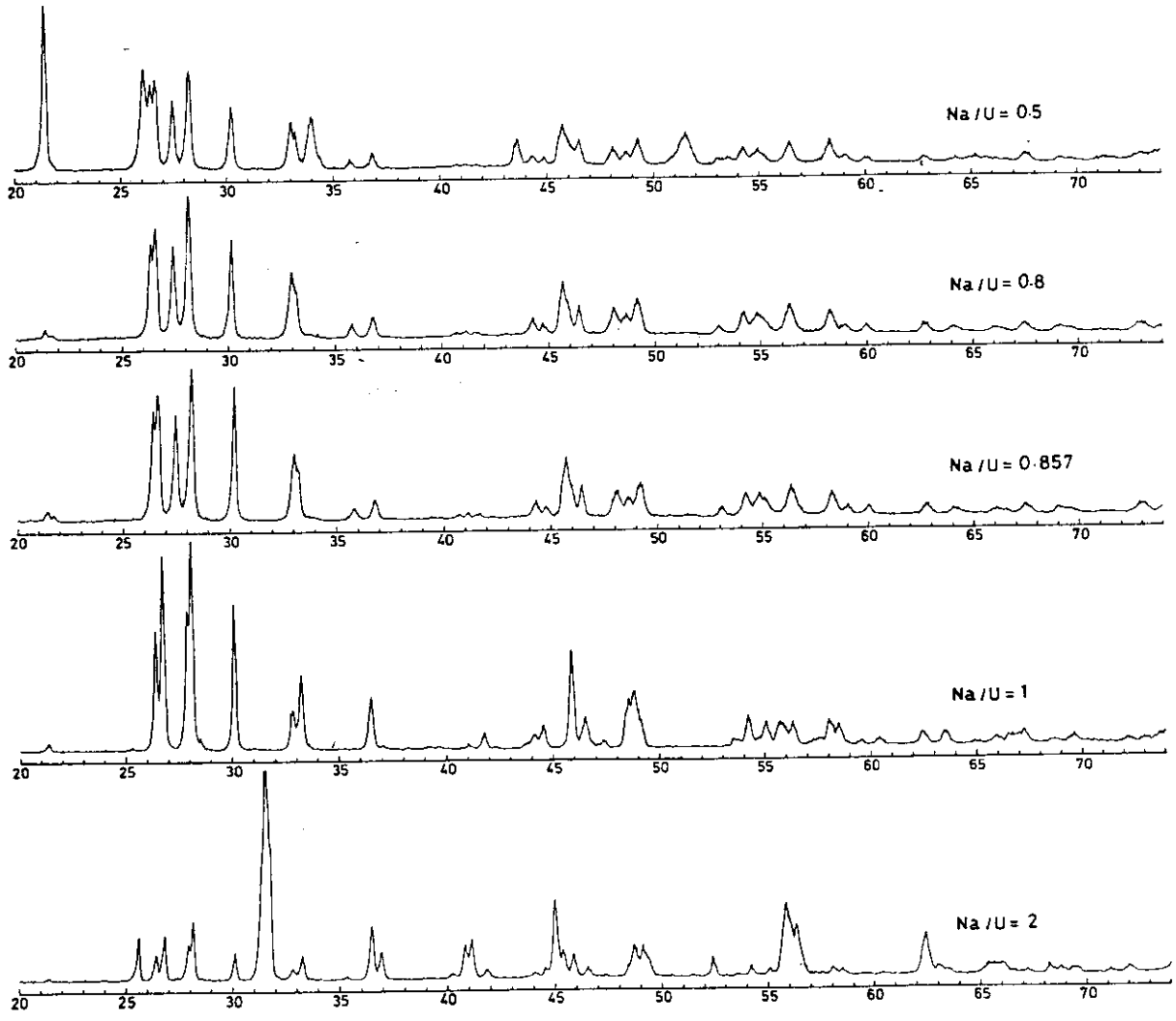

Fig. 7-3 X-ray diffraction patterns of the sodium uranates formed by the reactions between sodium carbonate and U_3O_8. Mixtures were heated in air at 1073 K for 48 h. Diffraction angle is given in 2θ.

7.3.2 Reactivity of lithium nitrate on UO_2

The known amount of lithium nitrate was added to UO_2 powder in the crucible. The furnace temperature was raised at a rate of 3 K/min in a stream of oxygen. After maintained at 673 K for 3 h, the temperature was raised to 873 K at which the samples were held for 3h, and then furnace cooled to room temperature. The nitrate melted on heating and reacted with UO_2 evolving brown NO_2 gas. X-ray diffraction patterns of the products are shown in **Fig. 7-4**. For the Li/U = 0.1891 product, large peaks observed at 2θ = 21.4, 26, 26.50, 34, 34.3, 44 deg etc. are all those of α-U_3O_8, i.e., U_3O_8 is the major component. When the lithium to uranium ratio was increased to 0.3024, the diffraction peaks of uranate grew up although the α-U_3O_8 peaks were still larger. The uranate peaks, however, do not coincide with those of the 0.667 phase which is the uranate phase having the minimum Li/U ratio described in the previous section. This fact may be ascribed to the difference in starting materials and reaction conditions. Both Li/U = 0.1891 and 0.3024 specimens were heterogenerous with tan and yellow colors. In the Li/U = 0.5342 specimen, there remains U_3O_8, but its amount is markedly reduced and the greatest part of the mixture is a lithium uranate. The peak positions for this

uranate basically agree with those for the 0.3024 specimen. The 0.5342 product shows yellow color. It is known from the X-ray pattern that the Li/U = 0.7929 compound is a mixture of the Li/U = 0.667 and 1.205 phases shown in the previous section. No peaks of α-U_3O_8 were found in the pattern. The pattern of the Li/U = 1.9483 compound was well consistent with that of the Li/U = 2 standard. The peak positions of the Li/U = 7.5756 were in accord with those of the Li/U = 6 standard. The products with Li/U ratios above 0.7929 gave a homogeneous yellow color.

From the reactivity experiments with lithium nitrate, it was found that the uranates were produced without U_3O_8 if the lithium to uranium atom ratio was equal or larger than 0.667. Although the crystal structure of the uranate formed was different from that of the standard 0.667 phase when Li/U < 0.5324, the products having the same structure were formed in the product with the ratio 0.7929.

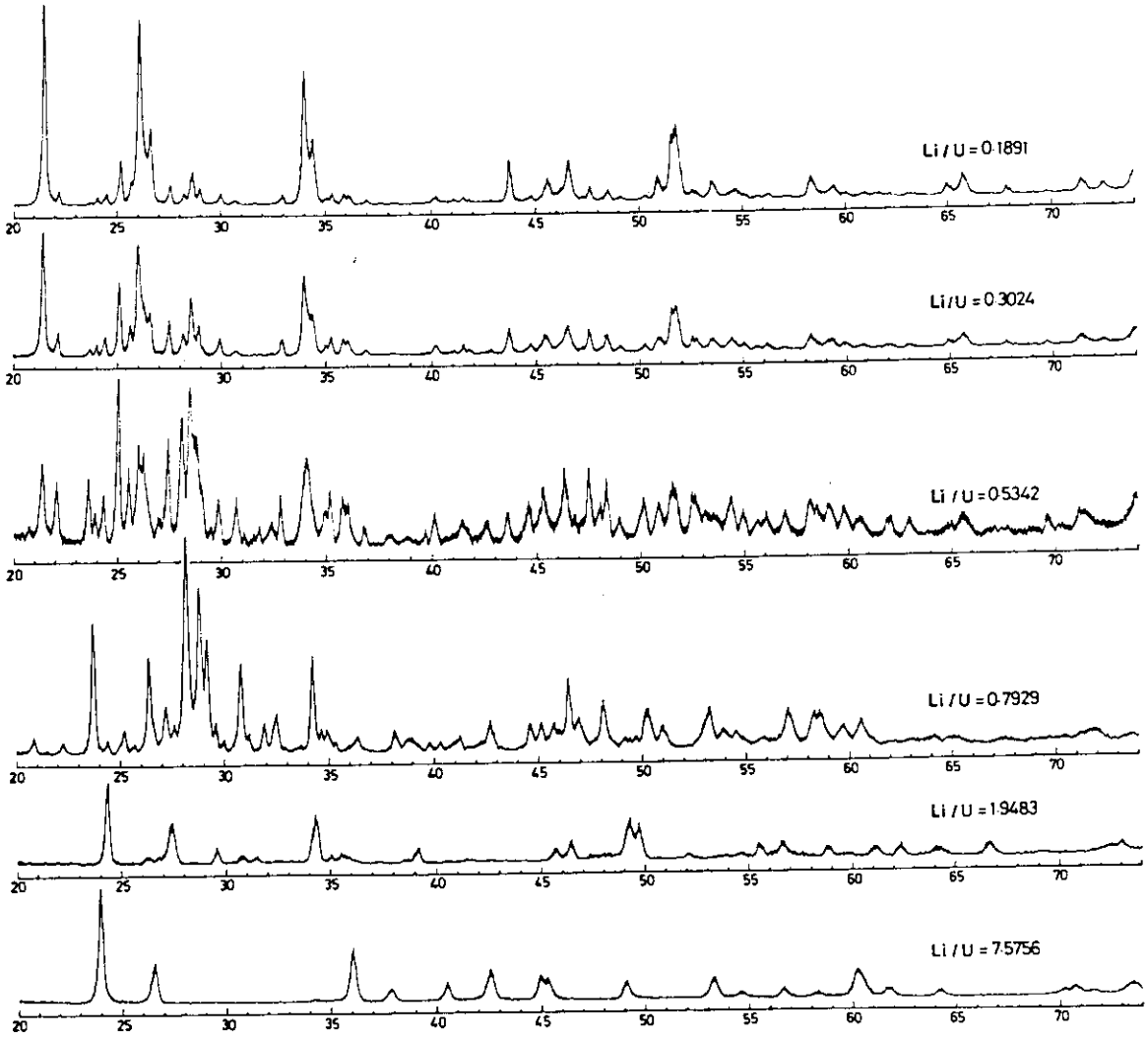

Fig. 7-4 Reaction between lithium nitrate and UO_2. Solid nitrate was added on UO_2 powder. Heating rate was 3 K/min in O_2. Heated at 673 K for 3 h, then at 873 K for 3 h. Horizontal axes show diffraction angle in 2θ.

7.3.3 Reactivity of sodium nitrate on UO_2

Sodium nitrate was added to UO_2 as solution. This technique was used only to know precise Na/U ratios in the products. The other reaction conditions were the same as those for the lithium nitrate. The X-ray patterns of the products obtained by heating at 873 K are shown in **Fig. 7-5**. It is seen from the figure that the Na/U = 0.1955 product is mainly composed of α-U_3O_8. In the 0.3225 product, the U_3O_8 still prevails, but small amount of uranate is formed as shown in the peaks between 27 and 30 deg. It was anticipated that the peaks for the Na/U = 0.4879 specimen were the same as those for the Na/U = 0.5 standard written in section 7.3.1. This was actually the case, but crystal growth is inadequate in the products from nitrate, i.e., the diffraction peaks are smaller and broader than those of the Na/U = 1 standard from carbonate. In the former experiments using carbonate and U_3O_8 (section 7.3.1), the reaction temperature did not greatly affect the X-ray peak shapes between 923 and 1073 K. Because the reactivity of sodium nitrate was studied at 873 K which differs only 50 K from 923 K of those experiments, the poor crystallinity may mainly be caused by the starting materials rather than by the temperature differences of the reactions. The peak positions for the Na/U = 0.9689 compound were in good agreement with those of the Na/U = 1 standard. No peaks of α-U_3O_8 were observed in the pattern. The peaks of the 0.9689 specimen are also weak and broad. The 0.1955, 0.3225 and 0.4879 products were brown colored, while the 0.9689 product was yellow ochre which is to some extent different from orange yellow of the Na/U = 1 standard. From the reactivity experiments with sodium nitrate it was found that sodium uranates free from U_3O_8 were obtained with the ratios Na/U $\geq$ 0.8, reaction temperatures between 873 and 923 K and reaction time 3 h.

In the separate series of experiments, the sodium nitrate reaction with pieces of sintered UO_2 pellets was studied. The pellets were completely pulverized with the formation of uranates. There were no significant differences between the reactions on pellet and powder in this case.

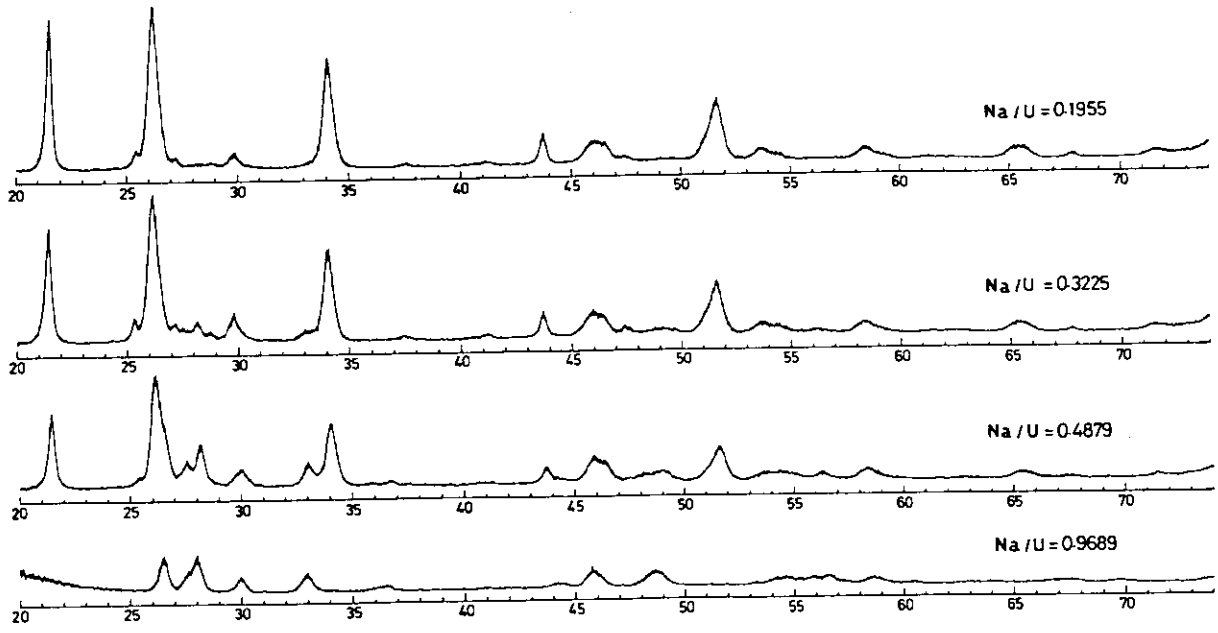

Fig. 7-5 Reaction between sodium nitrate and UO_2. Aliquots of sodium nitrate solution was added on UO_2 powder. Heating rate was 3 K/min in O_2. Heated at 673 K for 3 h, then at 873 K for 3h. Horizontal axes show diffraction angle in 2θ.

7.3.4 Thermogravimetric observations of the reaction of lithium and sodium carbonates with U_3O_8

The reaction of U_3O_8 with lithium and sodium carbonates was studied using an electrobalance. The calculated amount of alkali metal carbonate and U_3O_8 was intimately mixed in an agate mortar, pressed into a pellet of 10 mm diameter at 3 ton. The pellet was then heated at a rate of 2 K/min in air. Several were then for 15 h continuously kept at a temperature of 923 K. The results are shown in **Fig. 7-6**. Theoretical weight decrease in the figure indicates the weight difference between the hexavalent uranates which should be formed as the result of the reaction and the sum of alkali metal carbonate and U_3O_8 before the reaction. The experimental fact that the uranium valency is +6 in the uranates formed in air if the M/U ratios (M = Li, Na) are sufficiently large is generally admitted [9, 183]. The reaction can be expressed as:

$$\frac{p}{2}M_2CO_3(g) + \frac{1}{3}U_3O_8 + [\frac{1}{6} - \frac{p}{4}(1-x)]O_2(g) = M_p^{1+}U^{6+}O_{3+p/2}(s) + \frac{p}{2}CO_{1+x}(g),$$

where p represents M/U atom ratios. In **Fig. 7-6**, M/U = 0.5 curves (curves 1 and 3) exceed 100% theroretical weight decrease (TWD) to a large extent. This fact means that the mean

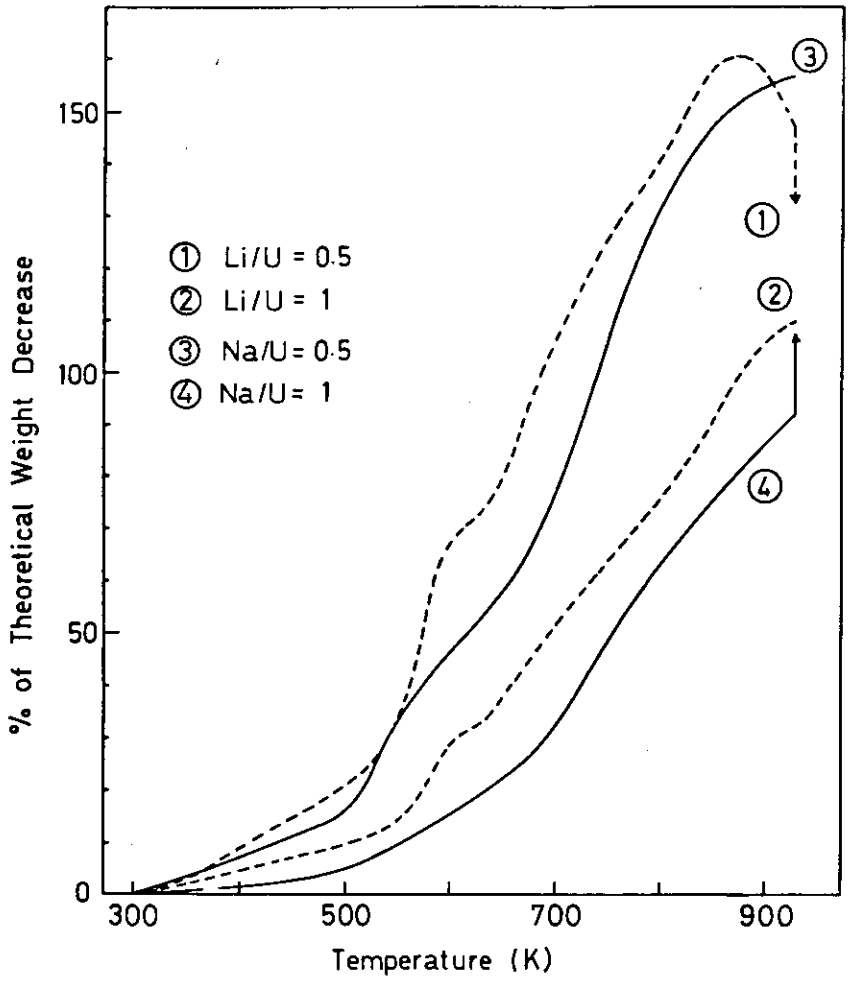

Fig. 7-6 Thermogravimetric analysis of the reactions between alkali metal carbonates and U_3O_8. Mixture pellets were heated in air at a heating rate 2 K/min. Arrows show the change in theoretical weight decrease while keeping the temperature for about 5 h at 923 K (cf. **Fig. 7-7**).

valency of uranium in the products is considerably smaller than +6. At the maximum of the Li/U = 0.5 curve (curve 1) the valency is +5.57. At the back and the top ends of the arrow of curve 1 at 923 K, the valencies are 5.67 and 5.77, respectively. The arrow indicates that the TWD decreases during the holding time of about 5 h at 923 K. The product is actually a mixture of the uranate with Li/U = 0.667 and U_3O_8. Calculation shows that the mole ratio of this uranate and U_3O_8 is 0.90:0.10 in the mixture, and the uranium valencies in the 0.667 uranate at 923 K are 5.78 and 5.92, which correspond to above two respective valencies. The reason for the appearing of the maximum in curve 1 may be that after the reaction between lithium carbonate and U_3O_8 with the formation of carbon dioxide or monoxide, the oxidation reaction of the formed lithium uranate in air proceeds rather slowly. In the reaction of sodium carbonate with the ratio Na/U = 0.5, this maximum does not appear. This would be due to a much lower rate of the reaction to oxidize the uranate. At the end of curve 3 at 923 K, the uranium valency becomes 5.60. On the basis that the uranate formed in this mixture has the Na/U ratio of 0.8, it can be calculated that the mixture is $Na_{0.8}UO_{3.28}$ and U_3O_8 in a ratio 0.83:0.17, the uranium valency in the uranate being 5.76. The larger TWD of curve 3 than that of curve 1 at 923 K is mainly because the least M/U ratio required to form sodium uranate is larger than that to form lithium uranate.

The reaction behavior at the ratio M/U = 1 is shown in curves 2 and 4. The compounds of this ratio should be uranates only. In contrast to the case with M/U = 0.5, the Li/U = 1 curve does not decrease during heating at 923 K. The valency of uranium at 923 K is 5.81. On the other hand, in the curve of the Na/U = 1 specimen (curve 4), the TWD increases on standing at 923 K. The valency was at first 6.18, and at the top end of the arrow it became 5.85. The value of 6.18 can be interpreted as an indication of insufficient reaction. The existence of unreacted sodium carbonate would give rise to such a high valency in calculation. The fact above shows that the reaction rate is lower when the Na/U ratio is larger in the reactions to form sodium uranates.

Figure 7-7 shows the variation of TWD with the holding time at 923 K (the time after

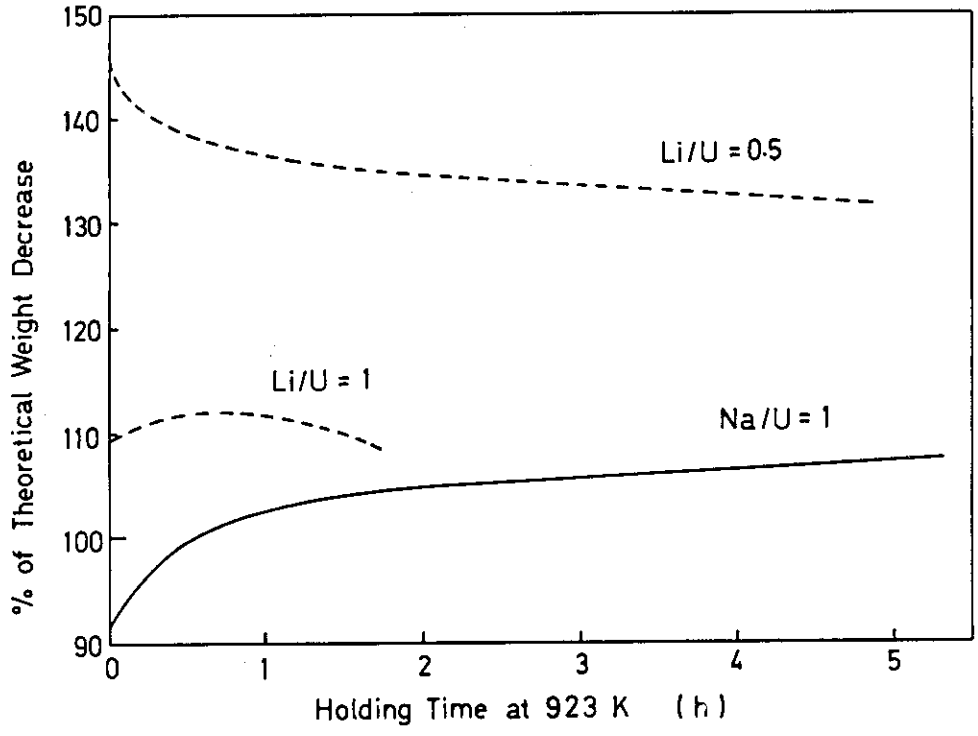

Fig. 7-7 Variation of the theoretical weight decrease while keeping the temperature at 923 K.

having reached that temperature). The decrease of TWD for Li/U = 0.5 curve shows that the oxidation reaction of the uranate continues, but after one hour its rate becomes much lower. On the other hand, it is seen that the main reactions are still the decomposition of carbonate and the formation of the uranate in the case of sodium carbonate reaction with the ratio Na/U = 1. The reaction in the specimen with Li/U = 1 is between these two cases. At first, there remain the decomposition and the uranate formation reactions. After about one hour, the oxidation reaction becomes predominant. It is concluded that these reactions between carbonates and U_3O_8 do not produce hexavalent uranates at 923 K. Higher heating temperatures or repeated mixing process may be needed to complete the reactions. These results can be compared with the reactions between lithium nitrate and uranium oxides where the uranium was exactly hexavalent in the uranates formed at 923 K for 3 h [197].

7.3.5 Dissolution of the uranates in nitric acid

The products obtained by heating sodium nitrate and UO_2 in oxygen at 873 K were used for these experiments. For small amounts of powder specimens having the ratios Na/U = 0.3225 and 0.4879 in beakers, 1 M HNO_3 was added. Although the most part of the solids were dissolved in the first one minute, a small amount of residue of U_3O_8 remained undissolved which was not dissolved after one hour. However, for the specimen of the ratio Na/U = 0.9689 which contains no U_3O_8, the dissolution was complete in 1 M HNO_3 in one minute. This fact shows that the uranates can be easily dissolved in dilute nitric acid if U_3O_8 is not present in the samples.

8. Conclusions

The phase relations of some ternary uranium oxides were studied with the aim to analyze the irradiation behavior of UO_2 type nuclear fuels from chemical and thermodynamic point of view. The standpoint of the present study is to understand the effects of fission products on the nuclear fuels as an overlap of ternary uranium oxides. That is to say, instead of investigating directly the complicated behavior of the oxide fuel which contains numerous fission products, the system is divided into ternary uranium oxides with individual fission product. Then, the results of the study of the phase relations and the thermodynamic properties for these ternary uranium oxides are combined together to elucidate the irradiation behavior of the oxide fuel in question.

In the present work, analytical methods were first studied to determine the composition of ternary uranium oxides with high accuracies, since high accuracy determination of the composition is essential in studying the change of properties of the oxides in relation to their compositions. Next, the formation reactions of alkaline earth monouranates were investigated to establish preparative conditions of these monouranates. In the course of the study, an anomalous change in the oxygen nonstoichiometry was found when the phase transformation took place in strontium monouranate from α to β phase. The phase transformation of cadmium monouranate was found to be similar to that of strontium monouranate. Then, the crystal structure of cadmium monouranates was studied to have an insight into the phase transformation of $CdUO_4$ from structural point of view. With use of the techniques and results so far obtained, the phase relations of ternary calcium-uranium-oxygen and praseodymium-uranium-oxygen systems were studied in detail. The reactivity and reaction conditions to form lithium and sodium uranates were studied. This basic knowledge was shown to be applicable to the fuel dissolution in nuclear fuel reprocessing.

The main results and conclusions obtained from the present work are as follows:

In Chapter 1, the purpose of the study and its outline were shown. Phase relations, crystal structures and some thermodynamic properties of ternary uranium oxides with alkaline earth metals were also reviewed.

In Chapter 2, two analytical methods were developed for the determination of the composition, x and y, in the ternary uranium oxides, $M_yU_{1-y}O_{2+x}$. These methods showed high accuracies for even small amount of sample, with easy operations and without expensive equipments.

(A) Gravimetric method for the determination of oxygen content.

The principle of the gravimetric method by the addition of alkali or alkaline earth metal nitrates is based on the fact that the oxidation state of uranium in most uranates containing alkali and/or alkaline earth metal is exactly +6 when they are formed in oxidizing atmosphers.

The point of the present method is that lithium nitrate or calcium nitrate solution was used as an additives instead of solid compounds in order to avoid tedious mixing procedure as well as to lower reaction temperatures and to reduce reaction period.

Applicatility of the present method was examined for test samples of UO_{2+x}, $Sr_yU_{1-y}O_{2+x}$, $Mg_yU_{1-y}O_{2+x}$ and $Th_yU_{1-y}O_{2+x}$. The oxygen content in these samples, of which the weight were about 200 mg, could be determined with an estimated standard deviation of ±0.005.

This error was considered to arise mainly from volumetric error when the solution was added to the oxide samples. To minimizing the error, the solution was weighed using a micro-

balance. The x values in the ternary uranium oxides were able to be determined with a standard deviation of ±0.002 by this procedure.

The reaction temperature and period required to decompose the nitrates and to form uranates were 920 K and 3 h for the lithium nitrate, and 1070 K and 3 h for the calcium nitrate, respectively.

(B) Cerium(IV)-iron(II) back titration method

By use of cerium(IV)-iron(II) backtitration method, the composition of ternary uranium oxides, both x and y in $M_yU_{1-y}O_{2+x}$, can be obtained by determining total amount of uranium as well as the amount of U^{4+} in the solution after dissolution of oxide samples in sulfuric acids. The present method was devised to give high accuracy with small amounts of samples. Main points of improvement were:

(1) Addition of excess cerium(IV) solution before dissolution of samples,

(2) Reduction of U^{6+} in a liquid-tight small glass bottle instead of the usual separatory funnel.

In the presence of excess cerium(IV), oxides were dissolved more rapidly. Moreover, no air oxidation of samples could be observed during the dissolution. The loss of the solution could be also reduced to a negligible amount by use of the small liquid-tight glass bottle.

Applicability of the present method was examined for a solid solution, $Sr_yU_{1-y}O_{2+x}$, having a known composition. The composition, x and y, of the test sample of c.a. 20 mg could be determined with standard deviations of ±0.004 and ±0.002 for x and y values, respectively. The accuracies for x and y values are estimated to be ±0.006 and ±0.004, respectively, if the volume error during titration is taking into account.

The determination of the composition of ternary uranium oxides are performed mainly by use of the cerium(IV)-iron(II) back titration method which enables us to determine both oxygen content and metal ratio with a small amount of sample. The gravimetric method is suitable for precise determination of oxygen content in specimens.

In chapter 3, the formation of monouranates of calcium, strontium and barium by the reactions of their carbonates with U_3O_8 in various atmosphers of air, carbon dioxide and hydrogen and in vacuum was studied by means of thermogravimetry and X-ray diffractometry. These monouranates were used as starting materials for the preparation of the ternary uranium oxides containing these metals.

The initiation temperatures of the reactions of $CaCO_3$, $SrCO_3$ and $BaCO_3$ with U_3O_8 (mixing ratio M/U = 1) in air were 850, 740 and 680 K, respectively. The composition of these products were $CaUO_{3.969}$, $SrUO_{3.997}$ and $BaUO_{4.000}$. From thermodynamic considerations, the reactions in air were deduced to proceed successively as follows:

$$MCO_3 \rightarrow MO + CO_2,$$

$$MO + UO_{8/3} + \frac{1}{6}O_2 \rightarrow MUO_4,$$

where M stands for Ca, Sr or Ba.

By reactions of carbonates and U_3O_8 under reducing atmospheres, oxygen-deficient monouranates were formed. However, if $CaCO_3$ was reacted with U_3O_8 in hydrogen atmosphere, the products were a two-phase mixture of CaO and $Ca_yU_{1-y}O_{2+x}$ with very low y values. The initiation temperatures of the reactions and the composition of the products are summarized in **Table 8-1**.

When heated in air, the rhombohedral compounds, $CaUO_4$ and α-$SrUO_4$, began to liberate oxygen above 970 and 770 K, respectively. These compounds showed a wide range of oxygen nonstoichiometry, while the orthorhombic compounds, β-$SrUO_4$ and $BaUO_4$, were almost stoichiometric up to 1370 K in air.

Table 8-1 The initiation temperatures of the reactions and the composition of the products

	atmosphere	ca	Sr	Ba
Initiation temperature (K)	air	850	740	680
	CO_2	920	810	800
	vac	770	680	700
	H_2	590	590	590
Composition	air	$CaUO_{3.969}$	$SrUO_{3.997}$	$BaUO_{4.000}$
	CO_2	$CaUO_{3.65}$	$SrUO_{3.673}$	$BaUO_{3.794}$
	vac	$CaUO_{3.50}$	$SrUO_{3.563}$	$BaUO_{3.651}$
	H_2	$CaUO_{3.03}$*	$SrUO_{3.175}$	$BaUO_{3.498}$

* Two-phase mixture of CaO and $Ca_yU_{1-y}O_{2+x}$ with very small y values.

In this study, the formation reaction of alkaline earth metal monouranates by heating the metal carbonates and U_3O_8 was clarified, and the composition of the formed monouranates was established. The phase behavior of the monouranates during heating in air was also clarified.

In Chapter 4, the crystal structures of α and β-$CdUO_4$ were determined by X-ray powder diffraction method. This study was carried out to have an insight into the phase transformation of $CdUO_4$ from structural point of view. Cadmium monouranate showed an anomalous oxygen nonstoichiometry change similar to that of strontium monouranate in the phase transformation from α to β phase.

α-$CdUO_4$ was rhombohedral with space group $R\bar{3}m$ and the lattice parameters were $a = 6.233 \pm 0.003$ Å and $\alpha = 36.12 \pm 0.05$ deg. The U-O_I bond length was obtained to be 1.98 Å which was somewhat longer than the usual uranyl bond length. This means that α-$CdUO_4$ is partly ionic and partly covalent. The crystal structure of α-$CdUO_4$ was isomorphous with that of α-$SrUO_4$.

β-$CdUO_4$ crystallized in a C-centered orthorhombic cell with $a = 7.023 \pm 0.004$, $b = 6.849 \pm 0.003$ and $c = 3.514 \pm 0.002$ Å. The space group was Cmmm. Collinear uranyl groups with a U-O_I distance of 1.91 Å were located either along or parallel to the c axis. The crystal structure of β-$CdUO_4$ was different from that of β-$SrUO_4$. Then, the infinite chains of $(UO_2)O_4$ octahedra in β-$CdUO_4$ were parallel to each other along c axis, whereas the distorted octahedra in β-$SrUO_4$ shared the corners to form infinite two-dimensional sheets in the plane with b and c axes. It is considered that the one-dimensional arrangement of the oxygen octahedra in β-$CdUO_4$ causes the thermal instability of this phase.

In this study, the crystal structure of nearly stoichiometric α and β-$CdUO_4$ has been established. It has been pointed out also that the difference in the macroscopic thermal stability of both phases could be explained by the difference in the microscopic crystal structure.

In Chapter 5, the phase behavior of $Ca_yU_{1-y}O_{2+x}$ solid solution was studied in the temperature range between 1473 and 1673 K by means of X-ray diffractometry and chemical analysis.

The single phase region of the cubic solid solution having the fluorite type structure was found to be extended $0 \leq y \leq 0.33$ in the temperature range from 1473 to 1673 K at oxygen partial pressures of 8 Pa. The lattice parameters were expressed as a linear equation of x and y in the range $x \geq 0$ to be:

$$a = 5.4704 - 0.102x - 0.310y \ (\text{Å}).$$

The coefficient of x, −0.102, which expresses the effect of excess oxygen on lattice parameter, was well comparable with that for $Mg_yU_{1-y}O_{2+x}$, $Sr_yU_{1-y}O_{2+x}$ and UO_{2+x}. Then, the defect type of oxygen in this solid solution can be assigned to oxygen interstitials.

The oxidation states of uranium in the solid solution were found to be U^{4+} and U^{5+} from a ionic model assuming rigid sphere ions. The partial molar enthalpies were estimated using calculated partial molar entropies. The enthalpy showed a maximum near $x = 0.01$ but became flattened to -72 ± 3 kcal/mol above $x = 0.1$.

In this work, a single phase region of the solid solution between uranium oxide and calcium oxide was clarified, and dependences of the lattice parameter and the partial molar enthalpy of oxygen on the composition of the solid solution were determined.

In Chapter 6, phase relations for praseodymium-uranium-oxygen ternary system were studied in the temperature range from 1473 to 1773 K and in various atmospheres of air, helium and high vacuum by means of X-ray diffraction method and chemical analysis. The knowledge of the phase relations in this system is of primary importance in order to estimate the effect of praseodymium on the chemical and thermodynamic properties of uranium dioxide fuels, since praseodymium is one of the major fission products with high yields.

From X-ray diffraction study, following phases were identified in this system: these were a β-U_3O_8 phase, a solid solution phase having fluorite structure ($Pr_yU_{1-y}O_{2+x}$), a rhombohedral phase (Pr_6UO_{12}) and an A-type rare earth sesquioxide phase.

The β-U_3O_8 phase existed in the composition range $0 \leq y \leq 0.32$ in air, and no solubility of praseodymium oxides in this phase could be observed. The single phase region of $Pr_yU_{1-y}O_{2+x}$ solid solution was from $y = 0.32$ to 0.71 when heated in air. On the other hand, the single phase region extended from $y = 0$ to 0.77 in the atmosphere of helium. This phase was classified in more detail by the mean valency of uranium and by the type of oxygen defects to explain the change of the lattice parameters. The rhombohedral phase existed in the range $\sim 0.7 < y \leq 0.9$ in all cases studied except for the condition of heating in air at 1473 K and in vacuum at 1773 K. The A-type Pr_2O_3 phase was formed under reducing atmospheres of helium and vacuum in the range $0.8 \leq y \leq 1.0$, and no solubility of uranium oxides could be observed. The C-type Pr_2O_3 phase of which the existence had been reported in literatures was not formed under the conditions of this study.

The lattice parameters of the solid solution phase were expressed as linear equations of x and y:

$$a = 5.4704 - 0.127x - 0.007y \ (\text{Å}), \text{ for } x \geq 0,$$

and

$$a = 5.4704 - 0.397x - 0.007y \ (\text{Å}), \text{ for } x < 0.$$

From the coefficients of x in these equations, the defect type of oxygen was deduced to be oxygen interstitials and oxygen vacancies for the region of $x \geq 0$ and $x < 0$. respectively. The change of the lattice parameter with y, $\partial a/\partial y$, in the solid solution of $RE_yU_{1-y}O_{2+x}$ (RE = rare earth elements) was found to change linearly with the ion size of trivalent rare earth elements which substitute for uranium. Since the present value of $\partial a/\partial y$ for praseodymium was on the line connecting those for the other $RE_{0.5}U_{0.5}O_{2.00}$ with trivalent rare earth elements, the oxidation state of praseodymium was considered to be trivalent.

It was confirmed that the reduced Pr_6UO_{12-x} phase existed under low oxygen partial pressures.

In this work, the phase relations of the ternary praseodymium-uranium-oxygen system

were established, which provide us useful data to estimate the behavior of fission product praseodymium in the uranium dioxide fuel.

In Chapter 7, the reactivity and reaction conditions to form lithium and sodium uranates were studied in an attempt ot grope some useful head-end processes in nuclear fuel reprocessing. In order to confine the increase of the high level wastes to a necessary minimum, it is important to know the minimum amounts of alkali metal salts which are required to form uranates.

The reactions between alkali nitrates and UO_2 with various M/U ratios showed that the minimum M/U ratios for obtaining the uranates free from U_3O_8 were 0.667 and 0.8 for lithium and sodium uranates, respectively. They were formed by heating at 873 K for 3 h in air or oxygen.

The uranates formed were found to be dissolved in 1 M HNO_3 within 1 min. This result shows that diluted acid can be employed to dissolve spent fuels, and hence this method would reduce the difficulties in dissolution of spent fuels to a large extent.

In order to elucidate and to establish the irradiation behavior of UO_2 type unclear fuels, we need a complete set of data base on the thermodynamic properties which describe the relation among the oxide fuels, fission products and cladding materials in the fuel pins. Although a number of thermodynamic studies on the ternary and/or polynary uranium oxides with fission product elements have been carried out until now, the knowledge and information available for that purpose are still fragmentary. Extensive and continuous efforts need to be paid to obtain such information as phase relations, thermodynamic properties of the polynary uranium oxides.

The same methods and approach as used in the present report can be applicable to the evaluation of the irradiation behavior of the plutonium-uranium mixed oxide fuel which will be employed in the fast breeder reactor, provided that appropriate modification due to introduction of new actinide element plutonium can be made.

Acknowledgments

The author wished to express his gratitude to Professors Keiji Naito and Shigeharu Naka, and Assistant Professor Toshihide Tsuji of Nagaya University for fruiful discussions and continuous encouragement.

He is also greatly indebted to Dr. Takeo Fujino for his help and valuable discussion throughout this work.

He gratefully acknowledges the significant contrubutions of several colleagues in conducting this study: Professor Hiroaki Tagawa of Yokohama National University, the former head of the Nuclear Fuel Chemistry Laboratory, for kind guidance and suggestions to the present study, Dr. Haruo Natsume and Dr. Kaoru Ueno for valuable discussions, Dr. Norio Masaki for the X-ray diffraction analyses, Dr. Ken Ohwada for the infrared absorption analyses, Mr. Kinji Ohuchi for the technical supports, Mr. Kikuo Kimura and Mr. Kazuhiro Obara for the glass blowing of the experimental apparatus, and the other members of the Nulear Fuel Chemistry Laboratory of Japan Atomic Energy Research Institute for their counsel and encouragements.

were established, which provide us useful data to estimate the behavior of fission product praseodymium in the uranium dioxide fuel.

In Chapter 7, the reactivity and reaction conditions to form lithium and sodium uranates were studied in an attempt ot grope some useful head-end processes in nuclear fuel reprocessing. In order to confine the increase of the high level wastes to a necessary minimum, it is important to know the minimum amounts of alkali metal salts which are required to form uranates.

The reactions between alkali nitrates and UO_2 with various M/U ratios showed that the minimum M/U ratios for obtaining the uranates free from U_3O_8 were 0.667 and 0.8 for lithium and sodium uranates, respectively. They were formed by heating at 873 K for 3 h in air or oxygen.

The uranates formed were found to be dissolved in 1 M HNO_3 within 1 min. This result shows that diluted acid can be employed to dissolve spent fuels, and hence this method would reduce the difficulties in dissolution of spent fuels to a large extent.

In order to elucidate and to establish the irradiation behavior of UO_2 type unclear fuels, we need a complete set of data base on the thermodynamic properties which describe the relation among the oxide fuels, fission products and cladding materials in the fuel pins. Although a number of thermodynamic studies on the ternary and/or polynary uranium oxides with fission product elements have been carried out until now, the knowledge and information available for that purpose are still fragmentary. Extensive and continuous efforts need to be paid to obtain such information as phase relations, thermodynamic properties of the polynary uranium oxides.

The same methods and approach as used in the present report can be applicable to the evaluation of the irradiation behavior of the plutonium-uranium mixed oxide fuel which will be employed in the fast breeder reactor, provided that appropriate modification due to introduction of new actinide element plutonium can be made.

Acknowledgments

The author wished to express his gratitude to Professors Keiji Naito and Shigeharu Naka, and Assistant Professor Toshihide Tsuji of Nagaya University for fruiful discussions and continuous encouragement.

He is also greatly indebted to Dr. Takeo Fujino for his help and valuable discussion throughout this work.

He gratefully acknowledges the significant contrubutions of several colleagues in conducting this study: Professor Hiroaki Tagawa of Yokohama National University, the former head of the Nuclear Fuel Chemistry Laboratory, for kind guidance and suggestions to the present study, Dr. Haruo Natsume and Dr. Kaoru Ueno for valuable discussions, Dr. Norio Masaki for the X-ray diffraction analyses, Dr. Ken Ohwada for the infrared absorption analyses, Mr. Kinji Ohuchi for the technical supports, Mr. Kikuo Kimura and Mr. Kazuhiro Obara for the glass blowing of the experimental apparatus, and the other members of the Nulear Fuel Chemistry Laboratory of Japan Atomic Energy Research Institute for their counsel and encouragements.

References

1) Waber J.E. and Jensen E.D. : Trans. Am. Nucl. Soc., **14**, 17 (1971).
2) Assmann H. and Stehle H. : "Behavior of Uranium Fuels in Nuclear Reactors, Gmelin Handbook of Inorganic Chemistry, Uranium", Springer-Verlag, Berlin, Sys. No.55, Suppl. Vol. A4, 1 (1981).
3) Research Committee on Nuclear Fuel Behavior : J. At. Energy Soc. Jpn., **19**, 303 (1977) [in Japanese].
4) Research Committee on Fuel Performance : J. At. Energy Soc. Jpn., **21**, 773 (1979) [in Japanese].
5) Research Committee on Fuel Performance, J. At. Energy Soc. Jpn., **23**, 571 (1981) [in Japanese].
6) Keller, C. : "MTP International Review of Science, Inorganic Chemistry", ed. Bagnall K.W., Butterworths, London, Vol. 7, 47 (1972).
7) Keller C. : "Ternäre und Polynäre Oxide des Urans, Gmelins Handbuch der anorganischen Chemie", Springer-Verlag, Berlin, Band 55, Ergänzungswerk, Teil C3, 70 (1975).
8) Potter P.E. : "Behavior and Chemical State of Irradiated Ceramic Fuels", IAEA, 115 (1974).
9) Fujino T. : J. At. Energy Soc. Jpn., **20**, 241 (1978) [in Japanese].
10) Tagawa H. and Jujino T. : J. At. Energy Soc. Jpn., **22**, 871 (1980) [in Japanese].
11) Lang S.M., Knudsen P.F., Fillmore C.L. and Roth R.C. : Nat. Bur. Std. (U.S.) Circ., **568** (1956).
12) Brisi C. : Ric. Sci., **30**, 2376 (1960).
13) Scholder R. and Brixner L. : Z. Naturforsch., **10b**, 178 (1955).
14) Furman S.C. : KAPL-1664 (1957).
15) Trzebiatowski W. and Jablonski A. : Nukleonika, **5**, 587 (1960).
16) Charvillat J.P., Band G. and Besse J.P. : Mater. Res. Bull., **5**, 587 (1960).
17) Brisi C. and Montorsi-Appendino M. : Ann. Chim. Rome, **59**, 400 (1969).
18) Young A.P. and Schwarz C.M. : J. Inorg. Nucl. Chem., **25**, 1133 (1963).
19) Keller C. : KFK-225 (1964).
20) Kemmler-Sack S. and Rüdorff W. : Z. Anorg. Allg. Chem., **354**, 255 (1967).
21) Fujino T. and Naito K. : J. Inorg. Nucl. Chem., **32**, 627 (1970).
22) Hoekstra H.R. and Katz J.J. : J. Am. Chem. Soc., **74**, 1683 (1952).
23) Brochu R. and Lucas J. : Bull. Soc. Chim. France, 4764 (1967).
24) Brisi C., Montorsi M. and Acquarone G.B. : Atti Accad. Sci. Torino Classe Sci. Fis. Mat. Nat., **106**, 257 (1972).
25) Voronov N.M. and Sofronova R.M. : "Physical Chemistry of Alloys and Refractory Compounds of Thorium and Uranium", ed. Ivanov O.S., Jerusalem, 204 (1972).
26) Kemmler-Sack S. : Z. Naturforsch., **23b**, 1260 (1968).
27) Kemmler-Sack S. and Seemann I. : Z. Anorg. Allg. Chem., **409**, 23 (1974).
28) Kemmler-Sack S. and Wall I. : Z. Naturforsch., **26b**, 1229 (1971).
29) Cordfunke E.H.P. and Loopstra B.O. : J. Inorg. Nucl. Chem., **29**, 51 (1967).
30) Polunina G.P., Kovba L.M. and Ippolitove E.A. : ANL-Trans-33, 224 (1961).
31) Klima J., Jakes D. and Moravec J. : J. Inorg. Nucl. Chem., **28**, 1861 (1966).
32) Allpress J.G. : J. Inorg. Nucl. Chem., **26**, 1847 (1964).
33) Allpress J.G. : J. Inorg. Nucl. Chem., **27**, 1521 (1965).
34) Zachariasen W.H. : Acta Cryst., **7**, 788 (1954).
35) Jakes D. and Krivy J. : J. Inorg. Nucl. Chem., **36**, 2885 (1974).
36) Zacharizsen W.H. : Acta Cryst., **1**, 281 (1948).
37) Loopstra B.O. and Rietveld H.M. : Acta Cryst., **B25**, 787 (1969).
38) Fujino T., Masaki N. and Tagawa H. : Z. Krist., **145**, 299 (1977).
39) Keller C. : Nukleonik, **4**, 271 (1962).
40) Samson S. and Sillen L.G. : Ark. Kemi. Min. Geol., **25A** No.21, 16 (1947).
41) Ippolitove E.A., Bereznikove I.A., Leonidov V.Y. and Kovba L.M. : ANL-Trans-33, 186 (1961).
42) Rietveld H.M. : Acta Cryst., **20**, 508 (1966).
43) Rüdorff W. and Pfitzer F. : Z. Naturforsch., **9b**, 568 (1954).
44) Kemmler-Sack S. and J. Seemann : Z. Anorg. Allg. Chem., **411**, 61 (1975).
45) Westrum Jr. E.F. : COO-1149-136 (1968).
46) O'Hare P.A.G., Boerio J., Fredrickson D.R. and Hoekstra H.R. : J. Chem. Thermodyn., **9**, 963 (1977).
47) Jakes D. and Schauer V. : Proc. Brit. Ceram. Soc., No.8, 123 (1967).
48) Lambertson W.H. and Mueller M.H. : ANL-5312 (1954).

49) Ippolitova E.A., Simanov Yu.P., Kovba L.M. Polunina G.P. and Bereznikova I.A. : Radiokhimiia, **1**, 660 (1959).
50) Fujino T. : J. Inorg. Nucl. Chem., **34**, 1563 (1972).
51) Fujino T. , Tateno J. and Tagawa H. : J. Solid State Chem., **24**, 11 (1978).
52) Tateno J., Fujino T. and Tagawa H. : J. Solid State Chem., **30**, 265 (1979).
53) Alberman K.B., Blakey R.C. and Anderson J.S. : J. Chem. Soc., 1352 (1951).
54) Hoekstra H.R. and Siegel S. : A/Conf., **7**, P/737, 394 (1956).
55) Bereznikova I.A., Ippolitove E.A., Simanov Yu.P. and Kovba L.M. : ANL-Trans-33, 176 (1961).
56) Wyckoff R.W.G. : "Crystal Structures", Interscience, New York, Vol. 2, 323 (1964).
57) Kovba L.M., Simanov Yu.P., Ippolitova E.A. and Spitsyn V.I. : ANL-Trans-33, 24 (1961).
58) Anderson J.S. and Barraclough C.G. : Trans. Faraday Soc., **59**, 1572 (1963).
59) Voronov N.M. and Sofronova R.M. : "Physical Chemistry of Alloys and Refractory Compounds of Thorium and Uranium", ed. Ivànov O.S., Jerusalem, 215 (1972).
60) Sawyer J.O. : J. Inorg. Nucl. Chem., **25**, 899 (1963).
61) Dayton R.W. and Tipton C.R. : BMI-1534 (1961).
62) Bobo J.C. : Rev. Chim. Minerale, **1**, 1 (1964).
63) Brisi C., Montorsi M. and Burlando G.A. : Rev. Intern. Hautes Temp. Refract., **8**, 37 (1971).
64) Tagawa H., Fujino T. and Tateno J. : Bull. Chem. Soc. Jpn, **50**, 2940 (1977).
65) Sawyer J.O. : J. Inorg. Nucl. Chem., **34**, 3268 (1972).
66) Ippolitova E.A., Bereznikova I.A., Kosynkin V.D., Simanov Yu.P. and Kovba L.M. : ANL-Trans-33, 180 (1961).
67) Sleight A.W. and Ward R. : Inorg. Chem., **1**, 790 (1962).
68) McIver E.J. : AERE-M-1612 (1966).
69) Hund F. : Ber. Deutsche Keram. Ges., **42**, 251 (1965).
70) Fujino T., Yamashita T. and Tagawa H. : to be published on J. Solid State Chem., **73** (1988).
71) Tagawa H. and Fujino T. : J. Inorg. Nucl. Chem., **40**, 2033 (1978).
72) Voronov N.M., Sofronova R.M. and Voitekhova E.A. : "Physical Chemistry of Alloys and Referactory Compounds of Thorium and Uranium", ed. Ivanov O.S., Jerusalem, 222 (1972).
73) Gifford F.E. and Hill R.F. : J. Appl. Phys., **38**, 2261 (1967).
74) Voronov N.M. and Sofronova R.M. : "Tr. Inst. Met. im A.A. Baikova Stroenie Splavov Nekotorykh s Uranom i Toriem", 482 (1961).
75) Florence T.M. : "Analytical Methods in the Nuclear Fuel Cycle, Proceedings of a Symposium, Vienna, 29 November-2 December, 1971", IAEA, Vienna, 45 (1972).
76) Petit G.S. and Kienberger C.A. : Anal. Chim. Acta, **25**, 579 (1961).
77) Ackermann R.J., Chang A.T. and Sorrell C.A. : J. Inorg. Nucl. Chem., **39**, 75 (1977).
78) Swanson G.C. : AEC-Reports LA-6083-T (1975).
79) Markin T.L., Walter A.J. and Bones R.J. : AERE-R-4608 (1964).
80) Markin T.L. and McIver E.J. : "Proc. 3rd Intern. Conf. on Plutonium", Inst. Metals, London, 845 (1965).
81) Braun R., Kemmler-Sack S., Roller H., Seemann I. and Wall I. : Z. Anorg. Allg. Chem., **415**, 133 (1975).
82) Hill D.C. : J. Am. Ceram. Soc., **45**, 258 (1962).
83) Wadier J.F. : CEA-R-4507 (1973).
84) Ohmichi T., Fukushima S., Maeda A. and Watanabe H. : J. Nucl. Mater., **102**, 40 (1981).
85) Fujino T., Tagawa H., Adachi T. and Hashitani H. : Anal. Chim. Acta, **98**, 373 (1978).
86) Fujino T. and Tagawa H. : Anal. Chim. Acta, **107**, 365 (1979).
87) Keller C. : "Ternäre und Polynäre Oxide des Urans, Gmelins Handbuch der anorganischen Chemie", Springer-Verlag, Berlin, Band 55, Ergänzungswerk, Teil C3, 213 (1975).
88) Hashitani H., Hoshino A. and Adachi T. : Japan Atomic Energy Research Institute Report, JAERI-M-5343 (1973).
89) Fujino T., Tagawa H. and Adachi T. : J. Nucl. Mater., **97**, 93 (1981).
90) Nickel H. : Nuklenik, **8**, 366 (1966).
91) Dharwadkar D.R. and Chandrasekharaiah M.S. : Anal. Chim. Acta, **45**, 545 (1969).
92) "Gmelins Handbuch der anorganischen Chemie, Lithium", Verlag Chemie, Berlin, No.20, 285 (1960).
93) Remy H. : "Treatise on Inorganic Chemistry", translated by Anderson J.S., Elsevier, Amsterdam, Vol. I, 272 (1956).
94) Canning R.G. and Dixon P. : Anal. Chem., **24**, 877 (1955).
95) Rao G.G. and Sagi S.R. : Talanta, **9**, 715 (1962).
96) Davies W. and Gray W. : Talanta, **11**, 1203 (1964).
97) Eberle A.E., Lerner M.W., Goldbeck C.G. and Rodden C.J., AEC/NBL/252 (1970).
98) Slanina J., Bakker F., Groen A.J.P. and Lingerak W.A. : Fresenius' Z. Anal. Chem., **289**, 102 (1978).

99) Corpel J. and Regnand F. : Anal. Chim. Acta, **27**, 36 (1962).
100) Sill C.W. and Peterson H.E. : Anal. Chem., **24**, 1175 (1952).
101) Stromatt R.W. and R.E. Connally R.E. : Anal. Chem., **33**, 345 (1961).
102) Viguie C.J. and Chabert J.P. : Anal. Chim. Acta, **48**, 367 (1969).
103) Burd R.M. and Goward G.W. : AEC-Reports WAPD-205 (1959).
104) Kubota H. : Anal. Chem., **32**, 611 (1960).
105) Shalgosky H.I., Smart R.C. and Watling J. : AERE-R-4270 (1964).
106) Kuhn E., Baumgartel G. and Schmieder H. : Fresenius' Z. Anal. Chem., **267**, 103 (1973).
107) Kihara S., Adachi T. and Hashitani H. : Fresenius' Z. Anal. Chem., **303**, 28 (1980).
108) Kemmler-Sack S. and Rüdorff W. : Z. Anorg. Allg. Chem., **344**, 23 (1966).
109) Diehl H.G. and Keller C. : J. Solid State Chem., **3**, 621 (1971).
110) Nakazono T. : J. Chem. Soc. Jpn. : **42**, 761 (1921).
111) Tagawa H., Fujino T. and Yamashita T. : J. Inorg. Nucl. Chem., **41**, 1729 (1979).
112) Rao G.G., Rao P.K. and Rahman M.A. : Talanta, **12**, 953 (1965).
113) Lundell G.E.F. and Knowles H.B. : J. Am. Chem. Soc., **47**, 2637 (1925).
114) Ryzhinskii M.V., Preobrazhenskaya L.D., Solntseva L.F. and Gromova E.A. : Zh. Anal. Khim., **33**, 1738 (1978).
115) Ippolitova E.A., Fanstova D.G. and Spitsyn V.I. : ANL-Trans-33, 170 (1961).
116) Jakes D. : Collection Czech. Chem. Commun., **38**, 1 (1973).
117) Reis A.H., Hoekstra H.R., Gebert E. and Peterson S.W. : J. Inorg. Nucl. Chem., **38**, 1481 (1976).
118) O'Hare P.A.G., Boerio J. and Hoekstra H.R. : J. Chem. Thermodyn., **8**, 845 (1976).
119) Allen G.C. and Griffiths A.J. : J. Chem. Soc. Dalton Trans., **1977**, 1144 (1977).
120) Mathews M.D., Momin A.C. and Karkhanavala M.D. : Indian J. Chem., **15A**, 192 (1977).
121) Tagawa H. and Fujino T. : Inorg. Nucl. Chem. Lett., **13**, 489 (1977).
122) Voronov N.M. and Sofronova R.M. : "Physical Chemistry of Alloys and Refractory Compounds of Thorium and Uranium", ed. Ivanov O.S., Jerusalem, 235 (1972).
123) "Experimental Chemistry", Edited by Chem. Soc. Jpn., Maruzen, Tokyo, Vol. 9, 176 (1958).
124) Barin I. and Knacke O. : "Thermochemical Properties of Inorganic Substances", Springer-Verlag, Berlin (1973).
125) Huber Jr. E.J. and Holley C.E. : J. Chem. Thermodyn., **1**, 267 (1969).
126) Cordfunke E.H.P., Ouweltjes W. and Prins G., J. Chem. Thermodyn., **7**, (1975) 1137.
127) Barin I., Knacke O. and Kubaschewski O. : "Thermochemical Properties of Inorganic Substances, Supplement", Springer-Verlag, Berlin (1977).
128) Girhar H.L. and Westrum Jr. E.F. : J. Chem. Eng. Data, **13**, 531 (1968).
129) Westrum Jr. E.F. : "Thermodynamics", IAEA, Vienna, Vol. II, 497 (1966).
130) Cordfunke E.H.P. and O'Hare P.A.G. : "The Chemical Thermodynamics of Actinide Elements and Compounds, Part 3, Miscellaneous Actinide Compounds", IAEA, Vienna (1978).
131) Ippolitova E.A., Simanov I.P., Kovba L.M., Polunina G.P. and Bereznikova I.A. : DEG-INF Ser. 145 (1961).
132) Reshetov K.V. and Kovba L.M. : J. Struct. Chem., **7**, 589 (1966).
133) Kovba L.M., Polunina G.P., Ippolitova E.A., Simanov Yu.P. and Spitsyn V.I. : Russ. J. Phys. Chem., **35**, 350 (1961).
134) Tagawa H. and Fujino T. : Inorg Nucl. Chem. Lett., **16**, 91 (1980).
135) Ibers J.A., Templeton D.H., Vainshtein B.K., Bacon G.E. and Lonsdale K. : "International Tables for X-ray Crystallography", Kynoch Press, Birmingham, Vol. III, 206 (1962).
136) Cromer D.T. and Waber J.T. : Acta Cryst., **18**, 104 (1965).
137) Cromer D.T. : Acta Cryst., **18**, 17 (1965).
138) Tokonami M. : Acta Cryst., **19**, 486 (1965).
139) Ohwada K. : Thesis, "Study on infrared Spectra of Uranium Compounds", The University of Tokyo, Tokyo (1977).
140) Naito K., Tsuji T., Matsui T. and Une K. : J. Nucl. Sci. Technol. (Tokyo) **11**, 22 (1974).
141) Keller C. and Boroujerdi A. : J. Inorg. Nucl. Chem., **34**, 1187 (1972).
142) Beals R.J. and Handwerk J.H. : J. Am. Ceram. Soc., **48**, 271 (1965).
143) Kolar D., Handwerk J.H. and Beals R.J. : ANL-6631 (1962).
144) Yamashita T., Fujino T. and Tagawa H. : J. Nucl. Mater., **132**, 192 (1985).
145) Füredi-Milhofer H., Despotović Z., Devidé Z. and Wrischer M. : J. Inorg. Nucl. Chem., **34**, 1961 (1972).
146) Zachariasen W.H. : Acta Cryst., **1**, 265 (1948).
147) Lynds L., Young W.A., Mohl J.S. and Libowitz G.G. : "Nonstoichiometric Compounds", Advances in Chemistry Series 39, American Chemical Society, Washington D.C., 58 (1963).
148) Shannon R.D. : Acta Cryst., **A32**, 751 (1976).

149) Aronson S. and Clayton J.C. : J. Chem. Phys., **32**, 749 (1960).
150) Une K. and Oguma M. : J. Nucl. Mater., **110**, 215 (1982).
151) Markin T.L. and Bones R.J. : AERE-R-4042 (1962).
152) Gerdanian P. : J. Phys. Chem. Solids, **35**, 163 (1974).
153) Kubaschewski O. and Slough S. : Progr. Mater. Sci., **14**, (1969).
154) Peehs M., Manzel R., Schweighofer W., Haas W., Haas E. and Würtz R. : J. Nucl. Mater., **97**, 157 (1981).
155) Keller C. : "Ternäre und Polynäre Oxide des Urans, Gmelins Handbuch der anorganischen Chemie", Springer-Verlag, Berlin, Band 55, Ergänzungswerk, Teil C3, 197 (1975).
156) Hund F. and Peetz U. : Z. Elektrochem., **56**, 223 (1952).
157) Jocher W.G. : KFK-2518 (1978).
158) De Alleluia I.B., Hoshi M., Jocher W.G. and Keller C. : J. Inorg. Nucl. Chem., **43**, 1831 (1981).
159) Aitken E.A., Bartram S.F. and Juenke E.F. : Inorg. Chem., **3**, 949 (1964).
160) Lowe A.T. : Diss. Srizona-State Univ. (1974).
161) Loopstra B.O. : Acta Cryst., **B26**, 656 (1970).
162) Burnham D.A. and Eyring L. : J. Phys. Chem., **72**, 4415 (1968).
163) Eyring L. and Holmberg B. : "Nonstoichiometric Compounds", Advances in Chemistry Series 39, American Chemical Society, Washington D.C., 46 (1963).
164) Chikalla T.D. and Eyring L. : J. Inorg. Nucl. Chem., **30**, 133 (1968).
165) Tagawa H. : J. Nucl. Mater., **51**, 78 (1974).
166) Keller C., Engerer H., Leitner L. and Sriyotha U. : J. Inorg. Nucl. Chem., **31**, 965 (1969).
167) Rüdorff W., Erfurth H. and Kemmler-Sack S. : Z. Anorg. Allg. Chem., **354**, 273 (1967).
168) Weitzel H. and Keller C. : J. Solid State Chem., **13**, 136 (1975).
169) Tanamas R. : KFK-1910 (1973).
170) Leitner L. : KFK-521 (1967).
171) Sriyotha U. : KFK-737 (1968).
172) Stadlbauer E., Wichmann U., Lott U. and Keller C. : J. Solid State Chem., **10**, 341 (1974).
173) Berndt U., Tanamas R. and Keller C. : J. Solid State Chem., **17**, 113 (1976).
174) Goode J.H. and Vaughen V.C.A. : CONF-720607-16 (1972).
175) Cadieux J.R. and Stone J.A. : DP-MS-80-10 (1980).
176) Groenier W.S. : ORNL-CF-77-67 (1977).
177) Baybarz R.D., Haire R.G., Clinton S.D., Tennery V.J., Farrar L.G., Vaughen V.C.A., Fitzgerald C.L. and Watson C.D. : ORNL-TM-3723 (1973).
178) Bähr W. and Vogg H. : Germany Patent 1,197, 630 (1964).
179) Milner G.W.C., Wood A.J., Weldrick G. and Phillips G. : Analyst, **92**, 239 (1967).
180) Maurice M.J., Angeletti L.M. and Buijs K. : EUR-4133 (1969).
181) Avogadro A. and De Plano A. : EUR-4784, (1972), English Translation, BNWL-TR-228 (1977).
182) Toussaint C.J. and Avogadro A. : J. Inorg. Nucl. Chem., **36**, 781 (1974).
183) Keller C. : "Ternäre und Polynäre Oxide des Urans, Gmelins Handbuch der anorganischen Chemie", Springer-Verlag, Berlin, Band 55, Ergänzungswerk, Teil C3, 1 (1975).
184) Kovba L.M. : Russ. J. Inorg. Chem., **16**, 1639 (1971).
185) Kovba L.M. : Sov. Radiochem., **12**, 486 (1970).
186) Hauck J. : J. Inorg. Nucl. Chem., **36**, 2291 (1974).
187) Gebert E., Hoekstra H.R., Reis Jr. A.H. and Peterson S.W. : J. Inorg. Nucl. Chem., **40**, 65 (1978).
188) Hauck J. : Z. Naturforsch., **28b**, 215 (1973).
189) Kovba L.M. : Sov. Radiochem., **13**, 319 (1971).
190) Kovba L.M. : Zh. Strukt. Khim., **3**, 159 (1962).
191) Carnall W.T., Walker A. and Neufeldt S.J. : Inorg. Chem., **5**, 2135 (1966).
192) Cordfunke E.H.P. and Loopstra B.O. : J. Inorg. Nucl. Chem., **33**, 2427 (1971).
193) Kovba L.M. : Sov. Radiochem., **14**, 746 (1972).
194) Kovba L.M., Polunina G.P., Simanov Yu.P. and Ippolitove E.A. : ANL-Trans-33, 17 (1961).
195) Hoekstra H.R. : J. Inorg. Nucl. Chem., **27**, 801 (1965).
196) Efremova K.M., Ippolitova E.A., Simanov Yu.P. and Spitsyn V.I. : Dokl. Akad. Nauk. SSSR, **124**, 1057 (1959).
197) Fujino T., Ouchi K. and Yamashita T., Anal. Chim. Acta, **147**, 423 (1983).